Geneeskundige Stichting Koningin Elisabeth
Fondation Médicale Reine Elisabeth
Königin-Elisabeth-Stiftung für Medizin
Queen Elisabeth Medical Foundation

Verslag – Rapport – Bericht – Report

2023

G.S.K.E. – F.M.R.E. – K.E.S.M. – Q.E.M.F.

www.fmre-gske.be
www.fmre-gske.eu
www.fmre-gske.com

Progress reports of the research projects of young researchers, supported by the Queen Elisabeth Medical Fondation in collaboration with the following professors and doctors (2023)

1. Interuniversity research projects

2. University research projects

3. Research projects of young researchers

Geneeskundige Stichting Koningin Elisabeth
Fondation Médicale Reine Elisabeth
Königin-Elisabeth-Stiftung für Medizin
Queen Elisabeth Medical Foundation

Interuniversitaire onderzoeksprojecten 2023-2025 gefinancierd door de G.S.K.E.

Projets de recherche interuniversitaire 2023-2025 subventionnés par la F.M.R.E.

Interuniversity research projects 2023-2025 funded by the Q.E.M.F.

Universiteiten met onderzoeksprogramma's die gesteund worden door de G.S.K.E.

Universités ayant des programmes de recherche subventionnés par la F.M.R.E.

Universities having research programs supported by the Q.E.M.F.

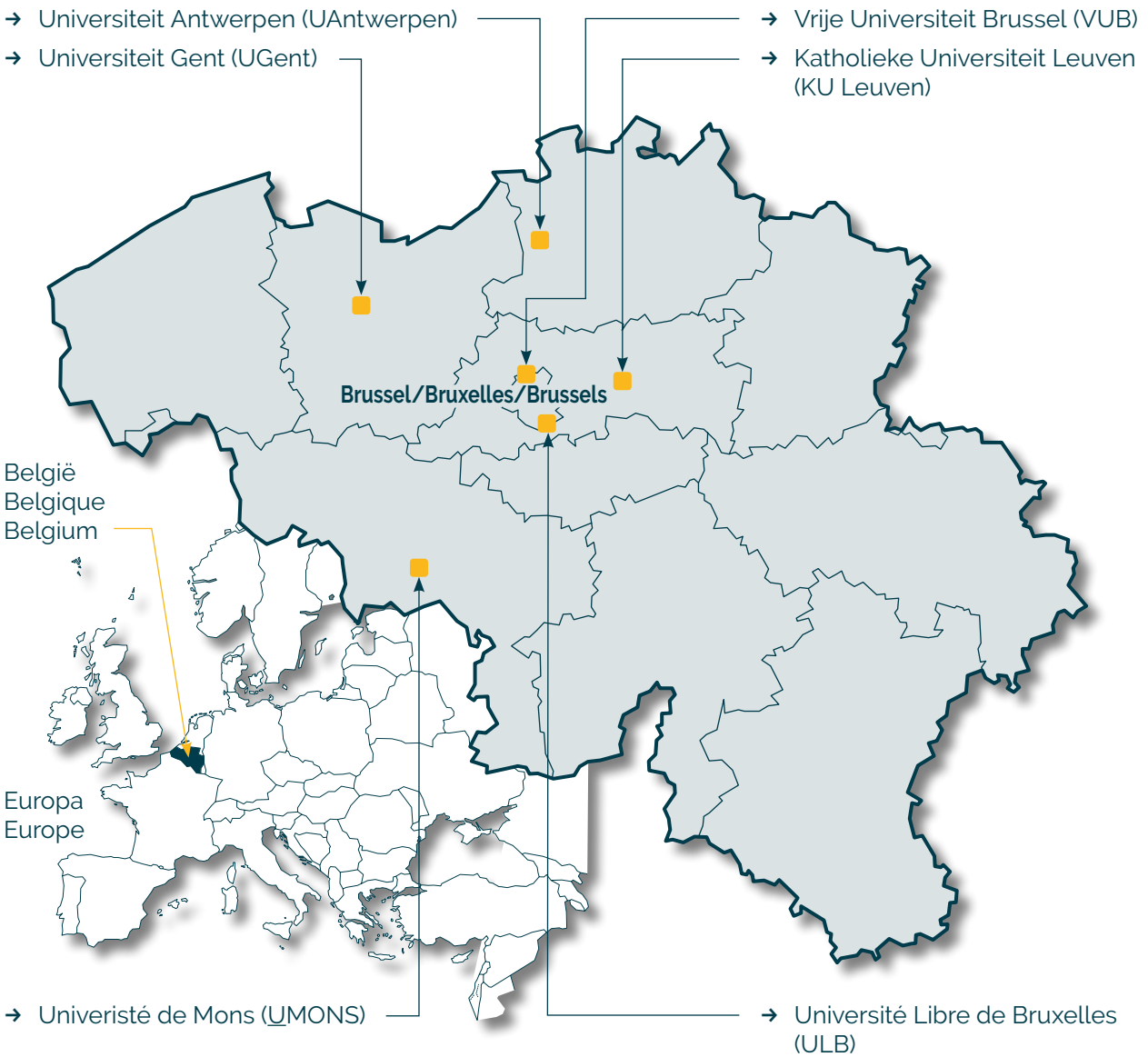

Interuniversitaire onderzoeksprojecten 2023-2025 gefinancierd door de G.S.K.E.

Projets de recherche interuniversitaire 2023-2025 subventionnés par la F.M.R.E.

Interuniversity research projects 2023-2025 funded by the Q.E.M.F.

Prof. dr. Geert Van Loo (UGent)
Prof. Kiavash Movahedi (VUB)
OTULIN in neuroinflammation and Alzheimer pathology

Prof. dr. Sarah Weckhuysen (UAntwerpen)
Prof. dr. Bjorn Menten (UGent)
Detection of somatic mutations and disease-defining methylation patterns in brain tissue and cerebrospinal fluid of patients with non-acquired focal epilepsy

Prof. dr. Renzo Manusco (UAntwerpen)
Prof. dr. Joris De Wit (KU Leuven)
Dissecting the molecular basis of microglia-synapse communication in AD

Prof. dr. Ann Massie (VUB)
Prof. dr. Lutgarde Arckens (KU Leuven)
The xCT-/- killifish to validate the potential of system xc- as therapeutic target in Parkinson's disease

Prof. dr. Karelle Leroy (ULB)
Prof. dr. Laurence Ris (UMONS)
Prof. dr. Kristel Sleegers (UAntwerpen)
Involvement of diabetes and antidiabetic treatment on tau pathology propagation

Geneeskundige Stichting Koningin Elisabeth
Fondation Médicale Reine Elisabeth
Königin-Elisabeth-Stiftung für Medizin
Queen Elisabeth Medical Foundation

Progress report of the interuniversity research project of

Prof. dr. Geert Van Loo (UGent)
Prof. Kiavash Movahedi (VUB)

Prof. dr. Geert van Loo (UGent)
VIB-UGent Inflammation
Technologiepark 71
9052 Gent-Zwijnaarde
Belgium
T +32-(0)9 3313761
Geert.vanloo@irc.vib-ugent.be

Prof. dr. Kiavash Movahedi (VUB)
Research Center Vrije Universiteit Brussel
Laarbeeklaan 103 building E, room E234
1090 Jette-Brussels
Belgium
T +32-(0)2 4774569
kiavash.movahedi@vub.be

OTULIN in neuroinflammation and Alzheimer pathology

1. Summary of the research project

Inflammatory signaling pathways are subjected to tight regulation to avoid chronic inflammation and the development of inflammatory pathology. One of the proteins involved in such regulation is the deubiquitinating enzyme OTULIN. In this project, we investigate the role of OTULIN in neuroinflammation and Alzheimer pathology.

2. Introduction

Inflammation is a protective response to induce repair in conditions of cellular damage and stress. **Strict control of inflammatory signaling pathways is however essential to prevent chronic inflammation and the development of inflammatory pathologies.** Such control is exercised at various levels, including the reversible modification of signaling proteins. Ubiquitination is a posttranslational protein modification in which ubiquitin chains are covalently attached to target proteins, thereby earmarking these proteins for proteasomal degradation or allowing them to function as a scaffold to recruit other proteins and mediate downstream signaling [1,2]. Linear ubiquitination involves the linkage of ubiquitin via its amino-terminal methionine residue (Met1 or M1) to another ubiquitin molecule, a process mediated by the linear ubiquitin chain assembly complex (LUBAC) (Figure 1). **LUBAC is the sole E3 ubiquitin ligase complex known to generate linear chains**, and is essential for i) NF-B-mediated inflammatory gene expression in response to various stimuli, including TNF, IL-1β, and ligands activating TLRs, NOD2 and NLRP3; and ii) for preventing TNF-induced cell death [3–12]. Genetic loss of LUBAC proteins causes immunodeficiency and auto-inflammation in humans [13,14], and embryonic lethality or inflammatory phenotypes in mice [4,10,11,15–17], establishing the importance of LUBAC-mediated M1 signaling for normal mammalian physiology.

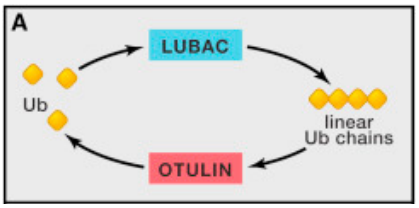

Ubiquitination is reversed by **deubiquitinating enzymes (DUBs)** that cleave ubiquitin chains from their substrate [2]. About hundred different DUBs have been identified so far, but mainly A20, Cylindromatosis (CYLD) and **OTULIN have been characterized as key DUBs involved in the negative regulation of NF-**B **activation and cell death** [18] (Figure 1). OTULIN (OTU Deubiquitinase with Linear Linkage Specificity), also known as Fam105b or Gumby, was only recently discovered in mice and human [19,20]. Homozygous hypomorphic mutations in the human *OTULIN* gene have been identified causing an early-onset, potentially fatal, autoinflammatory disease [21-24]. Mice harboring a point mutation in *OTULIN*, abolishing its activity to cleave M1 chains, are not viable and die during development [20,25], while mice with inducible (postnatal) deletion of *OTULIN* develop an acute systemic inflammation due to dysregulated NF-B activation and cytokine production [22]. **Together, these data identify OTULIN as a crucial regulatory mechanism in inflammatory signaling.**

Very little is known about the role of OTULIN in the central nervous system (CNS) and in CNS inflammation. A recent study showed that OTULIN controls microglia activation and suppresses neuroinflammation in a rat model of stroke [26]. Indeed, microglia, the resident tissue macrophages of the CNS, are important for the maintenance of CNS homeostasis, but

also critically contribute to CNS pathology [27]. Interestingly, **a recent genome-wide association study (GWAS) on human Alzheimer disease (AD) cases confirmed microglia implication and allowed identification of *OTULIN* as a new risk locus for AD** [28].
The aim of the project is to characterize the role of OTULIN in Alzheimer disease (AD), the most common progressive form of dementia, affecting over 25 million people worldwide [29,30]. Neuroinflammation is increasingly regarded as a key component that actively contributes to AD pathology. NF-κB signaling, activated by amyloid-β (Aβ) and/or by the microtubule-associated protein Tau, was shown to drive microglia-mediated Aβ and Tau toxicity leading to AD-associated learning and memory deficits [31-33]. However, **the specific immune mechanisms through which microglia contribute to AD-associated neuroinflammation, as well as the eventual role of OTULIN in this process, remain largely elusive and require further exploration.** In our project, using a CNS myeloid-specific OTULIN knockout model in combination with AD disease models, **we aim to investigate the specific role of OTULIN in the regulation of microglia activation, neuroinflammation and AD pathology.**

3. Results so far

To specifically address the role of OTULIN in microglia in CNS homeostasis and pathology, the van Loo lab generated mice with a 'floxed' *OTULIN* allele [34] and crossed these mice with *Cx3Cr1*-CreErt2 transgenic mice, allowing Cre-mediated gene deletion in myeloid cells following tamoxifen treatment [35] (Figure 2A). CNS-resident macrophage populations including microglia can be targeted using this approach which relies on microglial longevity and its self-renewing capacity [36, 37]. Tamoxifen-induced ablation of OTULIN in mice did not induce any gross abnormalities, however, immunohistochemical analysis using the microglial marker Iba-1 revealed a significant increase in microglia number in the CNS of OTULIN$^{Cx3Cr1\text{-}KO}$ mice compared to control littermates (Figure 2B, unpublished data). Single cell transcriptome analysis of microglia from **OTULIN-deficient mice revealed an altered microglia phenotype revealing** a strong upregulation of type I interferon response genes ('interferon response microglia'-IRM), genes associated with cell proliferation ('cycling and proliferating microglia'-CPM) and genes that have been linked to a **'disease-associated microglia' (DAM) phenotype** involved in inflammatory processes ('activated response microglia'-ARM) [38,39]. In agreement, OTULIN-deficient microglia display a suppressed "homeostatic gene signature", (H0M, H1M and H2M), also reminiscent of microglia in neurodegenerative conditions [38,39] (Figure 2C-D, unpublished data). **These strong preliminary data demonstrate the importance of OTULIN in microglia activation and suggest that defects in proper OTULIN function may contribute to CNS pathology and neurodegeneration**.

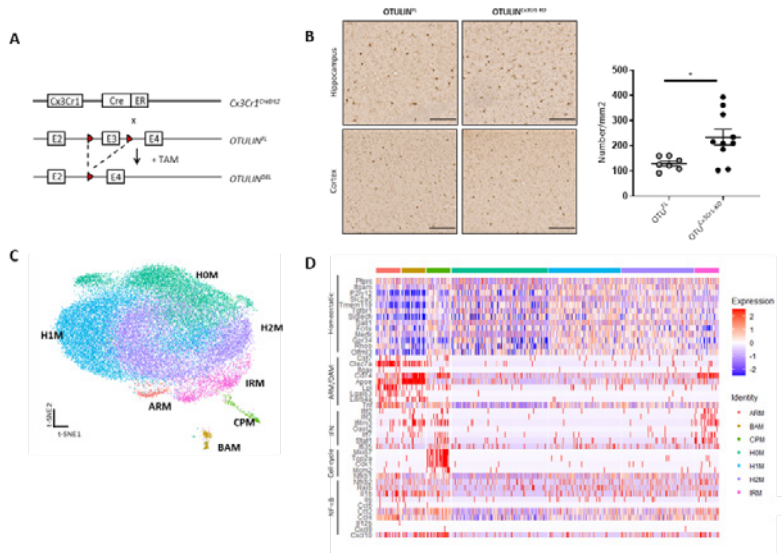

Figure 2 (A) Scheme for the Tam-inducible deletion of OTULIN in CNS-resident myeloid cells. (B) Immunohistochemistry for Iba-1+ microglia in the hippocampus and cerebral cortex of control (OTULIN^{FL}) and OTULIN$^{Cx3Cr1\text{-}KO}$ mice (left), and quantification of the number of Iba-1+ microglia. Each symbol represents one mouse. Data presented as mean ± SEM (right); $p<0.05$ (C) t-SNE plot visualizing 13500 single microglial cells per genotype depicting the separation into clusters. Cells are coloured according to clusters (H0M, H1M and H2M, homeostatic microglia; ARM, activated response microglia; IRM, interferon response microglia; CPM, cycling and proliferating microglia). (D) Heatmap showing clustering analysis of single cells, featuring most variable genes subdivided by cluster.

4. Methodology

To study the importance of OTULIN for microglia activation and AD pathology, OTULIN$^{Cx3Cr1\text{-}KO}$ mice have been crossed with three genetic models of AD : the *AppNL-G-F* knock-in mouse model of β-amyloid-induced neuropathology, the *APP/PS1* knock-in mouse model of β-amyloid-induced neuropathology, and the P301S Tau transgenic mouse model. *APP/PS1* mice ectopically overexpress the KM670/671NL 'Swedish' mutated amyloid precursor protein (APP) concomitant with mutant human PS1 (presenilin-1) in CNS neurons, and develop an early and robust AD pathology [40]. In contrast, *AppNL-G-F* mice express the human Aβ sequence which harbors the Swedisch (KM670/671NL), Beyreuther/Iberian (I716F) and Arctic (E693G) mutations in the *App* gene [41]. These mice develop typical Aβ pathology, neuroinflammation, synaptic defects and memory impairment in an age-dependent manner, most similar to the defects which develop in human AD patients [41]. P301S Tau transgenic mice develop filamentous Tau lesions in association with neuroinflammation, prominent microgliosis and neuron loss [42].

Meanwhile, the respective mouse lines (control OTULIN expressing mice and mice with tamoxifen-inducible OTULIN deficiency in microglia crossed into the *AppNL-G-F, APP/PS1* or P301S Tau AD background) have been generated and are being aged. Disease development in these mice will be evaluated by clinical disease assessment at different ages of the mice (20 weeks, 40 weeks and 60 weeks of age). At endpoint, brain sections will be evaluated for degree of Aβ deposition, Tau hyperphosphorylation, astro- and microgliosis, presence of inflammatory markers and neuronal cell death.

In parallel, we will perform CITE-seq of immune cells obtained from control and OTULIN$^{Cx3Cr1\text{-}KO}$ *AppNL-G-F, APP/PS1* and P301S Tau transgenic brains at young (20 weeks) and older (60 weeks) age. CITE-seq offers the possibility to combine transcriptome-wide gene expression analysis with simultaneous profiling of hundreds of surface protein markers, as previously shown by the Movahedi lab [43]. In-depth analysis of these single-cell RNA profiles will allow us to identify the tissue signals that drive neuroinflammation and AD pathology and help to understand the

molecular interplay between the different cell types (glial cells, neurons, immune cells) during AD development. CITE-Seq data will be complemented with single-cell spatial profiling using the newly introduced Akoya PhenoCycler-Fusion platform.

In the meantime, the Movahedi lab has been optimizing the Akoya Phenocycler-Fusion technology for fixed frozen brain tissue. In short, the Phenocycler-Fusion system is an automated fluidics control unit coupled to a microscope that allows automatic successive rounds of staining on the same tissue slide. To do so, Akoya uses barcoded antibodies and complementary oligonucleotides labeled with fluorophores. In each cycle, up to three oligonucleotides will specifically interact with their corresponding tissue-bound barcoded antibodies, thus allowing imaging of the corresponding antibodies. Afterwards, the imaged reporters will be washed away and new reporters will be added in a new cycle, altogether resulting in the visualization of up to 100 markers in the same tissue slide (Figure 3A).

Given the limited availability of barcoded antibodies for frozen murine brain tissue from commercial vendors, we successfully custom-conjugated several markers relevant for studying neurodegenerative disease and DAMs: GFAP (astrocytes), Iba1 (microglia), Clec7a (DAMs, figure 3B), Lyve-1 (border associated macrophages), ERTR7 (dural fibroblasts) or Nestin (neuronal stem cells). Together with commercially available antibodies, we compiled a 30-marker panel that allows in-depth characterization of different immune populations in the mouse brain, which will be used for disease profiling in *APP/PS1* and P301S mice. However, the first multiplexed immunostaining of frozen murine brain tissue revealed unexpected technical issues such as non-specific (mostly nuclear) and very faint primary staining (figure 3C) together with non-specific background in myelin-rich areas (figure 3D). Extensive troubleshooting allowed us to solve the non-specific primary staining with additional rounds of tissue blocking (Figure 3E) as well as to link the non-specific background in the myelin-rich areas to non-specific reporter binding (Figure 3F), which is reduced but not avoided under additional tissue blocking (Figure 3G). Currently, we are testing several approaches in collaboration with the Technical Service of Akoya to solve this issue as soon as possible. Although we prefer fixed frozen tissue because of its marker versatility and our established in-house experience with the tissue, we are considering FFPE murine brain tissue as a contingency approach if the non-specific reporter binding persists.

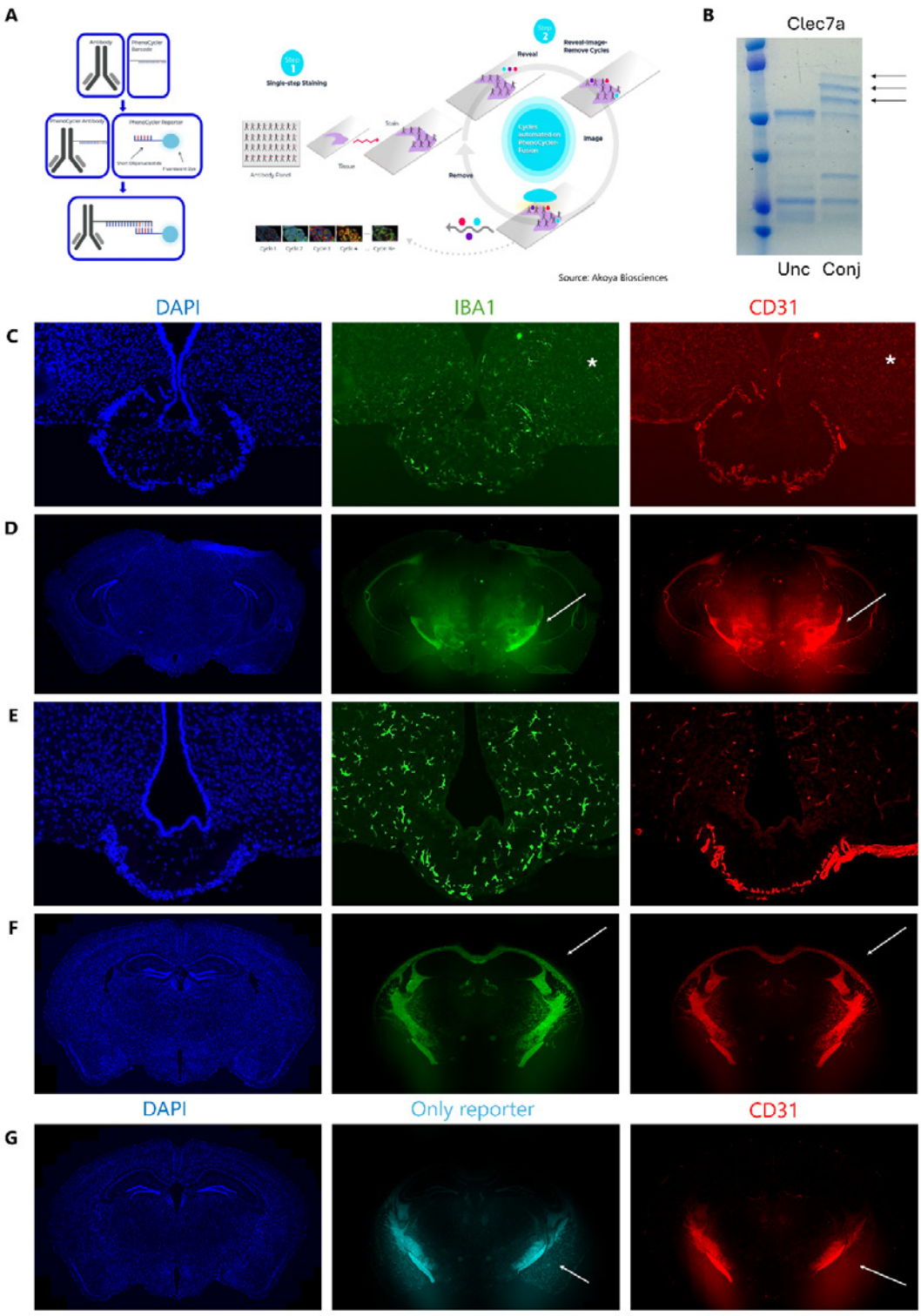

Figure 3: **(A)** Akoya's Phenocycler Fusion technology and workflow. Source: Akoya Biosciences. **(B)** Gel electrophoresis showing the successful conjugation of Clec7a (arrows depict the conjugated bands in the conjugated (Conj) sample while absent in the unconjugated (Unc) one). **(C-D)** First immunostaining of fixed frozen brain tissue using Akoya's Phenocycler Fusion technology. Channels depicting nuclei (DAPI, blue), microglia (IBA1, green) and blood vessels (CD31, red) are shown. (C) focuses in the median eminence region and the white asterisk marks an area with non-specific and faint staining. (D) shows the complete section and the white arrows mark myelin-rich areas showing non-specific staining in the brain parenchyma. **(E)** Regular Immunostaining of fixed frozen brain tissue following additional rounds of blocking. Channels depicting nuclei (DAPI, blue), microglia (IBA1, green) and blood vessels (CD31, red) are shown. **(F)** Immunostaining of fixed frozen brain tissue using Akoya's Phenocycler Fusion technology without primary antibodies, only reporters. Channels depicting nuclei (DAPI, blue), the binding of the corresponding reporter to IBA1 (green) and CD31 (red) are shown. White arrows mark myelin-rich areas showing non-specific staining in the brain parenchyma. **(G)** Immunostaining of fixed frozen brain tissue using Akoya's Phenocycler Fusion technology using only CD31 and a reporter without the corresponding primary. Channels depicting nuclei (DAPI, blue), a reporter without primary (cyan) and blood vessels (CD31, red) are shown. White arrows mark myelin-rich areas showing non-specific staining in the brain parenchyma.

Using *in vivo* mouse gene targeting and disease modelling, we hope to clarify the role of OTULIN in microglia neuroinflammation and AD disease pathology, which will provide new fundamental knowledge helping us to better understand the pathways and molecular mechanisms that control CNS inflammation in the context of AD. This knowledge may have important implications for the development of new therapeutics which may help in the treatment of patients suffering from AD and eventually other neuroinflammatory degenerative pathologies.

5. References

1. Iwai, K. et al. (2014) Linear ubiquitin chains: NF-B signalling, cell death and beyond. Nat. Rev. Mol. Cell Biol. 15, 503–508
2. Clague, M.J. et al. (2019) Breaking the chains: deubiquitylating enzyme specificity begets function. Nat. Rev. Mol. Cell Biol. 20, 338–352
3. Haas, T.L. et al. (2009) Recruitment of the Linear Ubiquitin Chain Assembly Complex Stabilizes the TNF-R1 Signaling Complex and Is Required for TNF-Mediated Gene Induction. Mol. Cell 36, 831–844
4. Gerlach, B. et al. (2011) Linear ubiquitination prevents inflammation and regulates immune signalling. Nature 471, 591
5. Zak, D.E. et al. (2011) Systems analysis identifies an essential role for SHANK-associated RH domain-interacting protein (SHARPIN) in macrophage Toll-like receptor 2 (TLR2) responses. Proc. Natl. Acad. Sci. 108, 11536–11541
6. Damgaard, R.B. et al. (2012) The Ubiquitin Ligase XIAP Recruits LUBAC for NOD2 Signaling in Inflammation and Innate Immunity. Mol. Cell 46, 746–758
7. Rodgers, M.A. et al. (2014) The linear ubiquitin assembly complex (LUBAC) is essential for NLRP3 inflammasome activation. J. Exp. Med. DOI: 10.1084/jem.20132486
8. Kumari, S. et al. (2014) Sharpin prevents skin inflammation by inhibiting TNFR1-induced keratinocyte apoptosis. eLife 3, e03422
9. Rickard, J.A. et al. (2014) TNFR1-dependent cell death drives inflammation in Sharpin-deficient mice. eLife 3, e03464
10. Peltzer, N. et al. (2014) HOIP Deficiency Causes Embryonic Lethality by Aberrant TNFR1-Mediated Endothelial Cell Death. Cell Rep. 9, 153–165
11. Peltzer, N. et al. (2018) LUBAC is essential for embryogenesis by preventing cell death and enabling haematopoiesis. Nature 557, 112–117
12. Taraborrelli, L. et al. (2018) LUBAC prevents lethal dermatitis by inhibiting cell death induced by TNF, TRAIL and CD95L. Nat. Commun. 9, 3910
13. Boisson, B. et al. (2012) Immunodeficiency, autoinflammation and amylopectinosis in humans with inherited HOIL-1 and LUBAC deficiency. Nat. Immunol. 13, 1178–1186
14. Boisson, B. et al. (2015) Human HOIP and LUBAC deficiency underlies autoinflammation, immunodeficiency, amylopectinosis, and lymphangiectasia. J. Exp. Med. 212, 939–951
15. Tokunaga, F. et al. (2011) SHARPIN is a component of the NF-B-activating linear ubiquitin chain assembly complex. Nature 471, 633–636
16. Ikeda, F. et al. (2011) SHARPIN forms a linear ubiquitin ligase complex regulating NF-B activity and apoptosis. Nature 471, 637
17. Zinngrebe, J. et al. (2016) LUBAC deficiency perturbs TLR3 signaling to cause immunodeficiency and autoinflammation. J. Exp. Med. 213, 2671–2689
18. Lork, M. et al. (2017) CYLD, A20 and OTULIN deubiquitinases in NF-B signaling and cell death: so similar, yet so different. Cell Death Differ. 24, 1172–1183
19. Keusekotten, K. et al. (2013) OTULIN Antagonizes LUBAC Signaling by Specifically Hydrolyzing Met1-Linked Polyubiquitin. Cell 153, 1312–1326
20. Rivkin, E. et al. (2013) The linear ubiquitin-specific deubiquitinase gumby regulates angiogenesis. Nature 498, nature12296
21. Zhou, Q. et al. (2016) Biallelic hypomorphic mutations in a linear deubiquitinase define otulipenia, an early-onset autoinflammatory disease. Proc. Natl. Acad. Sci. U. S. A. 113, 10127–10132
22. Damgaard, R.B. et al. (2016) The Deubiquitinase OTULIN Is an Essential Negative Regulator of Inflammation and Autoimmunity. Cell 166, 1215-1230.e20
23. Damgaard, R.B. et al. (2019) OTULIN deficiency in ORAS causes cell type-specific LUBAC degradation, dysregulated TNF signalling and cell death. EMBO Mol. Med. 11, e9324

24. Nabavi, M. et al. (2019) Auto-inflammation in a Patient with a Novel Homozygous OTULIN Mutation. J. Clin. Immunol. 39, 138–141
25. Heger, K. et al. (2018) OTULIN limits cell death and inflammation by deubiquitinating LUBAC. Nature 559, 120–124
26. Xu H, Qin W, Hu X, et al. (2018) Lentivirus-mediated overexpression of OTULIN ameliorates microglia activation and neuroinflammation by depressing the activation of the NF-B signaling pathway in cerebral ischemia/reperfusion rats. J Neuroinflammation.15(1).
27. Voet S, Prinz M, van Loo G. (2019) Microglia in Central Nervous System Inflammation and Multiple Sclerosis Pathology. Trends Mol Med. 25(2):112-123.
28. Bellenguez, C. et al. (2022) New insights into the genetic etiology of Alzheimer's disease and related dementias. Nat. Genet. 54(4):412-436.
29. Heppner, F. L., Ransohoff, R. M. & Becher, B. (2015) Immune attack: the role of inflammation in Alzheimer disease. Nat. Rev. Neurosci. 16, 358-372.
30. Scheltens, P. et al. (2016) Alzheimer's disease. Lancet 388, 505-517.
31. Kaltschmidt, B., Uherek, M., Volk, B., et al. (1997). Transcription factor NF-kappaB is activated in primary neurons by amyloid beta peptides and in neurons surrounding early plaques from patients with Alzheimer disease. Proc. Natl Acad. Sci. USA 94, 2642–2647.
32. Chen, J. et al. (2005) SIRT1 protects against microglia-dependent amyloid-beta toxicity through inhibiting NF-kappaB signaling. J. Biol. Chem. 280, 40364–40374.
33. Wang, C. et al (2022) Microglial NF-B drives tau spreading and toxicity in a mouse model of tauopathy. Nat. Commun. 13(1), 1969.
34. Verboom, L. et al. (2020) OTULIN Prevents Liver Inflammation and Hepatocellular Carcinoma by Inhibiting FADD- and RIPK1 Kinase-Mediated Hepatocyte Apoptosis. Cell Rep. 30, 2237-2247.e621
35. Goldmann T, Wieghofer P, Müller PF, et al. (2013) A new type of microglia gene targeting shows TAK1 to be pivotal in CNS autoimmune inflammation. Nat Neurosci. 16(11):1618-1626.
36. Goldmann T, Wieghofer P, Joana M, et al. (2016) Origin, fate and dynamics of macrophages at central nervous system interfaces. Nat Immunol.17(7):797-805.
37. Van Hove, H., Martens, L., Scheyltjens, I et al. (2019) A single-cell atlas of mouse brain macrophages reveals unique transcriptional identities shaped by ontogeny and tissue environment. Nat. Neurosci., 22, 1021-1035.
38. Sala Frigerio C, Wolfs L, Fattorelli N, et al. (2019) The Major Risk Factors for Alzheimer's Disease: Age, Sex, and Genes Modulate the Microglia Response to Aβ Plaques. Cell Rep. 27(4):1293-1306.e6.
39. Keren-Shaul H, Spinrad A, Weiner A, et al. (2017) A Unique Microglia Type Associated with Restricting Development of Alzheimer's Disease. Cell.169(7):1276-1290.e17.
40. Radde, R., Bolmont, T., Kaeser, S.A., et al. (2006). Abeta42-driven cerebral amyloidosis in transgenic mice reveals early and robust pathology. EMBO Rep 7, 940-946.
41. Saito, T. et al. (2014) Single App knock-in mouse models of Alzheimer's disease. Nat. Neurosci. 17, 661-663.
42. Yoshiyama, Y. et al. (2007) Synapse loss and microglial activation precede tangles in a P301S tauopathy mouse model. Neuron 53, 337-351.
43. Pombo Antunes, A.R., Scheyltjens, I., Lodi, F., et al. (2021) Single-cell profiling of myeloid cells in glioblastoma across species and disease stage reveals macrophage competition and specialization. Nat. Neurosci., 24, 595-610.
44. Browaeys, R., Saelens, W. & Saeys, Y. (2020) NicheNet: modeling intercellular communication by linking ligands to target genes. Nat Methods 17, 159-162.

6. Publications van Loo-Movahedi groups 2023 (acknowledging GSKE support)

– Srinivasan, S*., Kancheva, D*., De Ren, S*., Saito, T*., Jans, M., Boone, F., Vandendriessche, C., Paesmans, I., Maurin, H., Vandenbroucke, R.E., Hoste, E., Voet, S., Scheyltjens, I., Pavie, B., Lippens, S., Schwabenland, M., Prinz, M., Saido, T., Bottelbergs, A+., Movahedi, K+., Lamkanfi, M.+ and **van Loo, G+**. Inflammasome signaling is dispensable for β-amyloid-induced neuropathology in preclinical models of Alzheimer's disease. Frontiers Immunol., in press. (IF : 7.3).

*shared first author
+shared last author

Geneeskundige Stichting Koningin Elisabeth
Fondation Médicale Reine Elisabeth
Königin-Elisabeth-Stiftung für Medizin
Queen Elisabeth Medical Foundation

Progress report of the interuniversity research project of

Prof. dr. Renzo Manusco (UAntwerpen)
Prof. dr. Joris De Wit (KU Leuven)

Dr. Renzo Mancuso (he/him/his) (UAntwerpen)
Group Leader
Laboratory of Microglia and Inflammation in Neurological Disorders (MIND)
VIB-Center for Molecular Neurology (CMN), VIB.

Universiteit Antwerpen-CDE, Parking P4, Gebouw V 0.10
Universiteitsplein 1, B-2610 Antwerpen
T +32 (0) 3 265 25 28

Prof. Joris De Wit (KU Leuven)
Group Leader at VIB-KU Leuven
Center for Brain & Disease Research
Department of Neurosciences
ON5 Herestraat 49 – bus 602
3000 Leuven

Microglia-synapse molecular interactions in neurodegenerative disease (MicroSyn-MIND)

The goal of this project is to identify proteins that play a role in microglia-synapse interactions, and specifically those proteins whose expression is affected in Alzheimer's Disease (AD). We are currently well underway with aim 1, and provide an update on our findings and progress below.

First, a short description of our projects' original aim and strategy. It is unclear what drives AD progression. Genetic risk[1], Amyloid- (A) plaques, neurofibrillary tau tangles, and vascular alterations lead to a loss of neurons and synapses[2–4], followed by the patient's memory, cognition, and grasp on reality. However, A builds up years before cognitive symptoms set-in[5], and is not always followed by neurodegeneration[3]. Microglia prune synapses during development and could be key players in mediating synaptic loss in AD[6]. However, how microglia interact with neurons and synapses, and how AD affects these interactions, is poorly understood. Here, we combine the expertise of two labs to transplant human microglia in a mouse model of AD, perform a deep characterization of human microglia-synapse interactions at the molecular level using split-TurboID proximity labeling, and determine how these interactions are impacted by AD pathology. To address this overall goal, we formulated two main aims:

1. Identify AD-related changes to the microglial-synaptic cell surface interactome.

We are currently proceeding with aim 1. Originally, we intended to use split-TurboID proximity-based labeling (PL) to identify cell surface proteins (CSPs) at microglia-synapse contact sites. Our goal was to use Split-TurboID[7] PL with dual, inactive N- and C-terminal TurboID fragments, which would be expressed on the microglial- and synaptic surfaces. At spots where microglia and synapses interact, TurboID reconstitutes and biotinylates nearby proteins, which we would isolate using streptavidin beads and analyze using mass spectrometry (MS).

Extensive work on aim 1, however, has provided several key insights. The original strategy using **Split-TurboID**, based on published work[7], is not a viable option. We have tested the original published split-TurboID constructs *in vitro*, in various cell types (HEK293T, HMC3, human iPSC-derived microglia), and were not able to replicate the proper expression of the constructs as they are presented in the original publication. Aside from the original construct, we have designed and tested various modifications to the original design to improve expression and functionality, including different promotors (ubiquitin, EF1) and expression cassettes, but none improved functionality of the Split-TurboID system to an acceptable level.

Subsequently, we have adjusted our strategy, and have elected to express the **full TurboID** (non-split) on the microglial outer membrane. *In vivo* expression of full TurboID on the microglial outer membrane will still allow us to target and identify both microglial- and neuronal cell surface proteins that are located at interaction sites. Furthermore, by using full TurboID and a basic lentiviral expression vector, and combining these with specific baits, we have succeeded in targeting not only the outside of outer microglial membrane, but also the inside of the outer membrane, the lysosomal membrane, the endoplasmic reticulum, the cytoplasm, and a suspected key microglial transcription factor. A second benefit of this system is that we can generate iPSC lines

that stably express these constructs, and can be used flexibly. We have confirmed that these constructs are expressed at their target subcellular location within the iPSC-derived microglia, and are currently processing *in vitro* samples for validation with mass spectrometry. These *in vitro* samples will provide a detailed map of the subcellular compartmental proteomes of human *in vitro* microglia, which will serve as a valuable resource to the field in general. In parallel, we have transplanted these "stable" iPSC-derived microglia that express these various constructs, *in vivo* in immunosuppressed WT mice as well as AD model mice. Once these mature to an age where sufficient cortical A build-up has occurred (6 months of age), we will activate the TurboID through biotin injections, and attempt to extract protein for mass spectrometry analysis, like we originally intended in our proposal. Once these data are in, we can proceed with the analysis as intended, to identify cell-type specific cell surface proteins, and infer potential ligand-receptor pairs of interest. From the differential expression of these proteins, comparing microglia from healthy WT mice compared to our AD model mice, we should be able to infer potential targets to study in aim 2.

2. Identify microglial cell surface proteins that mediate excessive synaptic loss in AD.

The original strategy for aim 2 still stands. The goal here is to determine which of the identified proteins are involved in the excessive microglial synaptic phagocytosis observed in AD[8], using a CRISPR/Cas9 knockout screen[9]. Together with a sgRNA library (and a negative control condition with a mock sgRNA library), we add Cas9 enzyme to facilitate gene-editing. GFP-labeled isolated synaptosomes will then be added to cultured microglia to monitor phagocytic uptake of fluorescent synaptic material, allowing us to group phagocytic- and non-phagocytic microglia using fluorescence-activated cell sorting (FACS). We will monitor the control condition for negative effects of the knockout screen, in the form of cell death and the expression of inflammatory markers. We will sequence the genomic DNA to identify the gene knockouts that most strongly affect synaptosome phagocytosis, and use this as proxy for a potential role in the synaptic loss seen in AD.

We remain confident that we can fulfil aim 2 and provide the key datapoints that we originally promised. However, completion of objective #1 has required more time than we originally estimated, specifically to generate and optimize the use of various TurboID constructs, *in vivo*. To account for the fact that we will likely have less time to complete objective #3 than we originally estimated, we have already prepared a robust back up plan that would allow us to reduce the timeline and still deliver the key data. Specifically, instead of applying a large general CRISPR-screen to filter targets, we will select several key targets from the bioinformatics analysis in aim 1, which we will directly be knockout in iPSCs using CRISPR-Cas9. These, we will use to generate iPSC-derived microglia, which we will use in a synaptosome phagocytosis assay, to test the effects of the knockouts on the microglial capacity to phagocytose synapses. We will activate this alternative strategy if necessary, and we are confident this should provide an answer to our original question, of which key receptors-ligands affect the communication between microglia and synapses.

We hope this update provides sufficient information and are happy to answer any additional questions you might have regarding the progress of our project.

1. Bellenguez, C. *et al.* Large meta-analysis of genome-wide association studies expands knowledge of the genetic etiology of Alzheimer's disease and highlights potential translational opportunities. *medRxiv* 17, 10 (2020).
2. Mucke, L. & Selkoe, D. J. Neurotoxicity of amyloid -protein: Synaptic and network dysfunction. *Cold Spring Harb Perspect Med* 2, (2012).
3. Serrano-Pozo, A., Frosch, M. P., Masliah, E. & Hyman, B. T. Neuropathological alterations in Alzheimer disease. *Cold Spring Harb Perspect Med* 1, 1–24 (2011).
4. Mecca, A. P. *et al.* In vivo measurement of widespread synaptic loss in Alzheimer's disease with SV2A PET. *Alzheimer's and Dementia* 16, 974–982 (2020).
5. Mintun, M. A. *et al.* PIB in a nondemented population. *Neurology* 67, 446 LP – 452 (2006).
6. Werneburg, S. *et al.* Targeted Complement Inhibition at Synapses Prevents Microglial Synaptic Engulfment and Synapse Loss in Demyelinating Disease. *Immunity* 52, 167-182.e7 (2020).
7. Cho, K. F. *et al.* Proximity labeling in mammalian cells with TurboID and split-TurboID. *Nat Protoc* 15, 3971–3999 (2020).
8. Tzioras, M. *et al.* Altered synaptic ingestion by human microglia in Alzheimer's disease. *bioRxiv* (2019) doi:10.1101/795930.
9. Pluvinage, J. V. *et al.* CD22 blockade restores homeostatic microglial phagocytosis in ageing brains. *Nature* 568, 187–192 (2019).

Geneeskundige Stichting Koningin Elisabeth
Fondation Médicale Reine Elisabeth
Königin-Elisabeth-Stiftung für Medizin
Queen Elisabeth Medical Foundation

Progress report of the interuniversity research project of

Prof. dr. Karelle Leroy (ULB)
Prof. dr. Laurence Ris (UMONS)
Prof. dr. Kristel Sleegers (UAntwerpen)

Prof. dr. Karelle Leroy (ULB)
Assistant professor, ULB
Head of the Alzheimer
research group in the
laboratory of Histology
https://alzheimer-research.medecine.ulb.be

Prof. dr. Laurence Ris (UMONS)
Department of
Neurosciences

Prof. dr. Kristel Sleegers (UAntwerpen)
Dr Sleegers Kristel
Professor, UA
Head of the Complex Genetics of
Alzheimer's disease group at
VIB – UA Center for Molecular
Neurology
https://uantwerpen.vib.be/group/kristelSleegers

Involvement of diabetes and antidiabetic treatment on tau pathology propagation

1. State of the art:

The etiopathogeny of Alzheimer's disease (AD) is relatively unknown as only 5 % of AD cases can be explained by familial mutations. However, several risk factors have been described in AD. Among them, epidemiological studies showed a clear link between AD and type 2 diabetes mellitus (T2D), a medical condition frequent in industrial but also in developing countries. Indeed, T2D increases the risk of AD by at least twice. Moreover, a study has shown that T2D in elderly population with mild cognitive impairment influences the progression to dementia. The features of T2D are high levels of blood glucose (hyperglycemia) and insulin resistance. Most of insulin is produced by beta-pancreatic cells and is transported to the brain by crossing the blood brain barrier. Insulin binds to the insulin receptors that are present in neurons triggering the brain insulin signalling pathway by activating AKT resulting in the inhibition of GSK3beta. Interestingly, a recent study has shown that beta-pancreatic cells and neurons shared common mechanisms such as the ability to express tau proteins or shared causal genes or pathways. Under conditions of insulin resistance, GSK3beta is converted to its active form by the decrease of the inhibitory serine 9 phosphorylation therefore conducting to the degradation of IRS1 (Insulin receptor 1) leading to insulin pathway disturbances. As the activity of GSK3beta is increased in AD and is involved in tau phosphorylation in this disease, this kinase could be the possible link between these two pathologies. Indeed, an abnormal tau phosphorylation appears in beta-pancreatic cells of T2D patients and in the brain of T2D mouse models (High fat diet model) in which the brain insulin signaling pathway is impaired. The possibility that targeting AD and T2D through antidiabetic agents may constitute an approach to treat defective brain insulin signaling, cognitive impairment and neurodegeneration.

2. Aim of the study

This study will be devoted to the analysis of the role played by **metabolic disturbances observed in type 2 diabetes mellitus (T2D)** but also the **effect of an anti-diabetic treatment** on tau seeding and on the **propagation of tau pathology in Alzheimer's models** mice fed with high fat diet (HFD) to mimic T2D. Those experiments will be conducted in mice models in which tau seeding will be induced by intracerebral injection of PHF-tau proteins from AD brain.

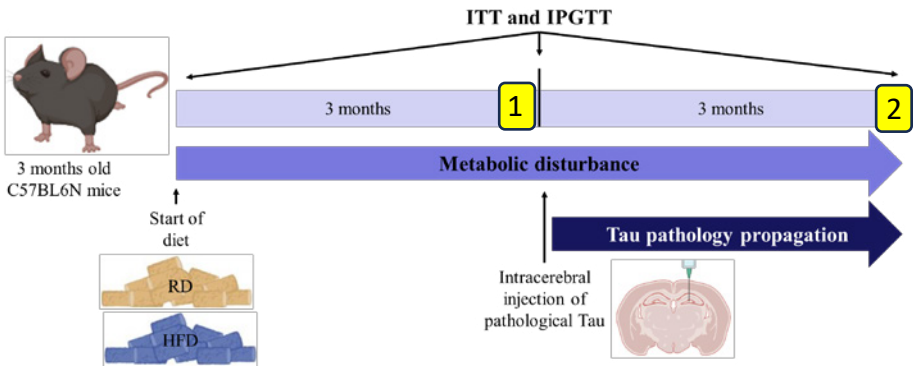

3. Results

3.1. Validation of the effect of HFD to mimic diabetic disturbances (1 In the timeline).

WT mice

3 months-old WT mice were fed with a regular diet (RD) or a High-fat diet (HFD) (60 % lipids) for 3 months. At the end of this period, metabolic parameters have been analysed with ITT, IPGTT and insulin quantification to confirm the effect of HFD to generate metabolic disturbances.

Protocol for the Insulin Tolerance Test (ITT). (BioRender)

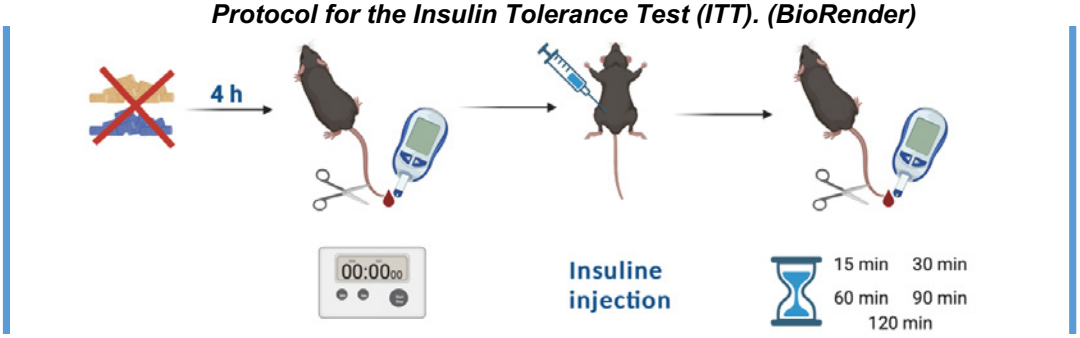

For the ITT, 4-hour–fasted mice were given insulin IP (0.75 mU Actrapid/g weight, Novo Nordisk), and glycemia was measured before and after 15, 30, 60, 90, and 120 minutes. Insulin sensitivity was calculated as the AOC from 0 to 30 minutes in the ITT. We observed an insulin resistance in mice fed with HFD compared to mice fed with RD (multiple t-tests, ***=p< 0.001; ****=p<0.0001).

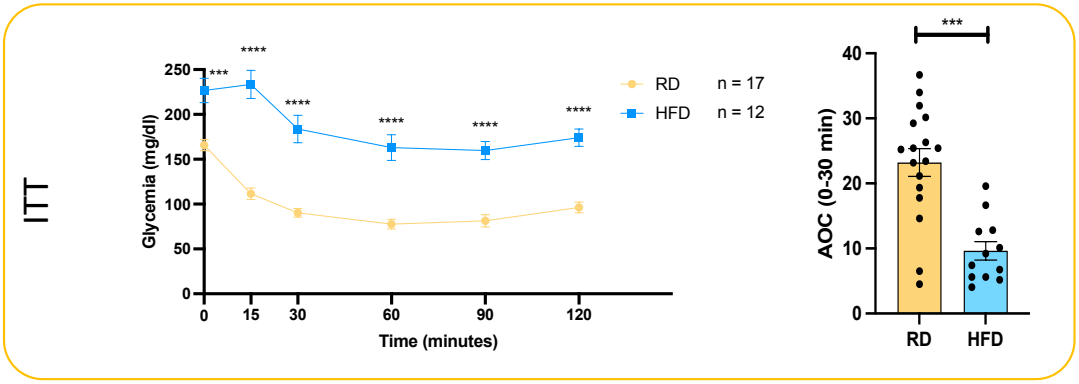

Protocol for the intraperitoneal Glucose Tolerance Test (IPGTT) and insulin quantification. (Biorender).

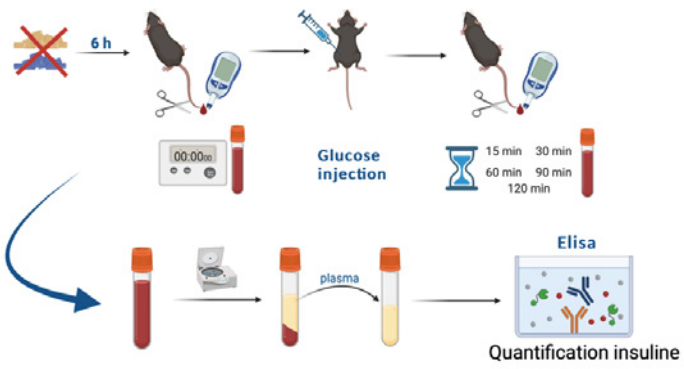

For the IPGTT, after a 6-hour fast, 2 mg glucose/g body weight was administered and glycemia measured (glucometer Accu-Chek Aviva Nano, Roche) before and after 15, 30, 60, 90, and 120 minutes. Blood was collected from the tail vein and plasma insulin measured using ultrasensitive mouse insulin ELISA (Crystal Chem). Glucose tolerance was calculated as the AUC from 0 to 120 minutes. We observed an intolerance to glucose and hyperinsulinemia in mice fed with HFD compared to mice fed with RD (multiple t-tests, ***=p< 0.001; ****=p<0.0001).

(multiple t-tests, ***=p< 0.001; ****=p<0.0001).

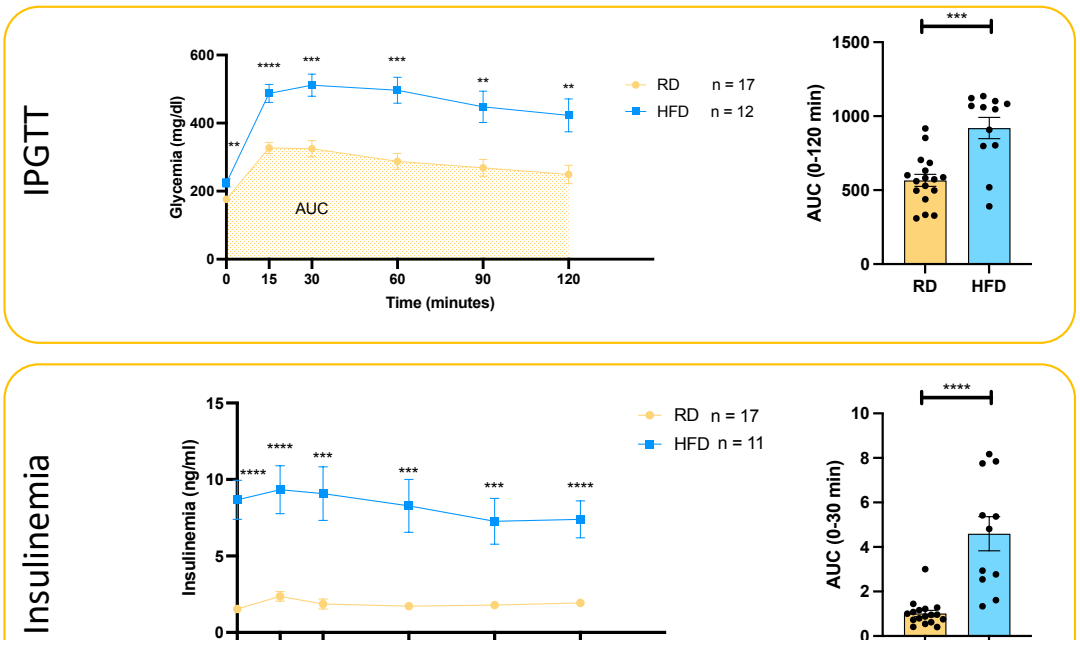

MAPTKI mice

We also performed metabolic tests before and after 3 months od diet in MAPT KI mice in which the entire human tau gene was inserted at the murine tau gene locus. In a previous study, it has been shown in these mice that there is no overexpression of tau proteins and the relative ratio for 3R/4R tau is close to that of human brain. Surprisingly, we observed significant metabolic differences in MAPTKI mice compared WT mice. Moreover, after 3 months of RD or HFD, MAPTKI mice do not develop metabolic disturbances as in WT mice indicating that these mice are not a good model to study the effect of HFD (and the HFD-induced metabolic disturbances) on tau pathology propagation. Indeed, these mice showed abnormal insulin sensitivity, glucose intolerance and hypoinsulinemia before starting the diet and we are not able to induce glucose intolerance in HFD mice after 3 months of diet. We decided to discard this mouse model and to continue our study on WT mice.

Before Diet

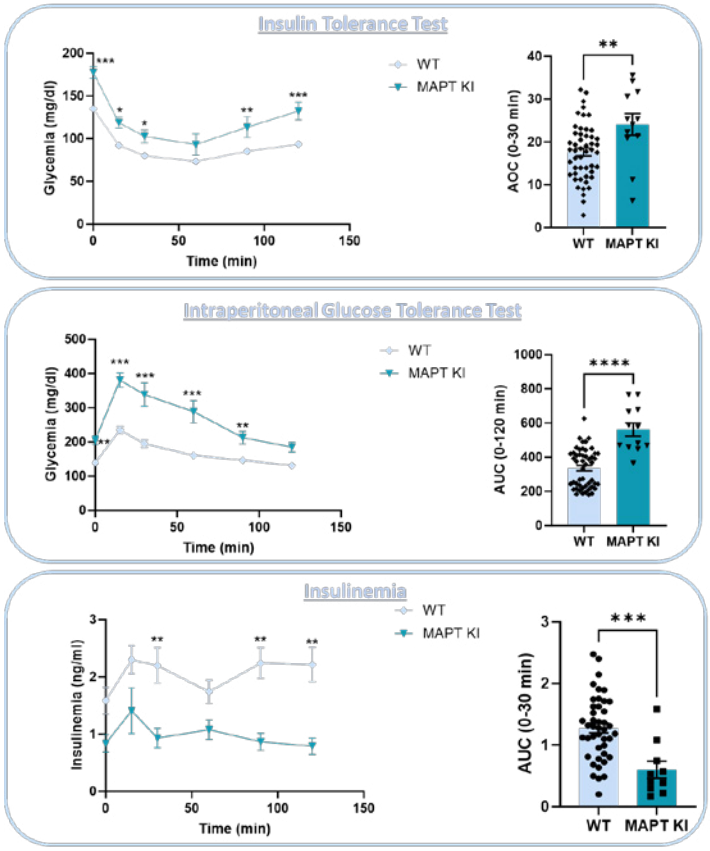

After 3 months of diet

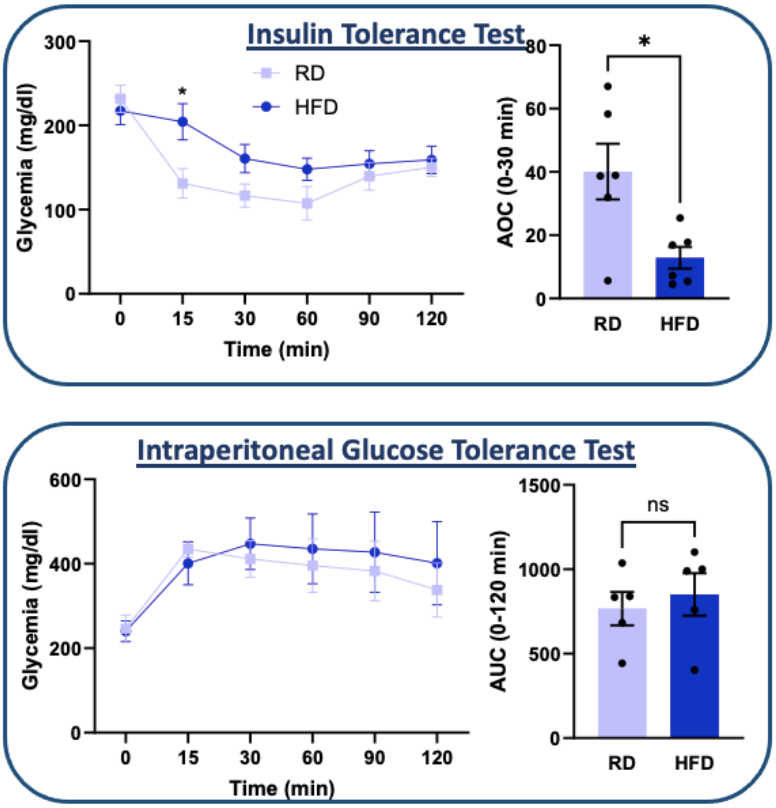

3.2. Characterization of sarkosyl fractions

Temporal cortex from AD subject was homogenized and treated with sarkosyl to solubilize proteins. Pathological tau proteins forming paired helical filaments (PHF) were resistant to sarkosyl treatment and can still be detected by western blotting in the AD sarkosyl fractions (lane AD in A). This AD sarkosyl fraction has been immunodepleted for tau with anti-total tau antibody and did not show tau expression (lane ADID in A). The seeding ability of these sarkosyl fractions have been evaluated in a bioassay based on the formation of a FRET signal when tau is seeded. We observed a FRET signal when cells were treated with AD sarkosyl fraction (B) but not with ADID sarkosyl fraction (C). These results confirmed that AD sarkosyl fraction can be used in vivo to induce tau pathology propagation and that ADID sarkosyl fraction can be used as a control.

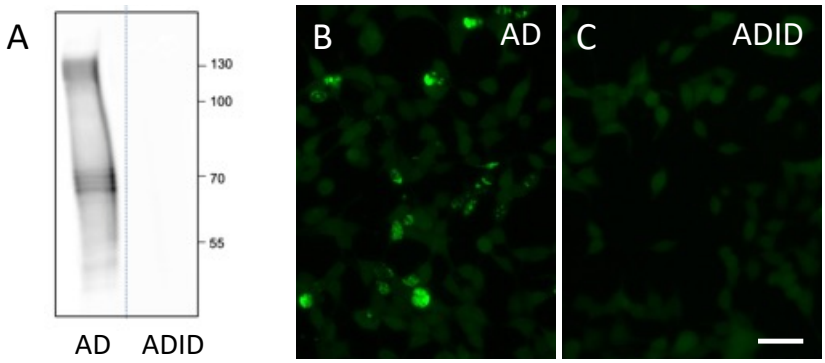

A: Western blotting of sarkosyl fractions with anti-tau antibody.
B-C: Cells treated with AD sarkosyl fractions showed a FRET signal (B) but not when they are treated with immunodepleted fraction.

3.3. Analysis of metabolic disturbances after the intracerebral injection of pathological tau (2 in the timeline).

3 months after the intracerebral injection of AD sarkosyl fraction containing pathological tau or ADID sarkosyl fraction, we analyzed the metabolic parameters in RD and HFD fed mice. As observed before the intracerebral injection, HFD fed mice showed insulin resistance, intolerance to glucose and hyperinsulinemia but, surprisingly, mice fed with RD and injected with AD sarkosyl fraction developed insulin resistance.

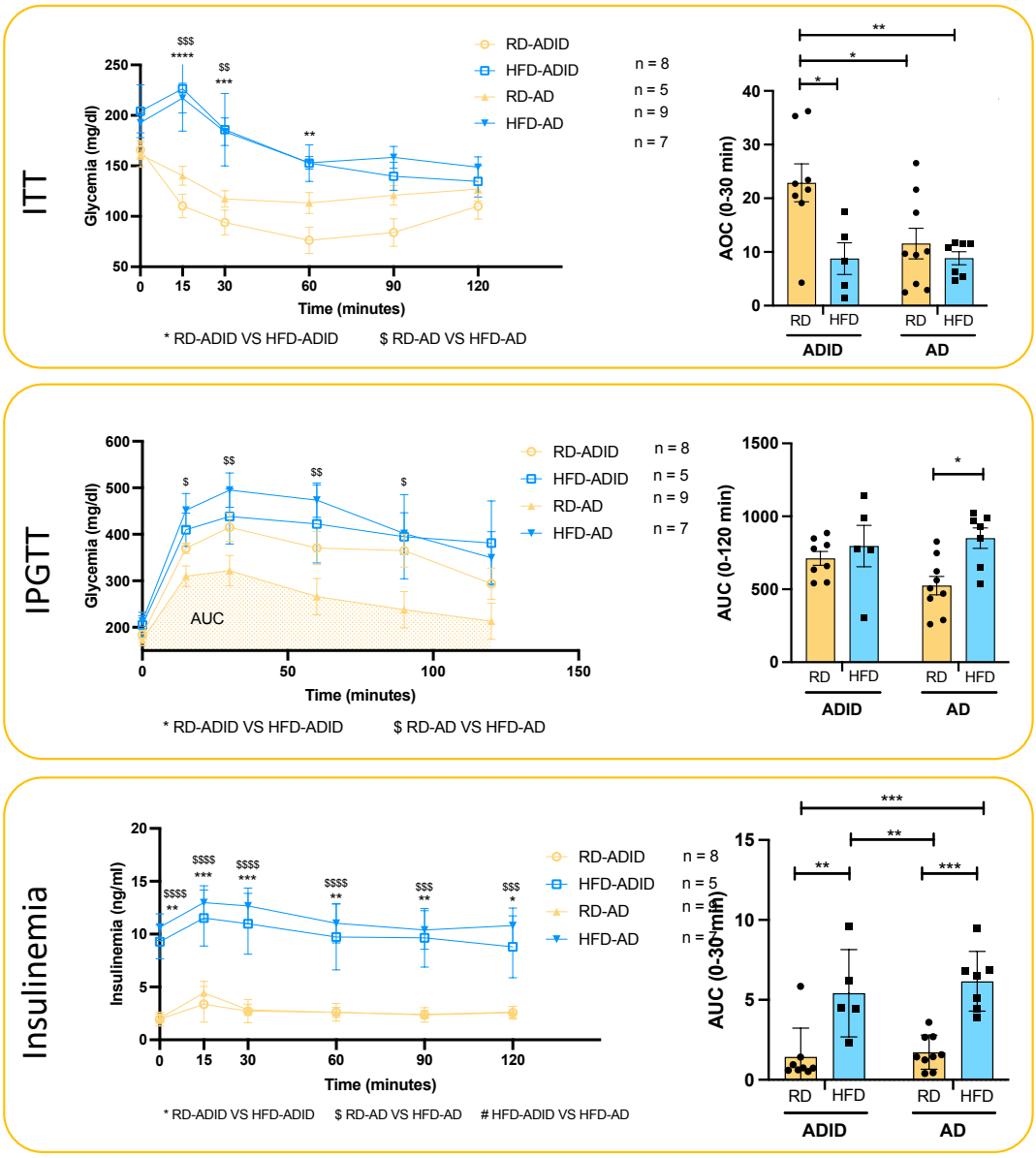

3.4. Analysis of tau pathology propagation

As expected, we didn't observe tau pathology in mice intracerebrally injected with ADID sarkosyl fractions and fed with RD (A) or HFD (B). In AD injected mice, mice developed a tau pathology as shown with the AT8 antibody (recognizing tau phosphorylated on Ser 202/thr 205) in C and D. There is a tendancy to an increased tau pathology in HFD fed mice (D) compared to RD fed mice (C) but it is not significant (E) probably due to the low number of mice analyzed (3 mice per conditions). The anteroposterior propagation of tau pathology is increased in HFD-AD compared to RD-AD mice but it is not significant probably for the same reason. Another group of mice are currently fed with RD and HFD and will be injected with AD and ADID in march 2024.

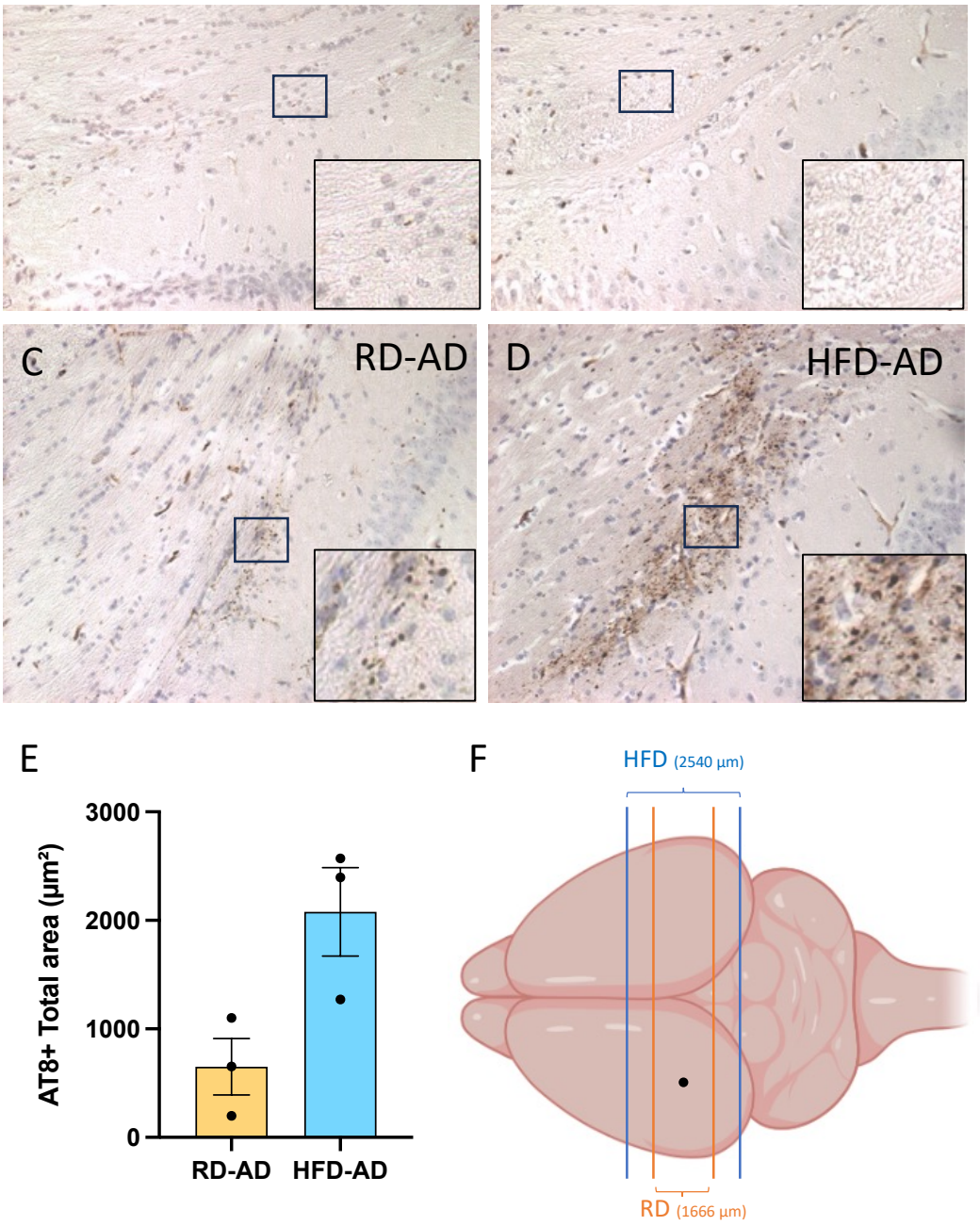

We performed immunolabellings with PHF1 antibody which recognizes tau proteins phosphorylated on Ser 396/404 (A and B). This epitope appeared after the AT8 epitope during

We performed immunolabellings with PHF1 antibody which recognizes tau proteins phosphorylated on Ser 396/404 (A and B). This epitope appeared after the AT8 epitope during the formation of tau pathology. The results are similar to those observed with AT8 antibody : tendancy to an increase of tau pathology propagation (C and D).

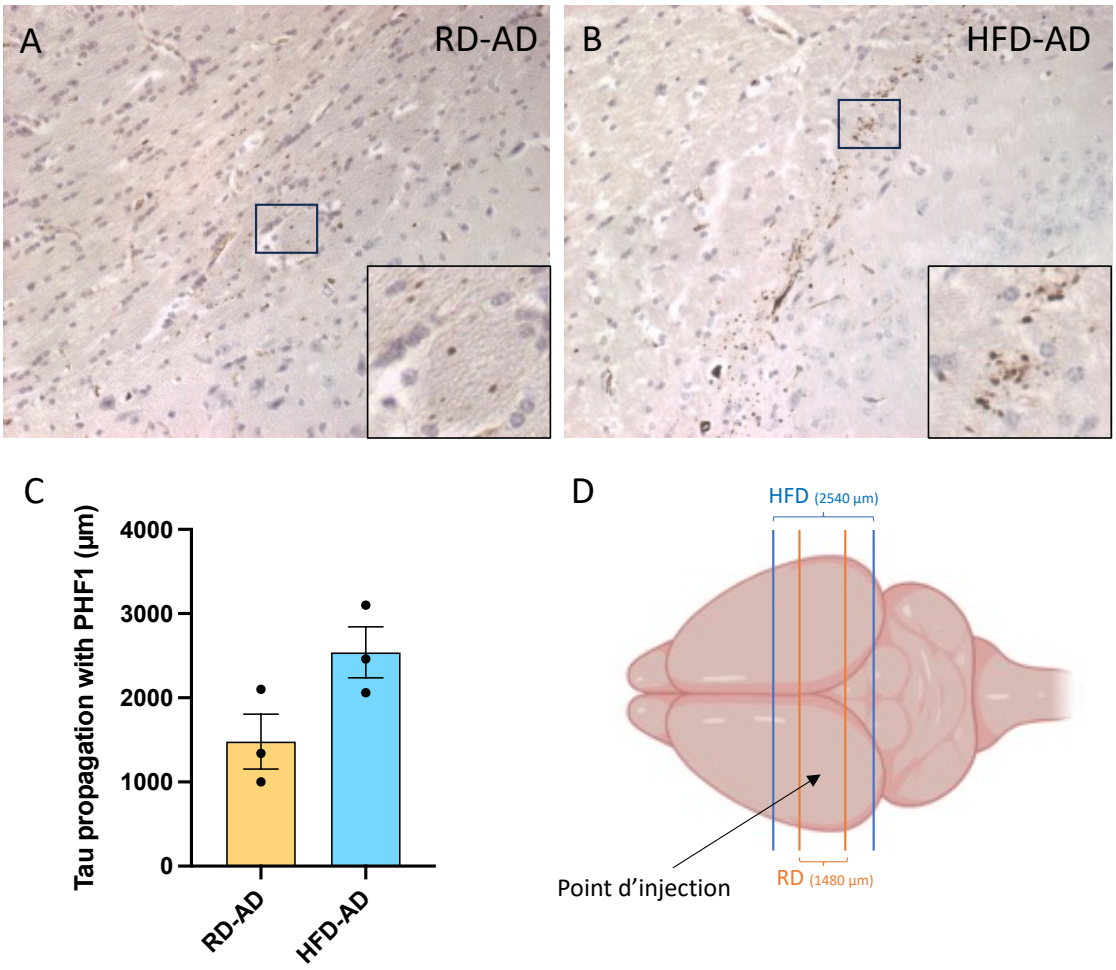

3.5. Analysis of tau pathology maturation

We also performed immunolabellings with T22 antibody which oligomers of tau proteins (A and B), with MC1 antibody which recognizes tai proteins in an abnormal conformation. A Gallyas staining was also performed to detect tau aggregates (C and D). In our injected model, we do not detect MC1 positives structures but with T22 and Gallyas, we observe a tendancy to an increase of tau pathology maturation (E and F).

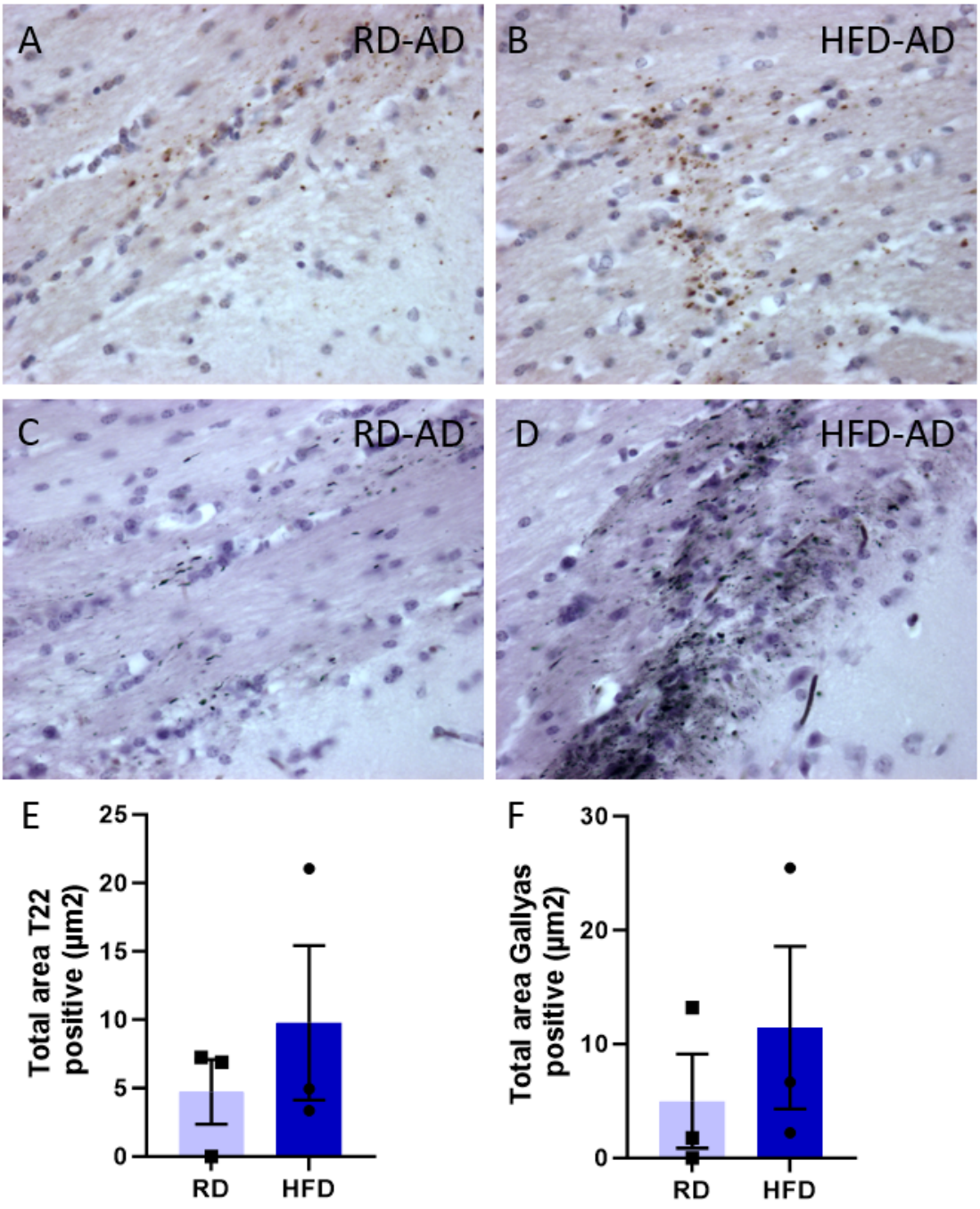

3.6. Analysis of the neuroinflammation

Because inflammation is a common risk factor for AD and T2D, we wanted to analyze the neuroinflammation and the neuronal loss after 3 months of diet and before the stereotaxic injection. For this, we performed immunolabellings with GFAP antibody which recognizes activated astrocytes (A and B) and with NeuN antibody which recognizes neurons nucleus (C and D). We did not observe a significant astrocyte activation or a neuronal loss (E and F) after 3 months of diet.

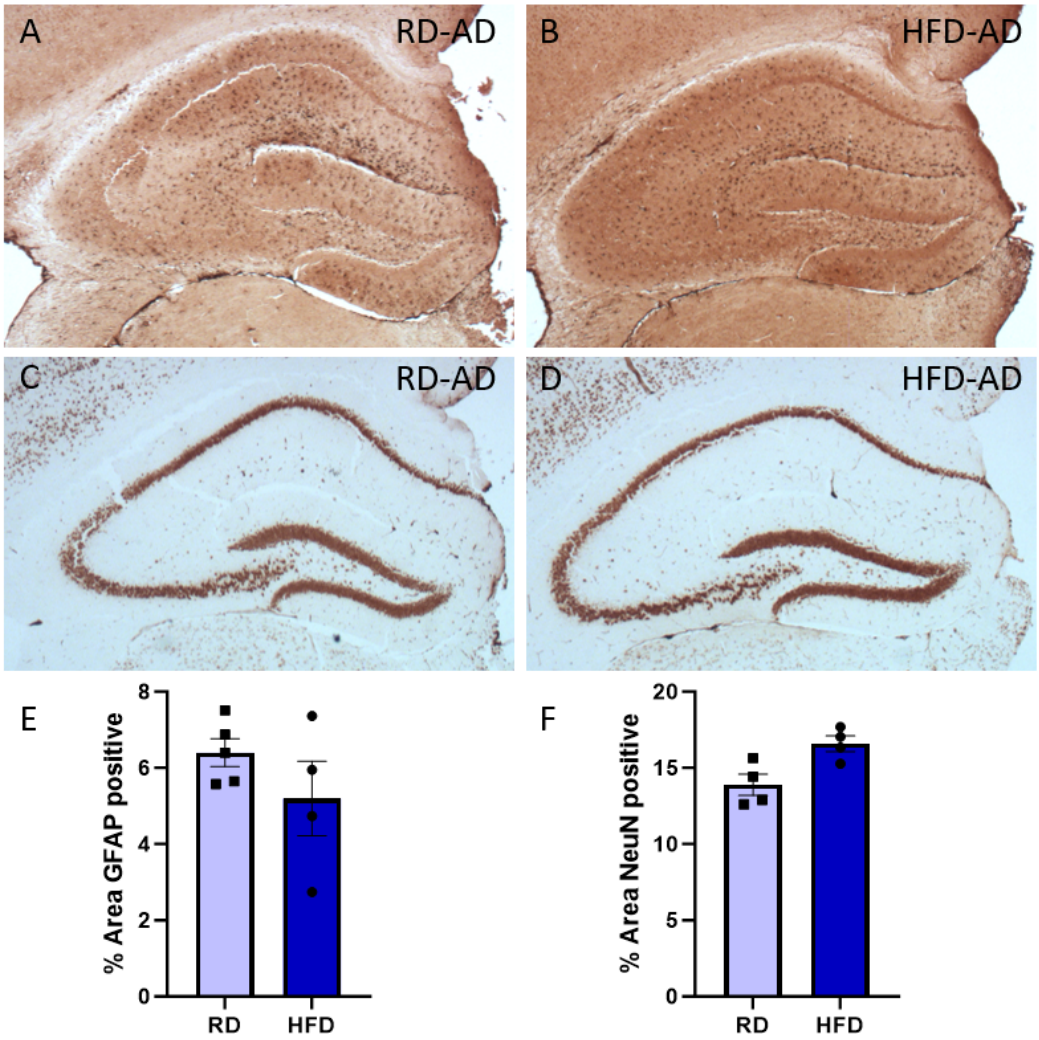

4. Conclusions and perspectives:

Metabolic tests showed that WT mice is a good model to study the effect of metabolic disturbances induced by high-fat diet on tau pathology propagation whereas MAPTKI mice can not be used. Sarkosyl fractions induced a tau pathology which was increased when the mice are fed with HFD compared to RD but it is not significant. New samples will be obtained in the following months to finish the analysis of tau pathology propagation and to start the transcriptomic analysis and electrophysiological experiments according to the calendar below. To study the effect of anti-diabetic treatment on tau pathology, Exendin will be replaced by liraglutide as exendin is no more used in humans. Treatments with liraglutide will start in July.

	Histology	Electrophysiology	Sequencing
RD-AD	5	5	10
RD-ADID	3	5	10
HFD-AD	5	5	10
HFD-ADID	4	5	10
Samples availability	07/2024	07/2024 11/2024 04/2025	

Geneeskundige Stichting Koningin Elisabeth
Fondation Médicale Reine Elisabeth
Königin-Elisabeth-Stiftung für Medizin
Queen Elisabeth Medical Foundation

Progress report of the interuniversity research project of

Prof. dr. Sarah Weckhuysen (UAntwerpen)
Prof. dr. Bjorn Menten (UGent)

Prof. dr. Sarah Weckhuysen, MD, PhD (UAntwerpen)
Applied&Translational Neurogenomics Group VIB-UAntwerp
Center for Molecular Neurology UAntwerp CDE
Parking P4, Building V Universiteitsplein 1, 2610 Antwerpen
Belgium
uantwerpen.vib.be

Neurology Department
Antwerp University Hospital
Drie Eikenstraat 655
2650 Edegem
www.UZA.be/neurologie

Prof. dr. ir. Björn Menten (UGent)
Lab for Genome Research, Center for Medical Genetics, Department of biomolecular Medicine (UGent)
Associate professor (Faculty of Medicine and Health Sciences, UGent)
Lab supervisor Cytogenomics Laboratory Center for Medical Genetics, UZGent
Lab address: UZ Gent, Medical Research Building 1 (entrance 34),
Corneel Heymanslaan 10
9000 Gent

Detection of somatic mutations and disease-defining methylation patterns in brain tissue and cerebrospinal fluid of patients with non-acquired focal epilepsy

1. Background

The majority of non-acquired focal epilepsies (NAFE) have a presumed genetic etiology. However, the current yield of diagnostic genetic testing in affected patients is very low. This diagnostic gap is an important barrier to the broader use of gene-targeted therapies. Increasing evidence from resected brain tissue of individuals with NAFE points towards an important role of pathogenic somatic variants and methylation abnormalities. Most NAFE patients however do not undergo brain surgery, and the lack of brain tissue precludes a genetic diagnosis. In this project, we aim to prove that cell-free DNA (cfDNA) circulating in cerebrospinal fluid (CSF) and serum of patients with NAFE can be used to bridge this diagnostic gap. 1) We will apply a deep- sequencing protocol to detect novel somatic variants and 2) pathognomonic methylation patterns in cfDNA from CSF. 3) We use nanopore sequencing on native cfDNA to both identify somatic copy number changes. We prioritize patients who undergo epilepsy surgery for our study cohort, to validate the detected somatic and epigenetic changes in paired brain tissue. By identifying the genetic etiology and disease methylation profiles from cfDNA, we can improve diagnostic yield and clinical decision-making in this severely affected population.
Over the past year, we have made significant in-roads in sample collection, sample preparation, and library preparation.

2. Summary of achievements

2.1. Sample Acquisition

In the past year, we have doubled our sample cohort to 30 surgical samples and 8 controls. As such we have achieved 2/3 of our desired $n = 45$ surgical cohort, and we anticipate exceeding this goal within the 2024 calendar year. The patients encompass a wide spectrum of focal epilepsy types, including FCD1 and FCD2 subtypes, temporal lope epilepsy, hippocampal sclerosis, and more.

Component	FCD	FE	Control	Total
Brain + CSF/Serum	12	18	0	30
CSF/Serum only	0	0	8	8

Table 1. Tissue Collection (31.21.23) FE: focal epilepsy other than FCD

All samples were collected in UZ Leuven, where an ethical approval for this project was already in place at the time of the project approval. In the last year, we have prepared the documents for the ethical committee agreement for the multicenter study including not only UZ Leuven but also UZ Antwerp/UA, UZ Gent/UGent, Hopital Erasme/ULB, Saint Luc/UCL. The 80 pages long dossier is submitted, and we hope to receive a positive feedback soon, so that sampling from other centers can be initiated.

2.2. Brain Sectioning and Staining

We receive brain tissue from epileptogenic and non-epileptogenic zones. These tissue samples are residual from those sent for pathological diagnosis. As such, the exact pathology will not clearly correlate in location between the diagnostic and research samples. In order to maximize identification of low frequency somatic mutations, it is essential to select the portion of tissue that has the most dysmorphic features consistent with the underlying diagnosis. To do this, we manually cryosection the brain tissue with intermittent histopathological staining to identify the best portions of the tissue to use for sequencing. We have completed this for all 30 surgical samples, including non-epileptogenic zones. Our local sectioning and staining corroborate the original pathological diagnoses thus far.

For each sample, we have selected the appropriate tissue section for extraction of DNA for sequencing. In the next week we'll start performing the library preparation for shipment of the samples (DNA from tissue, and cfDNA from CSF and serum) for sequencing for both the mosaic mutation analysis, as methylation analysis.

2.3. Library Preparation

- Targeted deep sequencing

  We have constructed the first set of sequencing libraries, with additional libraries to follow. To maximize sequencing cost-efficiency, we perform library preparation in batches of 16, with the goal of submitting a full set of libraries once we have acquired at least 32 surgical samples and 8 non-surgical samples (full use of a NovoSeq). The final two samples will be obtained in the coming months. As sequencing is the largest component of consumable costs, it is important to achieve a sufficient quantity of samples, which was almost achievable within the first calendar year, but could not be realized due to a lower-than-expected number of appropriate surgical cases at UZ Leuven alone. Nonetheless, the pace of library preparation and sequencing will further accelerate after approval of our submitted multicenter ethical committee agreement.

- Shallow whole genome nanopore sequencing

  At the same time we've been optimizing protocols to perform shallow whole genome sequencing with Oxford Nanopore Technologies (ONT) on cfDNA. This protocol is especially challenging as the techniques are optimized for very long DNA fragments in contrast to the very short cfDNA fragments. By performing ONT sequencing we can however interrogate both the methylome as copy number aberrations.

2.4. Further Planning

In the next months, we plan to start the analysis of the data generated from the first batch of samples from UZ Leuven. Once the ethical committee agreement for the multicenter study involving the other academic hospitals is received, we expect to start receiving samples also from these centers and exponentially increase our samples size. With this additional cohort we will be able to validate our results and/or increase our power for signal detection.

Geneeskundige Stichting Koningin Elisabeth
Fondation Médicale Reine Elisabeth
Königin-Elisabeth-Stiftung für Medizin
Queen Elisabeth Medical Foundation

Progress report of the interuniversity research project of

Prof. dr. Ann Massie (VUB)
Prof. dr. Lutgarde Arckens (KU Leuven)

Prof. dr. Ann Massie (VUB)
Vrije Universiteit Brussel
Center for Neurosciences
Laarbeeklaan 103
1090 Brussels
ann.massie@vub.be
T 02 477 45 02

Prof. dr. Lutgarde Arckens (KU Leuven)
Katholieke Universiteit Leuven
Department of Biology
Naamsestraat 59
3000 Leuven
lut.arckens@kuleuven.be
T 016 32 39 51

The xCT$^{-/-}$ killifish to validate the potential of system x_c^- as therapeutic target in Parkinson's disease

1. Summary

Targeting the cystine/glutamate antiporter system x_c^- has great potential in the treatment of age-related neurological diseases. We recently showed lifespan extension with reduced age-related *inflammaging*, and preservation of hippocampal function and memory in aged mice lacking the specific xCT subunit of this antiporter. xCT deletion in mice also results in protection of the nigrostriatal dopaminergic pathway against toxin-induced degeneration (as a model for Parkinson's disease; PD). This protection, however, seems to be age- and toxin-dependent. Access to a spontaneous -and therefore toxin free- PD animal model is of paramount importance to create indisputable evidence about the power of system x_c^- inhibitors for the treatment of PD patients.
The African turquoise killifish *Nothobranchius furzeri* is the shortest-living vertebrate laboratory species showing all cellular and molecular hallmarks of human aging, including spontaneous α-synuclein accumulation with degeneration of dopaminergic neurons. These features make the killifish an excellent model to study PD, as there is no need for toxins to induce dopaminergic neurodegeneration. In this project, we will therefore generate a transgenic killifish with a deletion of xCT. We will characterize the aging process of this fish and study its susceptibility to spontaneous age-related neurodegeneration. The severity of neurodegeneration will be correlated to changes in the activity of the most important transporters that regulate extracellular glutamate levels (as a first indication of excitotoxicity), to neuroinflammation, to metabolic changes in the killifish brain, and to function of the ubiquitin-proteasome system.
This study will not only allow us to confirm or refute the therapeutic potential of targeting system x_c^- in PD but will also generate a valuable tool to further investigate the function of system x_c^- in aging and age-related (neurological) diseases.

2. Project outline

State-of-the-art: The ***cystine/glutamate antiporter system x_c^-***, with xCT (Slc7a11) as specific subunit, imports cystine in exchange for glutamate and is the major source of extracellular glutamate in several mouse brain regions, including hippocampus and striatum[1,2]. In the central nervous system (CNS), system x_c^- is mainly expressed on astrocytes[3,4]. Glutamate released by system x_c^- is believed to be confined to the extrasynaptic space. This glutamate can act on metabotropic glutamate receptors to modulate glutamatergic transmission, and on ionotropic NMDA receptors thereby decreasing the threshold for glutamate toxicity (excitotoxicity). System x_c^- also regulates (neuro)inflammation: genetic xCT deletion (xCT$^{-/-}$) in mice[5] results in a faster normalization of peripheral cytokine levels after i.p. injection of a sublethal dose of bacterial lipopolysaccharide (LPS) -thereby reducing LPS-induced sickness and neuroinflammation[6]- and favors the anti- over the pro-inflammatory microglial phenotype in pathological conditions[7,8]. Accordingly, absence of system x_c^- is protective in neurological disorders that are characterized by excitotoxicity and (neuro)inflammation[1,2,9–11]. The therapeutic potential of targeting system x_c^- in age-related neurological disorders has however been questioned, as the oxidative shift in the plasma cystine/cysteine ratio of xCT$^{-/-}$ mice was suggested to accelerate the aging process[5]. We therefore studied the effect of genetic deletion of xCT on aging and indeed unveiled system x_c^- as a regulator of life- and healthspan[12]. Contrary to the expectations, however, mice with a genetic

deletion of xCT showed a significant lifespan extension, while preserving their hippocampal function and spatial memory[12]. Possible underlying mechanisms include attenuated *inflammaging* as well as metabolic changes at the level of the aged xCT$^{-/-}$ brain, including reduced levels of N6-carboxymethyllysine[12], an advanced glycation end product (AGE) that has been linked to cognitive decline and neurodegenerative disorders[13].
Glutamate toxicity and neuroinflammation are central to Parkinson's disease (PD) pathogenesis, and an accumulation of AGE levels has been linked to oxidative stress and α-synuclein (α-syn) aggregation in PD[14,15]. Given the effect of system x_c^- deficiency on these pathogenic mechanisms, we validated the therapeutic potential of targeting system x_c^- in PD, by comparing the impact of three different toxin-based PD models between young-adult and aged xCT$^{-/-}$ and xCT$^{+/+}$ mice[2,11]. Although we obtained very promising results, we remain somehow inconclusive. Whereas both young-adult and aged xCT$^{-/-}$ mice were protected against neurodegeneration induced by intrastriatal 6-hydroxydopamine injection[2], the dopaminergic neurons of only aged (and not adult) xCT$^{-/-}$ mice were protected against lactacystin (inhibitor of the ubiquitin proteasome system (UPS); intranigral injection)-induced degeneration, and neither young-adult nor aged xCT$^{-/-}$ mice showed reduced susceptibility in the chronic, progressive 1-methyl-4-phenyl-1,2,3,6-tetrahydropyridine (MPTP) model[11].

<u>Objectives</u>: With this project we aim at developing a novel short-lived vertebrate model with spontaneous age-related degeneration of dopaminergic neurons that will allow us to unambiguously -and independent of PD-inducing toxins- reinforce or refute the potential of system x_c^- as therapeutic target in PD and to study the mechanisms underlying the anticipated neuroprotection.
To reach our ***overarching goal***, i.e. reinforcing the validity of system x_c^- inhibition as a therapeutic target in PD, we defined four objectives:
The ***first objective*** is to create and validate an xCT$^{-/-}$ African turquoise killifish.
The ***second objective*** is to investigate whether the beneficial effects on lifespan and general health, that we observed in aged xCT$^{-/-}$ mice, can be replicated in aged xCT$^{-/-}$ killifish.
The ***third objective*** is to study the effect of xCT deletion on the spontaneous age-related α-syn accumulation and dopaminergic neurodegeneration in the killifish brain.
The ***fourth objective*** is to investigate how xCT deletion affects the age-related pathogenic mechanisms that underlie neurodegenerative disorders, in the fast-aging killifish.

3. Workplan *(results obtained in 2023 are in italic):*

3.1. Workpackage 1 (WP1): Generation and validation of an xCT$^{-/-}$ killifish

xCT is expressed in the killifish[16], showing a 73-75% DNA sequence homology with mouse and human xCT, and we have preliminary findings supporting the presence of system x_c^- activity in synaptosomes that were prepared from adult and aged killifish brains. In this WP we are generating a xCT$^{-/-}$ killifish that allows time-efficient and in-depth investigation of the molecular mechanisms of aging and spontaneous age-related neurodegeneration that are affected by system x_c^- and could underlie our promising observations -both in the context of aging and in PD- in mice[2,11,12].

*To induce **xCT deletion** by a CRISPR-Cas9 strategy, proven to be efficient in N. furzeri[17,18], the Cas9-sgRNA complex targeting slc7a11 is injected into the one-cell stage of killifish embryos, that are grown to adulthood. The knockout is confirmed on genomic DNA extracted from the caudal fin, followed by sequencing of the targeted region. After extensive training of our new PhD student for the injection of fish embryos, she obtained a heterozygous male fish. However, we lost this fish due*

to breeding issues (not related to the genotype) before he could fertilize eggs. We therefore started to inject new embryos. As the success rate to obtain heterozygous fish is too low, we are currently exploring possible alternative strategies to obtain a genetic deletion of xCT.

3.2. WP2: Characterization of the general health status and aging process of the xCT$^{-/-}$ killifish

We previously observed that xCT deletion results in lifespan extension without deterioration of general health status and with preservation of spatial memory in aged mice[12]. In this WP, we will evaluate whether these findings can be generalized to *N. furzeri* by comparing life- and healthspan of xCT$^{+/+}$ and xCT$^{-/-}$ killifish. The use of this short-lived small vertebrate will allow a longitudinal study including several life stages within six months.

While generating a xCT$^{-/-}$ killifish, we have been optimizing the behavioral test battery and a strategy for detailed analysis of longitudinal age-dependent changes in locomotor function in wildtype (WT) killifish. We used the open field and the novel tank diving test to study killifish locomotion, exploration-related behavior, and behavioral changes over their adult lifespan. The characterization of this behavioral baseline is important for future experiments in our xCT$^{-/-}$ fish. Fish were tested from the age of 6 weeks to the age of 24 weeks, and measurements were performed every 3 weeks. In the open field test, we found an increase in the time spent in the center zone from 18 weeks onward, which indicates altered exploration behavior. Upon aging, the fish also showed an increased immobility frequency and duration. In addition, after the age of 15 weeks, their locomotion decreased. In the novel tank diving test, we did not observe this aging effect on locomotion or exploration. Killifish spent around 80% of their time in the bottom half of the tank. We could not observe habituation effects, indicating slow habituation to novel environments. Moreover, we observed that killifish showed homebase behavior in both tests. These homebases are mostly located near the edges of the open field test and at the bottom of the novel tank diving test. Altogether, in the open field test, the largest impact of aging on locomotion and exploration was observed beyond the age of 15 weeks. In the novel tank diving test, no effect of age was found. Therefore, to test the effects of xCT-related interventions on the aging process, the open field test is ideally suited. The novel tank test is better suited to test possible effect on anxiety as there is no confounding effect of aging in this readout. Whether the preference to spend time at the bottom of the tank truly reflects anxiety still needs to be confirmed with proven anxiolytic drugs though. These data have been published (Mariën et al, 2024, Frontiers in Behavioral Neuroscience).

3.3. WP3: Validation of the protective effect of xCT deletion on the spontaneous age-related α-synuclein accumulation and dopaminergic neurodegeneration in the killifish brain

The neuroprotective effects of xCT deletion in mouse models for PD were shown to be age- and toxin/model-dependent[2,11]. We will therefore use the xCT$^{-/-}$ killifish to investigate how the absence of system x_c^- affects the occurrence and extent of spontaneous degeneration of dopaminergic neurons and the accumulation of α-syn, as was observed previously in WT killifish brain[19].

We have been optimizing the protocol to detect the presence of Aβ plaques and tauopathy in the aged WT killifish brain, using both dot blots and immunofluorescent stainings.

3.4. WP4: Identification of the mechanisms underlying the anticipated neuroprotective effect of xCT deletion in the aged killifish brain

Multiple mechanisms that can underlie the neuroprotective potential of genetic xCT deletion have been identified in the mouse brain. Using the xCT$^{-/-}$ killifish we will investigate how xCT deletion affects the (age-related) pathogenic mechanisms described below and correlate them

to the degree of neurodegeneration throughout the lifespan.
(WP4a) *Glutamate transporters: This WP was not initiated yet.*
(WP4b) *(Neuro)Inflammation: For this WP all methods are already optimized on WT fish (immunocytochemistry for L-Plastin; Hybridization Chain Reaction for APOEB; RT-qPCR for inflammatory marker genes il6, il8, il10 sirt, il1β, tnf, csfr1a)*
(WP4c) *Metabolic changes: This WP has not been initiated yet.*
(WP4d) *The ubiquitin-proteasome system: While generating the xCT$^{-/-}$ killifish, we familiarized ourselves with the techniques that are needed to study the ubiquitin-proteasome system (mRNA and protein levels, activity assays), using mouse samples.*

To conclude, although we do not have a xCT$^{-/-}$ killifish yet, we are ready to efficiently start the analyses proposed in our application, as soon as we have the transgenic fish.

4. References (own references are in bold)

1. **De Bundel, D. *et al.* Loss of system x_c^- does not induce oxidative stress but decreases extracellular glutamate in hippocampus and influences spatial working memory and limbic seizure susceptibility. *Journal of Neuroscience* 31, 5792–5803 (2011).**
2. **Massie, A. *et al.* Dopaminergic neurons of system x_c^-deficient mice are highly protected against 6 hydroxydopamineinduced toxicity. *The FASEB Journal* 25, 1359–1369 (2011).**
3. **Ottestad-Hansen, S. *et al.* The cystine-glutamate exchanger (xCT, Slc7a11) is expressed in significant concentrations in a subpopulation of astrocytes in the mouse brain. *Glia* 66, 951–970 (2018).**
4. Batiuk, M. Y. *et al.* Identification of region-specific astrocyte subtypes at single cell resolution. *Nature Communications* **11**, 1220 (2020).
5. Sato, H. *et al.* Redox imbalance in cystine/glutamate transporter-deficient mice. *Journal of Biological Chemistry* **280**, 37423–37429 (2005).
6. **Albertini, G. *et al.* Genetic deletion of xCT attenuates peripheral and central inflammation and mitigates LPS-induced sickness and depressive-like behavior in mice. *Glia* 66, 1845–1861 (2018).**
7. Mesci, P. *et al.* System xC- is a mediator of microglial function and its deletion slows symptoms in amyotrophic lateral sclerosis mice. *Brain* **138**, 53–68 (2015).
8. **Sprimont, L. *et al.* Cystine–glutamate antiporter deletion accelerates motor recovery and improves histological outcomes following spinal cord injury in mice. *Scientific Reports* 11, 12227 (2021).**
9. **Massie, A., Boillée, S., Hewett, S., Knackstedt, L. & Lewerenz, J. Main path and byways: Non-vesicular glutamate release by system x_c^- as an important modifier of glutamatergic neurotransmission. *Journal of Neurochemistry* 135, 1062–1079 (2015).**
10. **Leclercq, K. *et al.* Anticonvulsant and antiepileptogenic effects of system xc− inactivation in chronic epilepsy models. *Epilepsia* 60, 1412–1423 (2019).**
11. **Bentea, E. *et al.* Aged xCT-Deficient Mice Are Less Susceptible for Lactacystin-, but Not 1-Methyl-4-Phenyl-1,2,3,6- Tetrahydropyridine-, Induced Degeneration of the Nigrostriatal Pathway. *Frontiers in Cellular Neuroscience* 15, 796635 (2021).**
12. **Verbruggen, L. *et al.* Lifespan extension with preservation of hippocampal function in aged system xc- –deficient male mice. *Molecular Psychiatry* 27, 2355-2368 (2022).**
13. Akhter, F. *et al.* High Dietary Advanced Glycation End Products Impair Mitochondrial and Cognitive Function. *Journal of Alzheimer's Disease* **76**, 165–178 (2020).
14. Padmaraju, V., Bhaskar, J. J., Prasada Rao, U. J. S., Salimath, P. v. & Rao, K. S. Role of advanced glycation on aggregation and DNA binding properties of -synuclein. *Journal of Alzheimer's Disease* **24**, 211–221 (2011).
15. Li, J., Liu, D., Sun, L., Lu, Y. & Zhang, Z. Advanced glycation end products and neurodegenerative diseases: Mechanisms and perspective. *Journal of the Neurological Sciences* 317, 1–5 (2012).
16. Baumgart, M. *et al.* RNA-seq of the aging brain in the short-lived fish N. furzeri – conserved pathways and novel genes associated with neurogenesis. *Aging Cell* **13**, 965–974 (2014).
17. Harel, I. *et al.* A platform for rapid exploration of aging and diseases in a naturally short-lived vertebrate. *Cell* **160**, 1013–1026 (2015).
18. Harel, I., Valenzano, D. R. & Brunet, A. Efficient genome engineering approaches for the short-lived African turquoise killifish. *Nature Protocols* **11**, 2010–2028 (2016).
19. Matsui, H., Kenmochi, N. & Namikawa, K. Age- and -Synuclein-Dependent Degeneration of Dopamine and Noradrenaline Neurons in the Annual Killifish Nothobranchius furzeri. *Cell Rep* **26**, 1727-1733.e6 (2019).

Geneeskundige Stichting Koningin Elisabeth
Fondation Médicale Reine Elisabeth
Königin-Elisabeth-Stiftung für Medizin
Queen Elisabeth Medical Foundation

Universitaire onderzoeksprojecten 2023-2025 gefinancierd door de G.S.K.E.

Projets de recherche universitaire 2023-2025 subventionnés par la F.M.R.E.

University research projects 2023-2025 funded by the Q.E.M.F.

Universiteiten met onderzoeksprogramma's die gesteund worden door de G.S.K.E.

Universités ayant des programmes de recherche subventionnés par la F.M.R.E.

Universities having research programs supported by the Q.E.M.F.

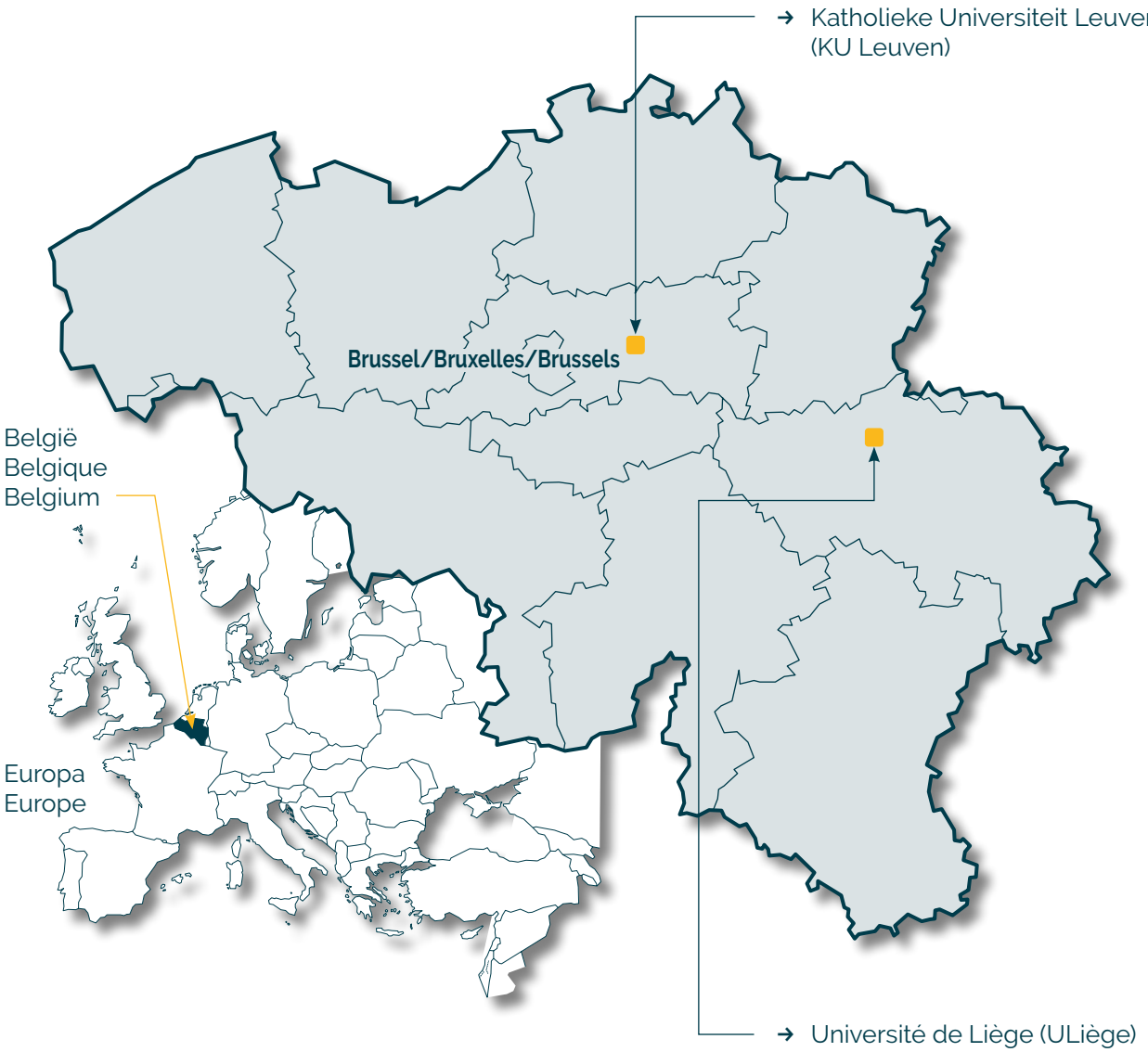

Universitaire onderzoeksprojecten 2023-2025 gefinancierd door de G.S.K.E.

Projets de recherche universitaire 2023-2025 subventionnés par la F.M.R.E.

University research projects 2023-2025 funded by the Q.E.M.F.

KU Leuven

Prof. dr. Bart De Strooper (VIB)
A vicious Aβ oligomers-dependent neuron-microglia cycle fuels Alzheimer's Disease

Prof. dr. Pierre Vanderhaeghen (VIB)
Deciphering the mechanisms underlying neurogenesis defects in mitochondrial diseases

Prof. dr. Veerle Baekelandt
The role of LRRK2 in the peripheral immune system and gut-to-brain spreading of alpha-synuclein pathology in Parkinson's disease

Prof. dr. Thomas Voets
Unraveling the etiology of TRPM3-dependent neurodevelopmental disorders

ULiège

Prof. dr. Pierre Maquet
Quantitative MRI at 7 Tesla addresses ten questions about brain small vessel diseases

Geneeskundige Stichting Koningin Elisabeth
Fondation Médicale Reine Elisabeth
Königin-Elisabeth-Stiftung für Medizin
Queen Elisabeth Medical Foundation

Progress report of the university research project of

Prof. dr. Bart De Strooper
Katholieke Universiteit Leuven
(KU Leuven-VIB)

Prof. dr. Bart De Strooper (KU Leuven-VIB)
VIB Center for Brain and Disease Research
Herestraat 49
3000 Leuven
Belgium
T +32 495 77 10 44
Bart.Destrooper@vib.be

A vicious Aβ oligomers-dependent neuron-microglia cycle fuels Alzheimer's Disease

INTERIM Scientific Progress Report 2023 – A vicious Aβ oligomers-dependent neuron-microglia cycle fuels Alzheimer's Disease (Bart De Strooper)

The overall aim of this project is to dissect how microglia-neuron interactions are affected by the accumulation of soluble Aβ species in Alzheimer's Disease and the effect of anti-Aβ antibodies on the neuroimmune crosstalk.

- **Aim 1: to study how neurons communicate with microglia in early AD, and address the question whether this is sufficient to induce their CRM state in response to soluble Aβ**

  Findings: Our hypothesis is that soluble Aβ influence microglial functions by causing hyperactivity of neurons (a very early sign of disease in patients and in our model[1]). To validate this hypothesis, we will manipulate neuronal activity and neuron-to-glia communication and study the consequences on microglial motility and their transcriptional state. No major progresses have been made on this work package as we encountered some issues with the brightness of the GFP reporter in the human microglia (needed to study their motility by 2P imaging) that we are currently troubleshooting. We are thinking to alternatives; for instance, we could tag H9 cells with m-Cherry or m-Ruby. We are also considering the possibility of conducting certain experiments in mouse microglia to obtain initial results and insights, before further troubleshooting the challenges we have been facing with human microglia. Furthermore, as we do not need a fluorescent reporter for studying whether manipulation of neuronal activity and neuron-to-glia communication alters microglial transcriptional states (i.e., CRM), we are now giving priority to those experiments.

- **Aim 2: to examine whether microglia and their response to soluble Aβ affect neuronal and synaptic function**

  Findings: Previous studies pointed to a causal involvement of microglia in the neurotoxic effects of soluble Aβ. Nonetheless, other evidence suggests that soluble Aβ neurotoxicity is neuronal cell autonomous. To increase insights in this unresolved issue, we started assessing the neurotoxic and synaptotoxic effects of soluble Aβ in mice depleted of microglia. Our preliminary data shows that pharmacological depletion of microglia in mice significantly attenuates the neurotoxicity (i.e., decreased NeuN expression) induced by Aβ aggregates in the medial prefrontal cortex. Furthermore, we compared the synaptic density in the medial prefrontal cortex of mice depleted of microglia and controls injected icv with soluble Aβ or scrambled peptide. Although soluble Aβ induces a significant synaptotoxicity in control mice, we could not detect a significant difference induced by the absence of microglia.

  Even though synaptic density is a good indicator of neuronal functions, we decided to further characterize the functional impact of soluble Aβ in mice depleted of microglia in acute slices collected from mice depleted of microglia. We collected acute hippocampal slices which were incubated with soluble Aβ or scrambled peptide, and placed onto a multielectrode array (MEA 2100, Multichannel Systems). Field excitatory postsynaptic potentials (fEPSPs) were recorded from Schaffer collateral–CA1 synapses by stimulating and recording from the appropriate electrodes. For LTP induction, we applied three high-frequency trains (100 stimuli; 100 Hz) with 5-min intervals. Subsequently, post-LTP fEPSPs were measured every 5 min for 55 min. The incubation with soluble Aβ significantly decreased post-LTP fEPSPs in presence of microglia, but the effects are attenuated by the absence of microglia. Furthermore, we performed 2P imaging to assess neuronal Ca2+ activity after local administration of soluble Aβ or scrambled peptide. To visualize the activity of CA1 neurons by 2P imaging, we performed local application (bolus loading with a micropipette) of the dye Cal-520. The aim here was to

reproduce the neuronal hyperactivity reported by Zott and colleagues[2], and study whether microglial depletion could rescue this phenotype. Preliminary observations indicated that – in our hands – Aβ application induces calcium overload rather than hyperactivity. Interestingly, the Aβ-induced calcium overload was significantly rescued by microglia depletion. This preliminary data needs further validation because Cal-520 is not a ratiometric dye. We will therefore confirm the calcium overload with a ratiometric fluorescent dye (i.e., FURA2/FURA8), whose emission is directly correlated to the amount of intracellular calcium (vs non-ratiometric dyes, where a relative change in fluorescence intensity is only indicative of a change in calcium). Overall, our preliminary data suggests that microglia are necessary transducers of Aβ neurotoxicity.

- **Aim 3: to assess the impact of anti-Aβ immunotherapy on microglia and neurons**
  Findings**:** There are now four anti-Aβ antibodies that have shown moderate positive effects in clinical trials, i.e., they are able to remove amyloid plaques; however, their clinical benefits are still under debate and it is unclear how they modulate the pathological response in AD. We have obtained from the patent literature the primary sequences of four antibodies used in clinical trials: Lecanemab (reacting with Aβ protofibrils), Aducanumab and Gantenerumab (targeting both soluble Aβ oligomers and plaques), and Donanemab (targeting Aβ plaques). We ordered their synthesis in the company, Genscript, supported by our collaborator Prof. Maarten Dewilde, who is an expert in antibodies synthesis. We already evaluated their binding to Aβ by ELISA and Dot Blot and our results consistently showed that Lecanemab and Gantenerumab have a high affinity to aggregated Aβ, whereas the profile seems worse for Aducanumab. Donanemab does not bind to the aggregated Aβ42 generated in the lab, which is in line with its specificity to pyroglutamate domain found only in dense core plaques. We also performed immunohistochemistry to see if these antibodies can bind to Aβ in AppNL-G-F mice, and we could only detect binding with Lecanemab. Together with the promising data reported for Lecanemab[3], and its high specificity for soluble Aβ, our data convinced us to start performing the experiments listed in WP3.1 and WP3.2 with Lecanemab. Furthermore, as we wanted to obtain preliminary data on this topic as soon as possible in order to wrap up a publication by the end of the year, we started the Lecanemab treatment in mice transplanted with human microglia only (rather than mice transplanted with both human microglia and neurons). After treating our xenotransplanted mice for 8 weeks, we can detect a significant decrease in plaque load compared to mice treated with a control IgG1. Furthermore, our preliminary data show that Lecanemab ameliorates not only Aβ pathology, but also the dystrophic neurons and synaptic loss around the plaques, as well as the cognitive impairment observed in AppNL-G-F mice. We also performed single-cell RNA sequencing of the Lecanemab treated microglia, which shows an enrichment of DAM state and related genes. This data was also confirmed at the protein level. Finally, we performed an *in vivo* phagocytosis assay, which indicates that Lecanemab-treated microglia are actively phagocyting Aβ in the brain of these mice. Overall, we are in the process of establishing the impact of anti-Aβ immunotherapy upon microglia in a highly humanized context to provide real insight into the working mechanisms of this first potential disease modifying therapy for AD. Notably, while treating the mice with Lecanemab, we also noticed that this antibody increases mortality rate in female mice. We are currently further investigating what could be underlying this phenotype and whether this could be linked with the side effects observed in patients.

– *1. Calafate, S. et al. Early alterations in the MCH system link aberrant neuronal activity and sleep disturbances in a mouse model of Alzheimer's disease. Nat Neurosci 26, 1021–1031 (2023). 2. Zott, B. et al. A vicious cycle of β amyloid–dependent neuronal hyperactivation. Science 365, 559–565 (2019).*
– *3. van Dyck, C. H. et al. Lecanemab in Early Alzheimer's Disease. N Engl J Med NEJMoa2212948 (2022) doi:10.1056/NEJMoa2212948.*

1. Publications that mention funding from GSKE over the last two years

- Balusu, S., Horré, K., Thrupp, N., Craessaerts, K., Snellinx, A., Serneels, L., T'Syen, D., Chrysidou, I., Arranz, A. M., Sierksma, A., Simrén, J., Karikari, T. K., Zetterberg, H., Chen, W.-T., Thal, D. R., Salta, E., Fiers, M., & De Strooper, B. (2023). MEG3 activates necroptosis in human neuron xenografts modeling Alzheimer's disease**.** ***Science*** *(New York, N.Y.)*, *381*(6663), 1176–1182. https://doi.org/10.1126/science.abp9556
- Balusu, S., Praschberger, R., Lauwers, E., De Strooper, B., & Verstreken, P. (2023). Neurodegeneration cell per cell. *Neuron*, *111*(6), 767–786. https://doi.org/10.1016/j.neuron.2023.01.016
- Calafate, S., Özturan, G., Thrupp, N., Vanderlinden, J., Santa-Marinha, L., Morais-Ribeiro, R., Ruggiero, A., Bozic, I., Rusterholz, T., Lorente-Echeverría, B., Dias, M., Chen, W.-T., Fiers, M., Lu, A., Vlaeminck, I., Creemers, E., Craessaerts, K., Vandenbempt, J., van Boekholdt, L., … de Wit, J. (2023). Early alterations in the MCH system link aberrant neuronal activity and sleep disturbances in a mouse model of Alzheimer's disease. ***Nature Neuroscience***, *26*(6), 1021–1031. https://doi.org/10.1038/s41593-023-01325-4
- Hardy, J., de Strooper, B., & Escott-Price, V. (2022). Diabetes and Alzheimer's disease: shared genetic susceptibility? *The Lancet. Neurology*, *21*(11), 962–964. https://doi.org/10.1016/S1474-4422(22)00395-7
- Hou, P., Zielonka, M., Serneels, L., Martinez-Muriana, A., Fattorelli, N., Wolfs, L., Poovathingal, S., T'Syen, D., Balusu, S., Theys, T., Fiers, M., Mancuso, R., Howden, A. J. M., & De Strooper, B. (2023). The -secretase substrate proteome and its role in cell signaling regulation. ***Molecular Cell***, *83*(22), 4106-4122.e10. https://doi.org/10.1016/j.molcel.2023.10.029
- Marino, M., Zhou, L., Rincon, M. Y., Callaerts-Vegh, Z., Verhaert, J., Wahis, J., Creemers, E., Yshii, L., Wierda, K., Saito, T., Marneffe, C., Voytyuk, I., Wouters, Y., Dewilde, M., Duqué, S. I., Vincke, C., Levites, Y., Golde, T. E., Saido, T. C., … Holt, M. G. (2022). AAV-mediated delivery of an anti-BACE1 VHH alleviates pathology in an Alzheimer's disease model. ***EMBO Molecular Medicine***, *14*(4), e09824. https://doi.org/10.15252/emmm.201809824
- Rué, L., Jaspers, T., Degors, I. M. S., Noppen, S., Schols, D., De Strooper, B., & Dewilde, M. (2023). Novel Human/Non-Human Primate Cross-Reactive Anti-Transferrin Receptor Nanobodies for Brain Delivery of Biologics. ***Pharmaceutics***, *15*(6). https://doi.org/10.3390/pharmaceutics15061748
- Serneels, L., Narlawar, R., Perez-Benito, L., Municoy, M., Guallar, V., T'Syen, D., Dewilde, M., Bischoff, F., Fraiponts, E., Tresadern, G., Roevens, P. W. M., Gijsen, H. J. M., & De Strooper, B. (2023). Selective inhibitors of the PSEN1-gamma-secretase complex. ***The Journal of Biological Chemistry***, *299*(6), 104794. https://doi.org/10.1016/j.jbc.2023.104794
- Shah, D., Gsell, W., Wahis, J., Luckett, E. S., Jamoulle, T., Vermaercke, B., Preman, P., Moechars, D., Hendrickx, V., Jaspers, T., Craessaerts, K., Horré, K., Wolfs, L., Fiers, M., Holt, M., Thal, D. R., Callaerts-Vegh, Z., D'Hooge, R., Vandenberghe, R., … De Strooper, B. (2022). Astrocyte calcium dysfunction causes early network hyperactivity in Alzheimer's disease. ***Cell Reports***, *40*(8), 111280. https://doi.org/10.1016/j.celrep.2022.111280
- Wouters, Y., Jaspers, T., Rué, L., Serneels, L., De Strooper, B., & Dewilde, M. (2022). VHHs as tools for therapeutic protein delivery to the central nervous system**.** ***Fluids and Barriers of the CNS***, *19*(1), 79. https://doi.org/10.1186/s12987-022-00374-4

Geneeskundige Stichting Koningin Elisabeth
Fondation Médicale Reine Elisabeth
Königin-Elisabeth-Stiftung für Medizin
Queen Elisabeth Medical Foundation

Progress report of the university research project of

Prof. dr. Pierre Vanderhaeghen
Katholieke Universiteit Leuven
(KU Leuven-VIB)

Prof. dr. Pierre Vanderhaeghen (KU Leuven-VIB)
VIB Center for Brain & Disease Research
Department of Neurosciences, KU Leuven
Stem Cell and Developmental Neurobiology Lab
O&N5 Herestraat 49 box 602 | 3000 Leuven | Belgium
Email: pierre.vanderhaeghen@kuleuven.be
T +32 16 3 77038
F +32 16 3 30827
https://pvdhlab.org

Deciphering the mechanisms underlying neurogenesis defects in mitochondrial diseases.

1. State of the art and objectives

Mitochondrial dysfunction can result in various forms of neurodevelopmental diseases (NDD), from microcephaly to intellectual disability. This suggests important roles for mitochondria in neural development, but these have remained poorly known, as their links with diseases. We had previously shown that mitochondria dynamics play a key role in neurogenesis of mouse and human NSPCs of the cerebral cortex [1,2]. We also identified intriguing differences in this process between mouse and human cortical cells, which could be linked to increased cortical size and complexity in our species.

In this project we aim to study the molecular mechanisms by which mitochondria dynamics and metabolic activity impact neuronal fate aquisition, and relate these to human corticogenesis in normal and pathological conditions.
This project will yield to deep mechanistic insights on mitochondria function during neural development, and will enable to build a robust and diverse pipeline of analysis of mitochondria/ metabolic defects in human neural development, which could be applied further to dissect pathogenic mechanisms and to establish screening platforms for diagnostic or therapeutic purposes.

2. Results

We first profiled, across time and species, mitochondria morphology, gene expression, oxygen consumption, and glucose metabolism. Next we used pharmacological or genetic manipulation of human or mouse neurons to enhance or decrease their mitochondria function, and determined the consequences on speed of neuronal development. We found that mitochondria are initally low in size and quantity in newborn neurons, and then grow gradually as neurons undergo maturation, following a species-specific timeline: while in mouse neurons mitochondria reach mature patterns in 3-4 weeks, they only do so after several months in human neurons [3].
We next measured mitochondria oxidative activity and glucose metabolism in human and mouse developing cortical neurons. This revealed a species-specific timeline of functional maturation of mitochondria, with mouse neurons displaying much faster increase in mitochondria-dependent oxidative activity than human neurons. We also found that human cortical neurons display lower levels of mitochondria-driven glucose metabolism than those of mouse neurons at the same age.
Finally we tested whether mitochondria function impacts human neuronal developmental timing. We performed pharmacological or genetic manipulation of human developing cortical neurons to enhance mitochondria oxidative metabolism. This led to accelerated neuronal maturation, with neurons exhibiting more mature features weeks ahead of time, including complex morphology, increased electrical excitability and functional synapse formation [3].
This work identifies a species-specific temporal pattern of mitochondria and metabolic development, which sets the tempo of neuronal maturation. Accelerated human neuronal maturation using metabolic manipulation might benefit pluripotent stem cell-based modeling of neural diseases, which remains greatly hindered by protracted neuron development. Tools to accelerate or decelerate neuronal development could allow to test the impact of neuronal neoteny on brain function, plasticity, and disease [4].

In relation to the latter, we tested the effect of inhibition of mitochondria metabolism, using pharmacological agents blocking the entry of Pyruvate into the mitochondria (MPC blocker), in mouse cortical neurons, which led to a decrease in developmental rates of dendrites and cell body, consustent with delayed developmental timing following mitochondria dysfunction, which could have important implications for some forms of mitochondria diseases [5,6]. To test this we have now designed inducible constructs to enable the knock-down of the MPC transporter in vivo [7], to look at the longer term effects of mitochondria blockade on neuronal maturation in vivo.

On the other hand, we have started exploring more directly the impact of mitochondria metabolism of earlier steps of corticogenesis, both in vivo and *in vitro*, in mouse and human cortical cells. Using oxygraphy, we have now obtained interesting evidence that ETC activity is higher on mouse than human cortical progenitors, while it also increases with developmental time in the mouse. As these differences could lead to distinct NAD+/NADH metabolism, we have now implemented successfully ad hoc sensory imaging on cortical cultures (using sonar imaging [8]), to test this during neuronal fate acquisition, in relation to timing differences, species differences, or both.

In parallel we have started to explore the functional impact of mitochondria metabolism on cortical neurogenesis. Surprisingly, we have found, in addition to expected effects on proliferation and differentiation, changes in the fate of generated neurons, which could be compatible with an impact of mitochondria oxidative metabolism on cortical temporal patterning, in line with previous findings in the fly nervous system [9]. We are now consolidating these data using human cortical cultures and organoids, using systems developed in the lab to this purpose [10].

3. References

1. Iwata, R. & Vanderhaeghen, P. Regulatory Roles of Mitochondria and Metabolism in Neurogenesis. *Curr Opin Neurobiol* **69**, 231–240 (2021).
2. Iwata, R., Casimir, P. & Vanderhaeghen, P. Mitochondrial dynamics in postmitotic cells regulate neurogenesis. *Science (1979)* **862**, 858–862 (2020).
3. Iwata, R. *et al.* Mitochondria Metabolism Sets the Species-Specific Tempo of Neuronal Development. *Science* **379**, eabn4705 (2023).
4. Vanderhaeghen, P. & Polleux, F. Developmental mechanisms underlying the evolution of human cortical circuits. *Nat Rev Neurosci* (2023) doi:10.1038/s41583-023-00675-z.
5. Lorenz, C. & Prigione, A. Mitochondrial metabolism in early neural fate and its relevance for neuronal disease modeling. *Current Opinion in Cell Biology* Preprint at https://doi.org/10.1016/j.ceb.2017.12.004 (2017).
6. Inak, G. *et al.* Defective metabolic programming impairs early neuronal morphogenesis in neural cultures and an organoid model of Leigh syndrome. *Nat Commun* **12**, 1–22 (2021).
7. Schell, J. C. *et al.* Control of intestinal stem cell function and proliferation by mitochondrial pyruvate metabolism. *Nat Cell Biol* (2017) doi:10.1038/ncb3593.
8. Zhao, Y. *et al.* SoNar, a Highly Responsive NAD + /NADH Sensor, Allows High-Throughput Metabolic Screening of Anti-tumor Agents. *Cell Metab* (2015) doi:10.1016/j.cmet.2015.04.009.
9. Van Den Ameele, J. & Brand, A. H. Neural stem cell temporal patterning and brain tumour growth rely on oxidative phosphorylation. doi:10.7554/eLife.47887.001.
10. Van Heurck, R. *et al.* CROCCP2 acts as a human-specific modifier of cilia dynamics and mTOR signaling to promote expansion of cortical progenitors. *Neuron* **111**, 65–80 (2023).

4. Publications 2023 in the frame of GSKE

- LRRC37B is a human modifier of voltage-gated sodium channels and axon excitability in cortical neurons.
  Libé-Philippot B, Lejeune A, Wierda K, Vlaeminck I, Beckers S, Gaspariunaite V, Bilheu A, Nyitrai H, Vennekens KM, Bird TW, Soto D, Dennis MY, Comoletti D, Theys T, de Wit J, **Vanderhaeghen P**.
  Cell (2023) 186, 5766-5783. IF: 38
- Mitochondria Metabolism Sets the Species-Specific Tempo of Neuronal Development.
  Iwata, R., Casimir, P., Erkol, E., Boubakar, L., Planque, M., Ditkowska, M., Vints, K., Gaspariunaite, V., Bird, M., Corthout, N., Vermeersch, P., Davie, K., Gounko, V., Aerts, S., Ghesquière, B., Fendt, S-M, **Vanderhaeghen P.**
  Science (2023) 379, eabn4705 DOI: 10.1126/science.abn4705. IF: 41
- Developmental mechanisms underlying the evolution of human cortical circuits.
  Vanderhaeghen P, Franck Polleux.
  Nat. Rev. Neurosci. (2023) 24, 213-232 IF: 39
- CROCCP2 acts as a human-specific modifier of cilia dynamics and mTOR signalling to promote expansion of cortical progenitors
  Van Heurck R, Wojno M, Suzuki IK, Velez-Bravo FD, Bonnefont J, Erkol E, Nguyen DT, Herpoel A, Bilheu A, Ledent C, **Vanderhaeghen P.**
  Neuron (2023) 4;111(1):65-80. IF: 18

Geneeskundige Stichting Koningin Elisabeth
Fondation Médicale Reine Elisabeth
Königin-Elisabeth-Stiftung für Medizin
Queen Elisabeth Medical Foundation

Progress report of the university research project of

Prof. dr. Veerle Baekelandt
Katholieke Universiteit Leuven (KU Leuven)

Prof. dr. Veerle Baekelandt (KU Leuven)
Laboratory for Neurobiology and Gene Therapy
Division of Molecular Medicine K.U.Leuven –
Faculty of Medicine Kapucijnenvoer 33 VCTB+5
B-3000 Leuven
Belgium
Tel.: +32 16 37 40 61
Fax: +32 16 33 63 36
E-mail: Veerle.Baekelandt@kuleuven.be

The role of LRRK2 in the peripheral immune system and gut-to-brain spreading of alpha-synuclein pathology in Parkinson's disease

1. Introduction

Parkinson's disease (PD) is the second most common neurodegenerative disorder. The neuropathological hallmarks consist of dopaminergic (DA) neuron loss in the *substantia nigra pars compacta* (SNpc) and cytoplasmic alpha-synuclein (αSyn) aggregates, termed Lewy bodies. **Cell-to-cell transmission** of misfolded αSyn has been proposed to account for the pathology stages described by Braak[1,2], suggesting that synucleinopathy might start in the periphery within the gastrointestinal tract (GI) and progress towards the brain via the vagus nerve. Mutations and variations in **LRRK2** (leucine-rich repeat kinase 2) are the most common cause of both familial and sporadic forms of PD[3]. Most pathogenic mutations are associated with enhanced kinase activity, thus making LRRK2 a very attractive therapeutic target[4].
Despite the strong association between LRRK2 and PD and hence intense research focusing on its role in the brain, evidence for an important role for **LRRK2** in the **immune system** is emerging. Indeed, highest LRRK2 expression levels in humans are found in cells of the myeloid lineage like monocytes and dendritic cells and to a lower extent in B and T cells, which points to a role in peripheral inflammation[12,5,6,7]. Also, enhanced LRRK2 levels have been detected in sporadic PD cases in peripheral immune cells including both innate (distinct monocyte subpopulations) and adaptive immune counterparts (B and T cells). Interestingly, emerging data highlight the role of **LRRK2 in several inflammatory diseases**, including inflammatory bowel disease (IBD), Crohn's disease (CD), tuberculosis, leprosy as well as other acute peripheral infections[8]. The link between **PD and gut inflammation** is of particular interest, pinpointing to chronic inflammation and the gut-brain axis in the pathophysiology of both diseases. Numerous large-scale population studies revealed that IBD patients have significantly elevated risk to also develop PD. On the other hand, PD patients frequently demonstrate intestinal inflammation and microbial dysbiosis[9].
In summary, it is becoming clear that LRRK2 plays a pivotal role in IBD, probably by regulating immune responses during intestinal inflammation. However, many questions remain, especially on how LRRK2 gain-of-function affects disease pathophysiology and how it correlates with PD.

2. Hypothesis and research objectives

The **general aim** of this project is to examine whether and how **gut inflammation** may act as an environmental trigger for **PD** and what the role of **LRRK2** is in this process. We hypothesize that **LRRK2 contributes to spreading of PD-like pathology from the gut to the brain through its role in the peripheral immune system.**

We have defined the following specific objectives :

Obj. 1: Characterize the role of mutant LRRK2 in intestinal inflammation.
Here we aim to characterize in detail the response of wild type (WT) and G2019S LRRK2 knock-in (KI) mice in a dextran sulfate sodium (DSS)-induced experimental chronic colitis mouse model.

Obj. 2 : Determine the role of mutant LRRK2 in the peripheral immune response to intestinal inflammation.
Here, we aim to assess the effect of G2019S LRRK2 in colitis specifically in immune cells.

Obj. 3: Identify the role of gut inflammation and LRRK2 in gut-to-brain propagation of αSyn pathology.
Here, we aim to investigate whether LRRK2 influences the gut-to-brain αSyn propagation through its essential role in immune responses.

Obj. 4: Evaluate if pharmacological inhibition of LRRK2 can rescue from colitis and/or αSyn pathology.
Here we aim to evaluate the therapeutic potential and mechanism-of-action of LRRK2 inhibition in models of gut inflammation and αSyn propagation.

3. Results

3.1. WP1. Characterize the role of mutant LRRK2 in intestinal inflammation.[10]

To study experimental colitis we have optimized a chronic colitis model based on the administration of dextran sodium sulphate (DSS), which provokes significant colitis-induced pathology with symptoms such as weight loss, diarrhea, and hematochezia, by inducing toxicity to the colonic epithelial and subsequent compromised mucosal barrier function and inflammation[11]. We opted for a protocol where DSS is added to the drinking water 5 days per week, for 1 month with a progressively increasing dose (Fig. 1a). We are using the constitutive LRRK2 G2019S KI mice (B6. Cg-Lrrk2tm1.1Hlme/J, The Jackson Laboratory, already available in the lab). This mouse model is currently accepted to best represent the human condition, since the LRRK2 levels and pattern of expression remain unaltered, opposed to earlier transgenic models that rely on overexpression and exogenous promoters[12].
Our DSS protocol moderately reduced the body weight but did not cause lethality, with no differences between LRRK2 G2019S KI (GS LRRK2) and wild-type (WT) LRRK2 mice. The severity of the colitis was scored three times per week by assessing the stool consistency and presence of blood in the stool. Both parameters, as well as the combined score (disease index score), show that our chronic administration scheme induced mild experimental colitis in WT mice (Fig. 1b). Nevertheless, a significantly increased sensitivity was observed in the GS LRRK2 mice, which developed severe colitis symptoms. Additionally, the GS LRRK2 mice presented severe shrinkage of the colon, which is linked to the severity of the inflammation. The histological score based on crypt architecture, infiltration of immune cells, presence of oedema and goblet cell depletion also demonstrated more damage to the colonic epithelium after DSS in the GS LRRK2 mice compared to the controls (Fig. 1c, d).

The G2019S LRRK2 mutation has been reported to increase kinase activity by approximately 4 times. No difference in the basal LRRK2 protein levels was found in the colon of untreated GS and WT LRRK2 mice (Fig. 1e, f). In response to DSS however, a significant increase in LRRK2 was found in the colon of the GS LRRK2 mice. In order to assess the kinase activity of LRRK2, we measured the autophosphorylation on Serine 1292 (Fig. 1g). Phosphorylation on S-1292 was significantly increased in GS LRRK2 mice, but to the same extent in control and DSS conditions, indicating that the kinase activity of LRRK2 remains unaltered during colitis.

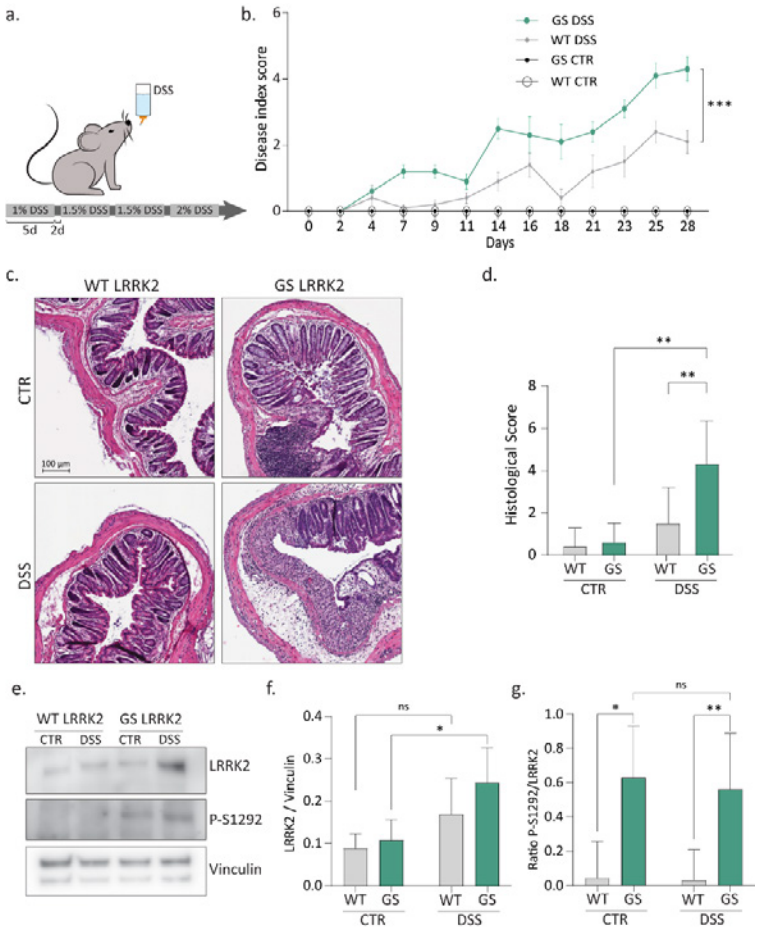

Figure 1 : The G2019S LRRK2 mutation increases the sensitivity to experimental colitis in mice. (**a**) DSS administration protocol. Mice received DSS in drinking water at increasing concentrations each time for 5 days with a pause of 2 days during one month. (**b**) Disease index score evaluation of stool consistency and haematochezia measured three times per week revealed a more severe phenotype in GS LRRK2 mice. Graph represents mean ± SD. Statistical differences were assessed using three-way ANOVA and Tukey's post hoc test, n = 10 animals/group. ***p < 0.001. (**c**) Representative image of Haematoxylin and Eosin (H&E) staining of the distal colon showing the damage to the epithelium and inflammation after DSS. Scale bar = 100 µm. (**d**) Histological scoring of the H&E images based on crypt architecture, infiltration of immune cells, presence of oedema and depletion of the goblet cells. (**e-g**) Immunoblot analysis of total and S-1292 phosphorylated LRRK2 in distal colon protein extracts of DSS-treated and control GS and WT mice. Graphs represent mean ± SD. Statistical differences were assessed using two-way ANOVA and Tukey's post hoc test, n = 10 animals/group. *p < 0.05, **p < 0.01, ***p < 0.001.

In order to characterise the inflammation in the colon we first used flow cytometry immunophenotyping (Fig. 2a). An overall increase in leukocytes (CD45+ cells) was found in the GS animals after DSS treatment. When looking at different subpopulations, we observed a significantly higher response in the GS LRRK2 animals treated with DSS for the non-classical (Ly6C-) monocytes, dendritic cells (CD11c+) and the lymphoid population (CD45hi, CD11b-), more specifically the CD8+ and CD4+ T cells. A similar trend that did not reach statistical significance was found for the myeloid cells (CD45hi, CD11b+), the classical (Ly6C+) monocytes and the granulocytes (defined as Ly6G+, Ly6C+, CD11b+ cells).

Next, we performed immunostaining in the distal colon for macrophages (F4/80), neutrophils (MPO) and for the major histocompatibility complex class II (MHC II) (Fig. 2b). In agreement with the higher level of inflammation detected by flow cytometry, the three markers were significantly increased in the GS LRRK2 mice treated with DSS (Fig. 2c-e).

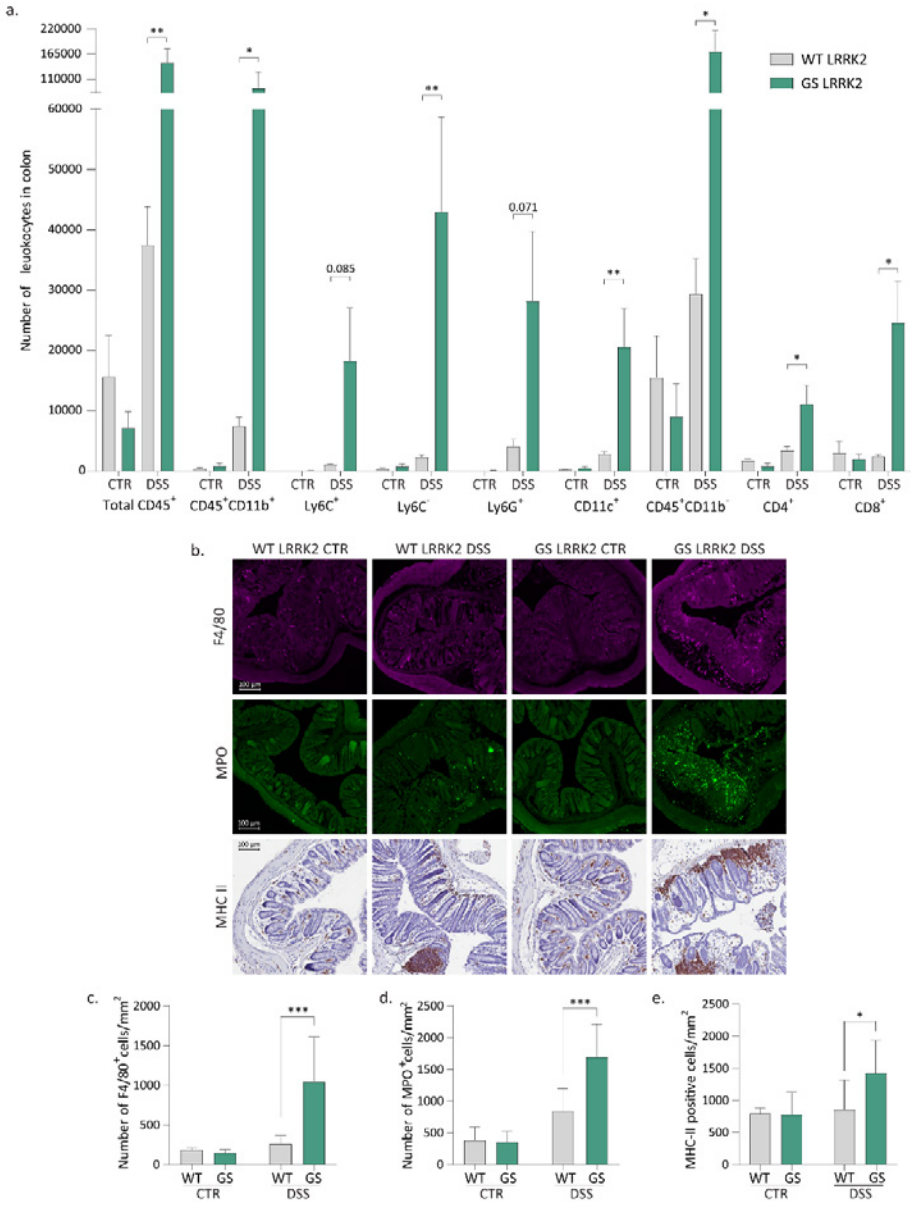

Figure 2. Increased inflammatory response in the colon of GS LRRK2 mice after DSS. (**a**) Flow cytometry immunophenotyping of the colon of WT and GS LRRK2 mice treated with DSS. Number of total leukocytes ($CD45^+$), myeloid cells ($CD45^+$ $CD11b^+$), $Ly6C^+$ and $Ly6C^-$ monocytes, dendritic cells ($CD11c^+$), neutrophils ($Ly6G^+$), lymphocytes ($CD45^+$ $CD11b^-$) and T cells ($CD8^+$ and $CD4^+$) are shown. Graphs represent mean ± SD. Statistical differences were assessed using Student's t-test between WT and GS DSS groups, n = 5 (DSS), 2 (CTR) animals/group. $^*p < 0.05$, $^{**}p < 0.01$ (**b**) Immunostaining of paraffin-embedded distal colon sections. Representative images of macrophage (F4/80), neutrophil (MPO) and MHC II immunostaining in the distal colon of WT and GS LRRK2 mice. Quantification of macrophages (**c**), neutrophils (**d**) and MHC II expressing cells (**e**). Graphs represent mean ± SD. Statistical differences were assessed using two-way ANOVA and Tukey's post hoc test, n = 10 animals/group. $^*p < 0.05$, $^{***}p < 0.001$.

Finally, a panel of cytokines was measured in colon homogenates from these animals (Fig. 3). An overall increase in cytokine levels was present in GS LRRK2 mice after experimental colitis. More specifically, significant differences were found between WT and GS LRRK2 mice for IL-33, CXCL10, CCL2, CCL3, CXCL2, IL-10, IL-12p70, IL-2 and TNF-, as well as a consistent trend for IFN-, IL-1β, IL-5, IL-6 and CXCL1.

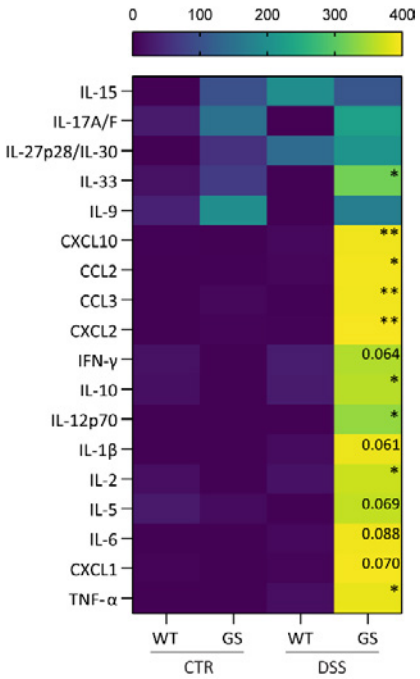

Figure 3. DSS induces higher levels of pro-inflammatory cytokines in the inflamed colon of GS LRKK2 mice. Cytokines were measured in colon protein extracts from WT and GS LRRK2 mice after DSS administration as well as WT and LRRK2 control mice (CTR). Increased levels of IL-33, IP-10, MCP-1, MIP-1, MIP-2, IL-10, IL12p27, IL-2 and TNF-, as well as trends towards increased levels of IFN-, IL-1β, IL-5, IL-6 and CXCL1 were found in GS mice. Graphs represent mean ± SD. Statistical differences were assessed using Student's t-test between WT and GSS DSS groups, n = 8 (DSS), 2 (CTR) animals/group. $^{*}p < 0.05$, $^{**}p < 0.01$.

3.2. WP2. Characterization of the role of mutant LRRK2 in immune cells in experimental colitis[10]

We hypothesised that the presence of mutant LRRK2 specifically in the immune cells might be responsible for the exacerbated inflammatory response of the GS mice towards DSS. Therefore, we transplanted the bone marrow of WT mice into lethally irradiated WT (WT^{WT}) and GS LRRK2 mice (GS^{WT}), as well as GS bone marrow into recipient GS LRRK2 (GS^{GS}) mice. In order to control for proper engraftment, we transplanted in parallel bone marrow from C57BL/6-Ly5.1 mice carrying the CD45.1 alloantigen of CD45 to our GS and WT LRRK2 mice which express CD45.2. 10 weeks post transplantation, engraftment was evaluated through flow cytometry. An average of 98.7% of engraftment was measured in every control animal. Next, we induced experimental colitis in the WT^{WT}, GS^{GS} and GS^{WT} mice 10 weeks after bone marrow transplantation. The disease index score of the GS^{WT} group was improved compared to the GS^{GS} group and reaching similar levels as the WT^{WT} mice (Figure 4a). The colon length was normalised in the GS^{WT} mice treated with DSS. Also, the histological score confirmed a reduction in the colonic epithelial damage in GS^{WT} mice (Fig. 4b).

Flow cytometry analysis of the colon revealed overall comparable immune cell numbers in the WT^{WT} and GS^{WT} animals in contrast to the increase seen in the GS^{GS} mice (Figure 4c). More specifically, a rescue was found by the WT bone marrow transplantation in the GS^{WT} mice for total myeloid cells ($CD45^{+}$ $CD11b^{+}$), $Ly6C^{+}$ and $Ly6C^{-}$ monocytes, granulocytes ($Ly6G^{+}$), dendritic cells ($CD11c^{+}$), MHC II+ leukocytes, NK cells ($CD161^{+}$), $CD4^{+}$ T cells, $CD25^{+}$ expressing CD4 T cells and B cells ($CD19^{+}$). These results demonstrate that the increased inflammation present in the GS LRRK2 mice after DSS is completely rescued by the bone marrow transplantation, suggesting that the DSS response is modulated by the activity of LRRK2 in the immune cells.

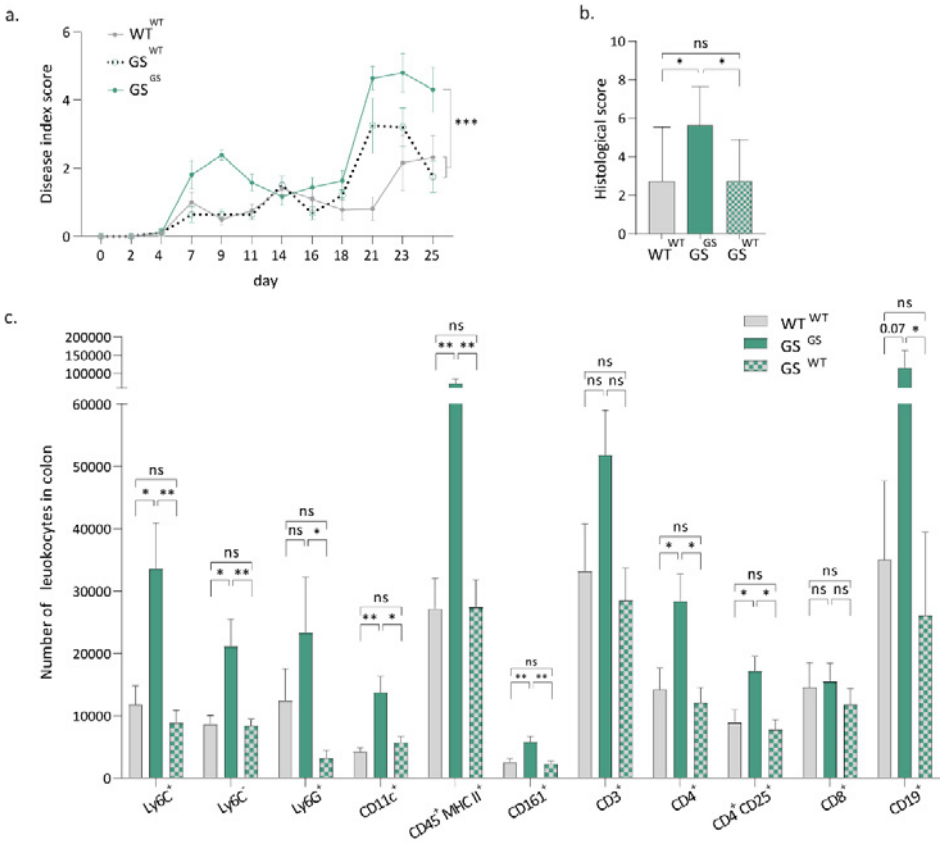

Figure 4. Bone marrow transplantation of wild type into GS LRRK2 mice reverts the susceptibility to DSS-induced colitis. (**a**) Disease index score of GS mice is normalised to WT levels after bone marrow transplantation from WT mice. Graph represents mean ± SD. Statistical differences were assessed using two-way ANOVA and Tukey's post hoc test, n = 8-9 animals/group. ***p < 0.001. (**b**) Histological score of GS mice is reduced to WT levels after bone marrow transplantation. Graph represents mean ± SD. Statistical differences were assessed using one-way ANOVA and Tukey's post hoc test, n = 8-9 animals/group. *p < 0.05. (**c**) Colonic immunophenotyping by flow cytometry of the GS^{WT} as well as the WT^{WT} and GS^{GS} mice treated with DSS. Quantification of total myeloid cells ($CD45^+$ $CD11b^+$), $Ly6C^+$ and $Ly6C^-$ monocytes, neutrophils ($Ly6G^+$), dendritic cells ($CD11c^+$), MHC II^+ antigen presenting cells, natural killer cells ($CD161^+$), lymphocytes ($CD45^+$ $CD11b^-$), T cells ($CD3^+$), CD4 T cells, $CD25^+$ CD4 T cells, CD8 T cells and B cells ($CD19^+$). Graphs represent mean ± SD. Statistical differences were assessed using one-way ANOVA and Tukey's post hoc test, n = 8-9 animals/group. *p < 0.05, **p < 0.01.

3.3. WP3. Identify the role of gut inflammation and LRRK2 in gut-to-brain propagation of αSyn pathology.

We have recently started to optimize the gut αSyn PFF injections and are currently characterizing the immune response and αSyn pathology.

3.4. WP4. Evaluate if pharmacological inhibition of LRRK2 can ameliorate colitis and/or αSyn pathology propagation.[10]

In order to determine whether or not the increased LRRK2 kinase activity is responsible for the enhanced DSS response in the GS mice, we treated the animals with the LRRK2 inhibitor MLi-2. MLi-2 was administered using an in-diet treatment protocol as previously described for 30 days starting 2 days before the DSS treatment[13]. The dose of ingested compound was estimated at 25 mg/kg/day (mean per animal). The treatment was well tolerated and no differences in animal weight between the treatment and placebo groups were observed. LRRK2 inhibition was confirmed by quantifying LRRK2 dephosphorylation at S935 in colon through western blot. Our protocol results in a reduction of 80% in the phosphorylation of S935, which suggests partial inhibition of LRRK2.

Pharmacological inhibition of LRRK2 significantly ameliorated the colitis phenotype based on the disease index score, especially in the last two weeks of the treatment (Fig. 5a). Nevertheless,

protection with the treatment was partial as the MLi-2 treated animals still responded more severely than the WT LRRK2 mice. The length of the colon was not significantly altered by the inhibition of LRRK2, suggesting that LRRK2 kinase inhibition at this dose and administration route could not completely counteract the GS mutation effect.

Quantification of the immune cells in the colon by flow cytometry revealed a reduction in the MLi-2 treated mice for the different immune populations tested, with the exception of Ly6C$^-$ monocytes, which didn't reach statistical significance (Fig. 5b). Overall, the results suggest a reduction of inflammation in the MLi-2 treated GS mice.

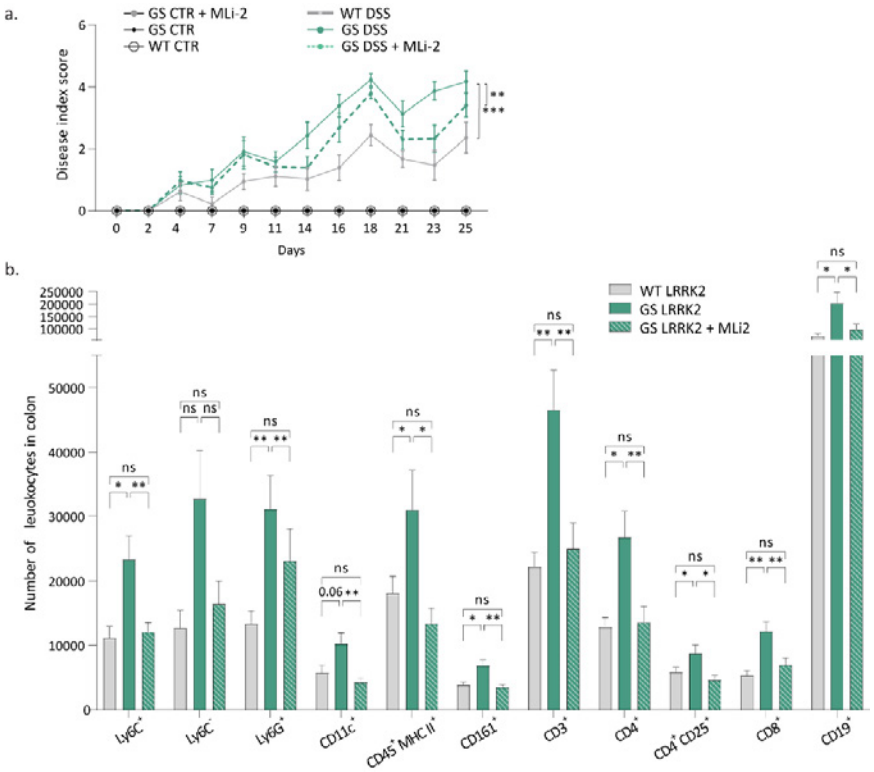

Figure 5. The LRRK2s kinase inhibitor MLi-2 partially rescues the enhanced susceptibility of GS LRRK2 mice to DSS. (**a**) Disease index score evaluation in WT and GS mice treated with placebo or MLi-2, as well as controls (CTR). Graph represents mean ± SD. Statistical differences were assessed using three-way ANOVA and Tukey's post hoc test, n = 9-15 animals/group. ***p < 0.001. (**b**) Colonic immunophenotyping by flow cytometry of GS mice treated with MLi-2 or placebo, as well as WT mice, after DSS administration. Quantification of total number of myeloid cells (CD45$^+$ CD11b$^+$), Ly6C$^+$ and Ly6C$^-$ monocytes, neutrophils (Ly6G$^+$), dendritic cells (CD11c$^+$), MHC II$^+$ antigen presenting cells, natural killer cells (CD161$^+$), lymphocytes (CD45$^+$ CD11b$^-$), T cells (CD3$^+$), CD4 T cells, CD25$^+$ CD4 T cells, CD8 T cells and B cells (CD19$^+$). Graphs represent mean ± SD. Statistical differences were assessed using one-way ANOVA and Tukey's post hoc test, n = 9-15 animals/group. *p < 0.05, **p < 0.01.

4. Publications 2023 with Q.E.M.F. acknowledgement

- Cabezudo D, Tsafaras G, Van Acker E, Van den Haute C, Baekelandt V. (2023) Mutant LRRK2 exacerbates immune response and neurodegeneration in a chronic model of experimental colitis. *Acta Neuropathologica*, 146(2):245-261. (IF 15.9, cit 4)

5. References

1. Braak, H., Tredici, K. D., Rub, U., de Vos, R. A., Jansen Steur, E. N. & Braak, E. Staging of brain pathology related to sporadic Parkinson's disease. *Neurobiol Aging* **24**, 197-211 (2003).
2. Peelaerts, W. & Baekelandt, V. a-Synuclein strains and the variable pathologies of synucleinopathies. *J Neurochem* **139 Suppl 1**, 256-274, doi:10.1111/jnc.13595 (2016).
3. Monfrini, E. & Di Fonzo, A. Leucine-Rich Repeat Kinase (LRRK2) Genetics and Parkinson's Disease. *Adv Neurobiol* **14**, 3-30, doi:10.1007/978-3-319-49969-7_1 (2017).
4. Tolosa, E., Vila, M., Klein, C. & Rascol, O. LRRK2 in Parkinson disease: challenges of clinical trials. *Nat Rev Neurol* **16**, 97-107, doi:10.1038/s41582-019-0301-2 (2020).
5. Gardet, A., Benita, Y., Li, C., Sands, B. E., Ballester, I., Stevens, C., Korzenik, J. R., Rioux, J. D., Daly, M. J., Xavier, R. J. & Podolsky, D. K. LRRK2 is involved in the IFN-gamma response and host response to pathogens. *Journal of immunology (Baltimore, Md. : 1950)* **185**, 5577-5585, doi:10.4049/jimmunol.1000548 (2010).
6. Sharma, S., Bandopadhyay, R., Lashley, T., Renton, A. E., Kingsbury, A. E., Kumaran, R., Kallis, C., Vilarino-Guell, C., O'Sullivan, S. S., Lees, A. J., Revesz, T., Wood, N. W. & Holton, J. L. LRRK2 expression in idiopathic and G2019S positive Parkinson's disease subjects: a morphological and quantitative study. *Neuropathol Appl Neurobiol* **37**, 777-790, doi:10.1111/j.1365-2990.2011.01187.x (2011).
7. Dzamko, N., Gysbers, A. M., Bandopadhyay, R., Bolliger, M. F., Uchino, A., Zhao, Y., Takao, M., Wauters, S., van de Berg, W. D., Takahashi-Fujigasaki, J., Nichols, R. J., Holton, J. L., Murayama, S. & Halliday, G. M. LRRK2 levels and phosphorylation in Parkinson's disease brain and cases with restricted Lewy bodies. *Mov Disord* **32**, 423-432, doi:10.1002/mds.26892 (2017).
8. Cabezudo, D., Baekelandt, V. & Lobbestael, E. Multiple-Hit Hypothesis in Parkinson's Disease: LRRK2 and Inflammation. *Front Neurosci* **14**, 376, doi:10.3389/fnins.2020.00376 (2020).
9. Lee, H. S., Lobbestael, E., Vermeire, S., Sabino, J. & Cleynen, I. Inflammatory bowel disease and Parkinson's disease: common pathophysiological links. *Gut* **70**, 408-417, doi:10.1136/gutjnl-2020-322429 (2021).
10. Cabezudo, D., Tsafaras, G., Van Acker, E., Van den Haute, C. & Baekelandt, V. Mutant LRRK2 exacerbates immune response and neurodegeneration in a chronic model of experimental colitis. *Acta Neuropathol* **146**, 245-261, doi:10.1007/s00401-023-02595-9 (2023).
11. Wirtz, S., Neufert, C., Weigmann, B. & Neurath, M. F. Chemically induced mouse models of intestinal inflammation. *Nat Protoc* **2**, 541-546, doi:10.1038/nprot.2007.41 (2007).
12. Chang, E. E. S., Ho, P. W., Liu, H. F., Pang, S. Y., Leung, C. T., Malki, Y., Choi, Z. Y., Ramsden, D. B. & Ho, S. L. LRRK2 mutant knock-in mouse models: therapeutic relevance in Parkinson's disease. *Transl Neurodegener* **11**, 10, doi:10.1186/s40035-022-00285-2 (2022).
13. Van der Perren, A., Cabezudo, D., Gelders, G., Peralta Ramos, J. M., Van den Haute, C., Baekelandt, V. & Lobbestael, E. LRRK2 ablation attenuates alpha-synuclein-induced neuroinflammation without affecting neurodegeneration or neuropathology in vivo. *Neurotherapeutics : the journal of the American Society for Experimental NeuroTherapeutics* **18**, 949-961, doi:10.1007/s13311-021-01007-8 (2021).

Geneeskundige Stichting Koningin Elisabeth
Fondation Médicale Reine Elisabeth
Königin-Elisabeth-Stiftung für Medizin
Queen Elisabeth Medical Foundation

Progress report of the university research project of

Prof. dr. Thomas Voets
Katholieke Universiteit Leuven (KU Leuven)

Prof. dr. Thomas Voets
Laboratory of Ion Channel Research
VIB-KU Leuven Center for Brain & Disease Research
KU Leuven, Department of Cellular and Molecular Medicine
Herestraat 49 bus 801
3000 Leuven
Tel: +32 16 33 02 17
Thomas.voets@kuleuven.vib.be

Table of contents

Unraveling the etiology of TRPM3-dependent neurodevelopmental disorders

1. Background and aim

TRPM3, a member of the transient receptor potential (TRP) superfamily of tetrameric ion channels, is a Ca^{2+}-permeable cation channel activated by increasing temperature and by ligands, including the endogenous neurosteroid pregnenolone sulphate (PS)[1-3]. Several studies, including pioneering work from our research group, have established the channel's role in peripheral somatosensory neurons, where it is involved in heat sensation and in the development of pathological pain[1,4-8]. In addition, TRPM3 is expressed in kidney, eye, pancreas, and several regions of the central nervous system, such as the hippocampal formation, the choroid plexus and the cerebellum, but little is known about the channel's physiological role in these tissues [11-15].

Recently, rare heterozygous *de novo* variants in TRPM3 were identified in patients with neurodevelopmental disorders, consistently presenting with global developmental delay and mild to severe intellectual disability, often in combination with childhood-onset epilepsy, hypotonia and altered heat and/or pain sensitivity[16-20]. At the start of this project, our team had performed for the first time a detailed analysis of the electrophysiological and pharmacological properties of two disease-associated TRPM3 variants, following heterologous expression in the HEK293 cell line[9,21]. We found that these variants show a dominant gain of function (GoF) when co-expressed with wild type TRPM3 (mimicking the situation in patients), seen as increased basal activity and enhanced responses to heat and PS. In particular, the recurrent $TRPM3^{V1002M}$ variant, which to data has been described in 16 patients worldwide, provokes a more than 10-fold increase in inward currents. Moreover, our team initiated an international consortium around TRPM3-related disease, via which we (1) facilitate rapid exchange of knowledge between geneticists, neurologists and basic scientists working on TRPM3[20], (2) perform functional characterization of new variants, thereby allowing the diagnosis in new patients, and (3) organize information and Q&A sessions with parents of affected children.

The aim of this project is to better understand how disease-associated TRPM3 variants lead to human neurodevelopmental disease, and use this knowledge as a basis for the development of TRPM3-based therapies to treat brain disease. In the past year, important progress was made regarding (1) further characterization of new patient variants and the corresponding phenotypes, (2) development of a mouse model of TRPM3-related brain disease, and (3) experimental treatment of a subset of patients.

2. Results

2.1. A spectrum of TRPM3 variants in patients with neurodevelopmental disorder

As initiating team in the international consortium around TRPM3-related neurodevelopmental disease, we have been directly involved in the biophysical characterization of disease-associated TRPM3 variants, and in the systematic description of the phenotype of the patients. These include 10 patients carrying 7 novel variants that were described in a first publication[10], and 6 additional variants in 6 patients, for which a publication is currently being prepared (Roelens et al., in preparation). The position of the different variants is indicated in Figure 1.

Importantly, we were able to show that all known disease-associated variants (15 in total) lead to a dominant gain-of-function channel, showing increased basal activity and increased responses to the neurosteroid agonist PS. Considering the high expression levels of TRPM3 in specific brain cells (including neurons and non-neuronal cells), these findings strongly suggest that increased TRPM3 channel activity lies at the root of the neurodevelopmental and epileptic symptoms in the patients. We have now also established a fluorescence-based analytical pipeline, which allows us to rapidly assess whether newly identified TRPM3 variants are likely pathogenic. In this assay, we co-express equal amounts of cDNA of wild type and variant TRPM3, cloned into an IRES-GFP vector, together with the red calcium indicator jRCAMP1b. Using a 96-well based fluorescence imaging plate reader system, quantification of the ration between the green and the red fluorescence allows us to accurately measure various aspects of the channel gating, including basal activity, response to PS and sensitivity to antagonists such as the anticonvulsant primidone. Using this assay, we have been able to confirm the diagnosis of TRPM3-dependent neurodevelopmental disease in more than 20 patients. Moreover, by determining the sensitivity of the mutant channel to primidone, the feasibility of drug treatment with this drug has been assessed (see below).

Fig.1: TRPM3 variants
Structure of a single TRPM3 subunit, indicating the location of disease-associated variants. The transmembrane region is indicated in gray, and the cytosolic N and C termini in cyan.
The location amino acids that are altered in the different disease associated variants are indicated as balls colored in orange (V1002 and P1102; described in ref.9), red (D614, L769, G1007, N1126 and S1113; described in ref.10) and in yellow (our unpublished data).

2.2. Primidone as an experimental treatment for patients with TRPM3-dependent neurodevelopmental disease

Based on our assessment of the sensitivity of disease-associated TRPM3 variants to the primidone, a well-known medication to treat epilepsy and tremor, several children suffering from TRPM3-dependent neurodevelopmental disease have been treated with primidone. In a first case report, we were involved in the description of two children suffering from pharmacoresistant developmental and epileptic encephalopathy with spike-and-wave activation in sleep (DEE-SWAS) due to TRPM3 mutations. Following treatment with primidone, developmental regression was stopped, psychomotor development improved, and epileptic activity was fully suppressed[22]. Currently, more than 50% of the known patients are being treated with primidone, often (but not

always) with profound beneficial effects on developmental progress and the occurrence of seizures. Unfortunately, some of the patients do not show any improvement following primidone treatment, and the cause of treatment failure is currently unknown. One issue is that primidone is not very selective, and can have central side effects that occlude potential beneficial effects of the suppression of overactive TRPM3. In this regard, our team is collaborating with the Center for Drug Design and Discovery (CD3; www.cd3.be), in partnership with the company Biohaven (www.biohaven.com), to develop highly potent and specific TRPM3 antagonists. Alternatively, there may be a window during development where primidone is effective, and later treatments may be with lesser or no effect. The availability of a mouse model of the human disease (see below) will allow to address some of these questions experimentally.

2.3. Impact of TRPM3^{V1002M} on development and disease progression in mice

We have succeeded in developing a mouse model that reproduces the genetic condition in patients that heterozygotic for the most recurrent disease-associated variant (V1002M), which causes a severe form of neurodevelopmental disorder in patients, including global developmental delay, hypotonia, musculoskeletal issues. By crossing a conditional knockin line, based on the cre-LoxP system, with Sox1-cre mice, we obtained mice that are heterozygotic for the mutation equivalent to the human V1002M. A first systematic analysis of these mice has revealed several (neuro)developmental deficits (Figure 2).

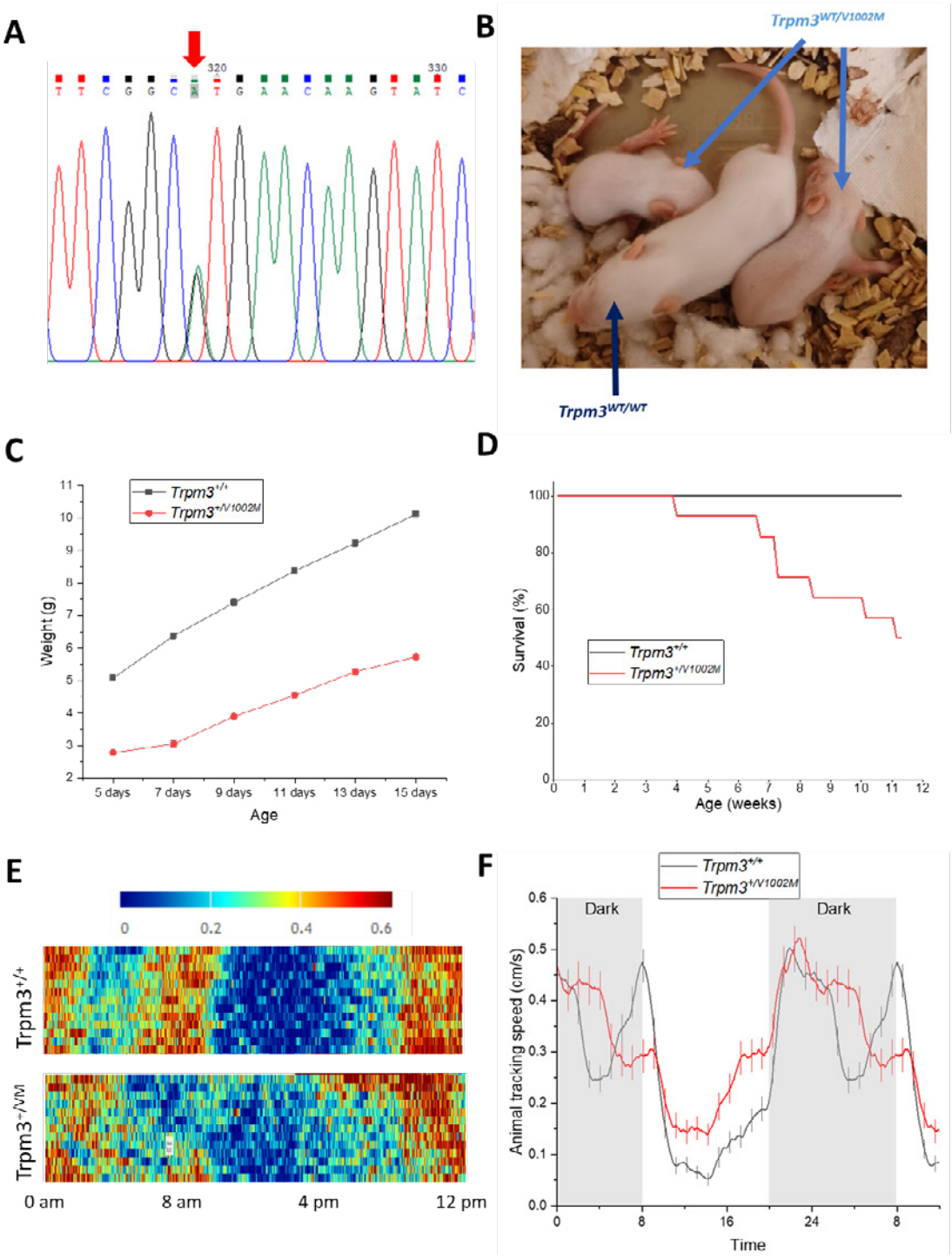

Fig. 2 Phenotype of Trpm3$^{+/V1002M}$ mice.
(A) Short sequence fragment of cDNA from a Trpm3$^{+/V1002M}$ mouse brain, showing equal expression of wt and mutant RNA. (B) Picture of a WT and two Trpm3$^{+/V1002M}$ littermates, clearly illustrating developmental delays in the mutant pups. (C) Body weight of WT and Trpm3$^{+/V1002M}$ mice (n=5 for each group), showing growth retardation. (D) Survival plot of WT and Trpm3$^{+/V1002M}$ mice, showing premature death of Trpm3$^{+/V1002M}$ mice. Notably, mice typically died following seizure-like hypomotor activity. (E,F) Alterations in circadian rhythm between WT and Trpm3$^{+/V1002M}$ mice. (E) Automated activity measurement using DVC cages – each row corresponds to one day, and warmer colors represent higher activity. Lights were on between 8am and 8 pm. (F) Comparison of the mean speed of WT and Trpm3$^{+/V1002M}$ mice show increased activity during the resting (light) phase in mice carrying the disease-associated mutation.

Indeed, Trpm3$^{+/V1002M}$ mice show growth retardation (Fig. 2B,C), severe seizure leading to premature death (Fig.2D), and alterations in diurnal activity, including increased activity during the resting phase of the day. Taken together, these findings indicate that Trpm3$^{+/V1002M}$ mice show a phenotype

that mimics various important aspects of the human disease, including developmental delay, epileptic seizures and abnormal activity during the resting period of the day.

3. Next steps and outlook

Thanks to the support of the GSKE , we have been able to make important progress in understanding TRPM3-dependent neurodevelopmental disease. By establishing a quantitative functional pipeline of novel TRPM3 variants, we were able to support the diagnosis of patients with neurodevelopmental disease by establishing gain of channel function as the underlying cause. As pioneers in the field, we are frequently contacted by geneticists treating patients with previously undescribed TRPM3 variants, but the costs to perform these assays, which amount to 2500 Euro/variant for cloning, cell culture, plate reader and analysis, are currently not covered by any running funding. With 8 new variants tested in 2023, we are currently searching for alternative funding in order to be able to further offer this service to patients and their caretakers.

Importantly, with the establishment of the $Trpm3^{+/V1002M}$ mice, whose breeding and first detailed behavioral analyses were partly enabled by the GSKE funding, we now have an excellent tool to study disease progression, pathological mechanisms and potential treatments. Currently, we are using this mouse model in various longitudinal tests: 1) in collaboration with the KU Leuven Molecular Small Animal Imaging Center (MoSAIC), we have initiated longitudinal imaging using µMRI and µCT, to follow brain and skeletal development; 2) in collaboration with the VIB-CBD single-cell expertise unit, we have initiated spatial transcriptomics (using the Vizgen MERSCOPE system), to evaluate changes in single cell identity and gene expression in the brain of mutant mice; 3) in our team, we are currently investing in a MOseq (motion sequencing[23]) behavioral imaging system to better identify behavioral fingerprints in epilepsy in the mutant mice[24]; 4) we are setting up cohorts of mutant mice that are treated daily with vehicle or TRPM3 antagonist (primidone or undisclosed brain-permeant TRPM3 antagonists developed in collaboration with CD3 and Biohaven), to evaluate whether inhibiting TRPM3 function can prevent/delay/counteract the (neuro)developmental phenotype of the mutant mice.

In parallel, experiments are ongoing to compare the differentiation process of human stem cells heterozygous for the V1002M mutation to isogenic controls. The results of these ongoing experiments will be reported in the coming year.

Overall, the project is yielding important new insights into TRPM3-dependent brain disease, with a high translational value, both for the diagnosis of the cause of disease in patients with newly identified variants in the TRPM3 gene, and for the development of therapy. Thanks to our close interactions with geneticists, neurologists and parents of affected children, new findings and potential treatments can be directly communicated to the relevant stakeholders.

4. Publications in 2023 with support from GSKE

(*: shared last and corresponding authors)

- Aloi, V. D., Pinto, S., Van Bree, R., Luyten, K., **Voets, T.**, & Vriens, J. (2023). TRPM3 as a novel target to alleviate acute oxaliplatin-induced peripheral neuropathic pain. *Pain*, *164*(9), 2060-2069. https://doi.org/10.1097/j.pain.0000000000002906
- Becker, L. L., Horn, D., Boschann, F., Van Hoeymissen, E., **Voets, T.**, Vriens, J., Prager, C., & Kaindl, A. M. (2023). Primidone improves symptoms in TRPM3-linked developmental and epileptic encephalopathy with spike-and-wave activation in sleep. *Epilepsia*, *64*(5), e61-e68. https://doi.org/10.1111/epi.17586
- Burglen, L., Van Hoeymissen, E., Qebibo, L., Barth, M., Belnap, N., Boschann, F., Depienne, C., De Clercq, K., Douglas, A. G. L., Fitzgerald, M. P., Foulds, N., Garel, C., Helbig, I., Held, K., Horn, D., Janssen, A., Kaindl, A. M., Narayanan, V., Prager, C., . . . **Voets, T.***, Vriens, J.* (2023). Gain-of-function variants in the ion channel gene TRPM3 underlie a spectrum of neurodevelopmental disorders. *Elife*, *12*. https://doi.org/10.7554/eLife.81032
- Daniluk, J., & **Voets, T.** (2023). pH-dependent modulation of TRPV1 by modality-selective antagonists. *Br J Pharmacol*, *180*(21), 2750-2761. https://doi.org/10.1111/bph.16173
- Luyts, N., Daniluk, J., Freitas, A. C. N., Bazeli, B., Janssens, A., Mulier, M., Everaerts, W., & **Voets, T.** (2023). Inhibition of TRPM8 by the urinary tract analgesic drug phenazopyridine. *Eur J Pharmacol*, *942*, 175512. https://doi.org/10.1016/j.ejphar.2023.175512

5. References

1. Vriens, J. *et al.* TRPM3 is a nociceptor channel involved in the detection of noxious heat. *Neuron* **70**, 482-494 (2011). https://doi.org/10.1016/j.neuron.2011.02.051
2. Wagner, T. F. *et al.* Transient receptor potential M3 channels are ionotropic steroid receptors in pancreatic beta cells. *Nat Cell Biol* **10**, 1421-1430 (2008). https://doi.org/10.1038/ncb1801
3. Held, K. *et al.* Activation of TRPM3 by a potent synthetic ligand reveals a role in peptide release. *Proc Natl Acad Sci U S A* **112**, E1363-1372 (2015). https://doi.org/10.1073/pnas.1419845112
4. Mulier, M. *et al.* Upregulation of TRPM3 in nociceptors innervating inflamed tissue. *Elife* **9** (2020). https://doi.org/10.7554/eLife.61103
5. Mulier, M., Vandewauw, I., Vriens, J. & Voets, T. Reply to: Heat detection by the TRPM2 ion channel. *Nature* **584**, E13-E15 (2020). https://doi.org/10.1038/s41586-020-2511-6
6. Su, S., Yudin, Y., Kim, N., Tao, Y. X. & Rohacs, T. TRPM3 channels play roles in heat hypersensitivity and spontaneous pain after nerve injury. *J Neurosci* **41**, 2457-2474 (2021). https://doi.org/10.1523/JNEUROSCI.1551-20.2020
7. Vangeel, L. *et al.* Functional expression and pharmacological modulation of TRPM3 in human sensory neurons. *Br J Pharmacol* **177**, 2683-2695 (2020). https://doi.org/10.1111/bph.14994
8. Vandewauw, I. *et al.* A TRP channel trio mediates acute noxious heat sensing. *Nature* **555**, 662-666 (2018).
9. Van Hoeymissen, E. *et al.* Gain of channel function and modified gating properties in TRPM3 mutants causing intellectual disability and epilepsy. *Elife* **9** (2020). https://doi.org/10.7554/eLife.57190
10. Burglen, L. *et al.* Gain-of-function variants in the ion channel gene TRPM3 underlie a spectrum of neurodevelopmental disorders. *Elife* **12** (2023). https://doi.org/10.7554/eLife.81032
11. Grimm, C., Kraft, R., Sauerbruch, S., Schultz, G. & Harteneck, C. Molecular and functional characterization of the melastatin-related cation channel TRPM3. *J Biol Chem* **278**, 21493-21501 (2003). https://doi.org/10.1074/jbc.M300945200
12. Oberwinkler, J., Lis, A., Giehl, K. M., Flockerzi, V. & Philipp, S. E. Alternative splicing switches the divalent cation selectivity of TRPM3 channels. *J Biol Chem* **280**, 22540-22548 (2005). https://doi.org/10.1074/jbc.M503092200
13. Zamudio-Bulcock, P. A., Everett, J., Harteneck, C. & Valenzuela, C. F. Activation of steroid-sensitive TRPM3 channels potentiates glutamatergic transmission at cerebellar Purkinje neurons from developing rats. *J Neurochem* **119**, 474-485 (2011). https://doi.org/10.1111/j.1471-4159.2011.07441.x
14. Becker, A. *et al.* Control of Insulin Release by Transient Receptor Potential Melastatin 3 (TRPM3) Ion Channels. *Cell Physiol Biochem* **54**, 1115-1131 (2020). https://doi.org/10.33594/000000304
15. Held, K. & Toth, B. I. TRPM3 in Brain (Patho)Physiology. *Front Cell Dev Biol* **9**, 635659 (2021). https://doi.org/10.3389/fcell.2021.635659
16. de Sainte Agathe, J. M. *et al.* Confirmation and Expansion of the Phenotype Associated with the Recurrent p.Val837Met Variant in TRPM3. *Eur J Med Genet* **63**, 103942 (2020). https://doi.org/10.1016/j.ejmg.2020.103942
17. Dyment, D. A. *et al.* De novo substitutions of TRPM3 cause intellectual disability and epilepsy. *Eur J Hum Genet* **27**, 1611-1618 (2019). https://doi.org/10.1038/s41431-019-0462-x

18. Gauthier, L. W. *et al.* Description of a novel patient with the TRPM3 recurrent p.Val837Met variant. *Eur J Med Genet* **64**, 104320 (2021). https://doi.org/10.1016/j.ejmg.2021.104320
19. Kang, Q. *et al.* A Chinese patient with developmental and epileptic encephalopathies (DEE) carrying a TRPM3 gene mutation: a paediatric case report. *BMC Pediatr* **21**, 256 (2021). https://doi.org/10.1186/s12887-021-02719-8
20. Lines, M. A. *et al.* Phenotypic spectrum of the recurrent TRPM3 p.(Val837Met) substitution in seven individuals with global developmental delay and hypotonia. *Am J Med Genet A* (2022). https://doi.org/10.1002/ajmg.a.62673
21. Zhao, S., Yudin, Y. & Rohacs, T. Disease-associated mutations in the human TRPM3 render the channel overactive via two distinct mechanisms. *Elife* **9** (2020). https://doi.org/10.7554/eLife.55634
22. Becker, L. L. *et al.* Primidone improves symptoms in TRPM3-linked developmental and epileptic encephalopathy with spike-and-wave activation in sleep. *Epilepsia* **64**, e61-e68 (2023). https://doi.org/10.1111/epi.17586
23. Wiltschko, A. B. *et al.* Mapping Sub-Second Structure in Mouse Behavior. *Neuron* **88**, 1121-1135 (2015). https://doi.org/10.1016/j.neuron.2015.11.031
24. Gschwind, T. *et al.* Hidden behavioral fingerprints in epilepsy. *Neuron* **111**, 1440-1452 e1445 (2023). https://doi.org/10.1016/j.neuron.2023.02.003

Geneeskundige Stichting Koningin Elisabeth
Fondation Médicale Reine Elisabeth
Königin-Elisabeth-Stiftung für Medizin
Queen Elisabeth Medical Foundation

Progress report of the university research project of

Prof. dr. Pierre Maquet
Université de Liège (ULiège)

Prof. dr. Pierre Maquet (ULiège)
Faculté de Médecine
Département des sciences cliniques
Neurologie
GIGA CRC In vivo Imaging – Sleep and chronobiology

Bât. B35 Neurologie
Quartier Hôpital
avenue de l'Hôpital 13
4000 Liège 1
Belgique
Téléphone de service: +32 4 366 23 67
Téléphone de service: +32 4 366 23 62

Quantitative MRI at 7 Tesla addresses ten questions about brain small vessel diseases

Our research project uses ultra-high field MRI to characterize the various aspects of brain small vessel diseases, frequent disorders that alter the cerebral small perforating arterioles, capillaries, and venules.
Most of activity this year has been devoted to the improvement of the multi-parameter protocol, which grounds most of the project. Indeed, the initial protocol was based on a single transmit coil and did not allow a proper investigation of the brainstem and cerebellum. It is well-known that ultra-high field MRI, as it is currently applied in neuroimaging, has substantial limitations in imaging the subtentorial regions. Due to the reduced wavelength of proton MRI at 7T, conventional MRI technology suffers from standing wave effects in whole-brain MRI, which often results in strongly reduced signal-to-noise ratio (SNR) in specific brain regions, mostly the lower part of the temporal lobes and the posterior fossa. The effect is also known as transmit field inhomogeneity, which is pronounced at 7 Tesla. This is inevitable if conventional excitation with a single radiofrequency (RF) transmit coil is performed. RF-coils specifically designed for the cerebellum would trade off other parts of the brain, which is not an option when critical measures must be extracted from the whole brain. Therefore, in the framework of an international collaboration on spinocerebellar ataxias (https://www.dzne.de/forschung/projekte/scaifield/about/), we considered parallel transmission (pTx) with multiple RF channels. While it has been known for a long time that pTx can mitigate transmit field inhomogeneity, the technology became mature to be applicable in larger studies only recently. Our 7T imaging device (Siemens Terra) has a fully integrated pTx system, which can be used in the standard workflow. We also took advantage of novel pTx pulse design methods that have been developed and enable fast and calibration-free routine application.

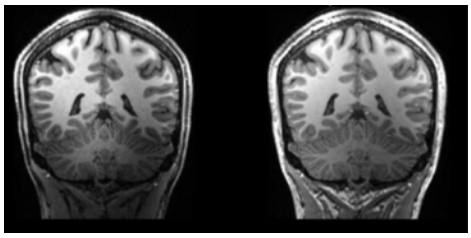

Illustration of the gain in signal homogeneity across the brain using pTX multiparameter protocol.
Left hand-side panel: Conventional single transmit T1 image. Right hand-side panel: Current achievement with parallel transmit coil, showing a better signal homogeneity, across the whole brain. Voxel size is 500 µm in both cases.

In parallel, we obtained the approval of the project by the local ethics committee and already identified about 50 potential participants with SVD of various causes, lesional load and cognitive status. Two medical doctors are currently working on this project and are applying for clinical PhD position at the FNRS. Data acquisition should begin in summer 2024.

Geneeskundige Stichting Koningin Elisabeth
Fondation Médicale Reine Elisabeth
Königin-Elisabeth-Stiftung für Medizin
Queen Elisabeth Medical Foundation

Projecten jonge onderzoekers 2023-2025 gefinancierd door de G.S.K.E.

Projets de recherche de jeunes chercheurs 2023-2025 subventionnés par la F.M.R.E.

Research projects of young researchers 2023-2025 funded by the Q.E.M.F.

Universiteiten met onderzoeksprogramma's die gesteund worden door de G.S.K.E.

Universités ayant des programmes de recherche subventionnés par la F.M.R.E.

Universities having research programs supported by the Q.E.M.F.

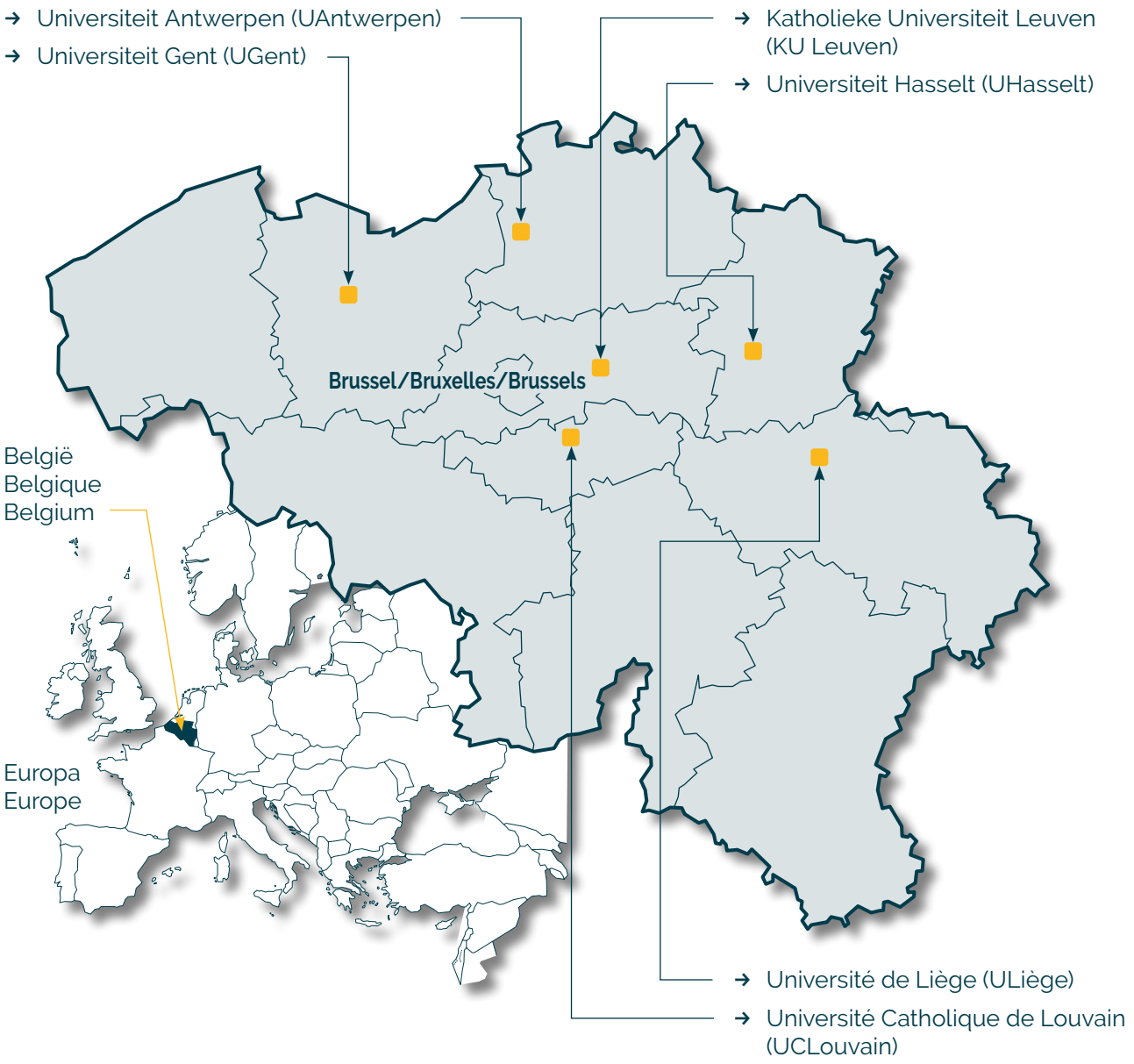

Projecten jonge onderzoekers 2023-2025 gefinancierd door de G.S.K.E.

Projets de recherche de jeunes chercheurs 2023-2025 subventionnés par la F.M.R.E.

Research projects of young researchers 2023-2025 funded by the Q.E.M.F.

UGent

Sielke Caestecker (PhD student) & promotor prof. Robrecht Raedt

The role of the locus coeruleus noradrenergic system in seizures and epilepsy

Dr. Delfien Syx

Zebrafish as a model to study pain in Ehlers-Danlos syndromes

UAntwerpen

Dr. Marijne Vandebergh

World-wide systematic characterization of TMEM106B and ATXN2 genetic status Towards implementation of genetic testing of modifiers in clinical practice

Dr. Barbara M.P. Willekens

Unravelling the role of antigen-specific T cells in NMOSD and MOGAD

KU Leuven

Dr. Wouter Peelaerts

Peripheral infections as a trigger of multiple system atrophy

Dr. Sarah van Veen

The impact of ATP13A4-mediated polyamine transport in astrocytes on synaptogenesis and neurodevelopmental disorders

UCLouvain

Prof. Giulia Liberati

STIM-WAVES: Identifying pain biomarkers with invasive and non-invasive brain stimulation targeting ongoing neural oscillations

(UHasselt)

Prof. dr. Jeroen Bogie

Getting a grip on slippery protein modifications in multiple sclerosis

Prof. dr. Bieke Broux

High salt diet causes blood-brain barrier disturbances in multiple sclerosis: involvement of the renin-angiotensin-aldosterone system

ULiège

Dr. Sophie Laguesse

Unveiling the alcohol-dependent alterations in mRNA local translation and its consequences on adolescent prefrontal cortex maturation and function

Geneeskundige Stichting Koningin Elisabeth
Fondation Médicale Reine Elisabeth
Königin-Elisabeth-Stiftung für Medizin
Queen Elisabeth Medical Foundation

Progress report of the research project of the young researcher

Sielke Caestecker (PhD student) &
promotor prof. Robrecht Raedt
Universiteit Gent (UGent)

Prof. dr. Robrecht Raedt (UGent)
Principal investigator – 4BRAIN
Associate Professor (Faculty of Medicine and Health Sciences)
Director of the Animal Facility of the Faculty of Medicine and Health Sciences
Member of GATE steering committee
Secretary of the Belgian Society for Neuroscience
Lab address: 4BRAIN,
Campus UZ Gent, 0 Blok B (entrance 36),
Corneel Heymanslaan 10,
9000 Gent, Belgium
Robrecht.Raedt@UGent.be

Sielke Caestecker (UGent)
PhD srtudent
Lab address: 4BRAIN,
Campus UZ Gent, 0 Blok B (entrance 36),
Corneel Heymanslaan 10,
9000 Gent, Belgium
sielke.caestecker@ugent.be

The role of the locus coeruleus noradrenergic system in seizures and epilepsy

Promotor: prof. dr. Lars Emil Larsen
Due to family reasons, my family and I have relocated to Denmark, which has forced me to leave my position at Ghent University. I have suggested that my close colleague, prof. Robrecht Raedt takes over the project responsibilities. Robrecht and I have been jointly supervising a PhD student, Sielke Caestecker, that has been working on this project and will continue to do so the following years.

1. Project overview

This project was based on preliminary data which showed changes in the firing of locus coeruleus (LC) neurons in relation to acute hippocampal seizures in rats and hippocampal release of noradrenaline (NA). Since the initiation of this project, we have completed these experiments and finalized and submitted a manuscript hereof in the Neurobiology of Disease (see attachment).

We have further initiated two of our intended subsequent experiments. First and foremost, we have invested additional time in studying methods for precision modulation of the LC. Secondly, we have accessed changes in noradrenergic transmission in relation to spontaneous seizures in chronically epileptic mice using a recently developed fluorescent biosensor for noradrenaline.

2. DREADD based modulation of the LC

The brainstem locus coeruleus (LC) is the sole source of noradrenaline in the neocortex, hippocampus and cerebellum. Noradrenaline is an endogenous neuromodulator involved in the regulation of excitability and plasticity of large-scale brain networks. Previous pharmacological studies have indicated that noradrenaline is able to potentiate dentate gyrus excitability and increases the population spike of perforant-path evoked potentials. These studies hold several limitations, since pharmacological interventions are likely to induce unintended off target effects. Recent development of tools for precision modulation of the LC, including Designer Receptors Exclusively Activated by Designer Drugs (DREADDs) allow the study of LC physiology with unprecedented detail. In this study, we assessed the influence of chemogenetically activating the LC on noradrenergic signaling and excitability in the hippocampus.

Male Sprague Dawley rats were injected with the viral vectors CAV2-PRSx8-hM3Dq-HA hSyn-mCherry in the LC and AAV9-hSyn-NE2m-mRuby3 in the hippocampus to induce expression of hM3Dq in LC neurons and the GRABNE2m biosensor in the hippocampus. All rats were implanted with a stimulation electrode in the perforant path and a recording electrode in the dentate gyrus, for registration of evoked potentials and local field potentials (EEG). An optical fiber was implanted for fiber photometry, to assess changes in hippocampal noradrenaline levels. Rats were injected with deschloroclozapine (DCZ) to activate the LC and to assess the effects on noradrenaline signaling and dentate gyrus electrophysiology.

Injection of DCZ resulted in a pronounced increase in $GRAB_{NE2m}$ fluorescence (z-score range: 5 - 15), a decrease in EEG power and an increase in the amplitude of the population spike of the

dentate gyrus evoked potential (a marker for postsynaptic activation of DG neurons), (**Figure 1**). No significant change in the slope of the evoked potential (a marker of synaptic strength) was found. In individual animals, changes in the population spike amplitude and EEG power were significantly correlated to the observed changes in GRABNE2m fluorescence.

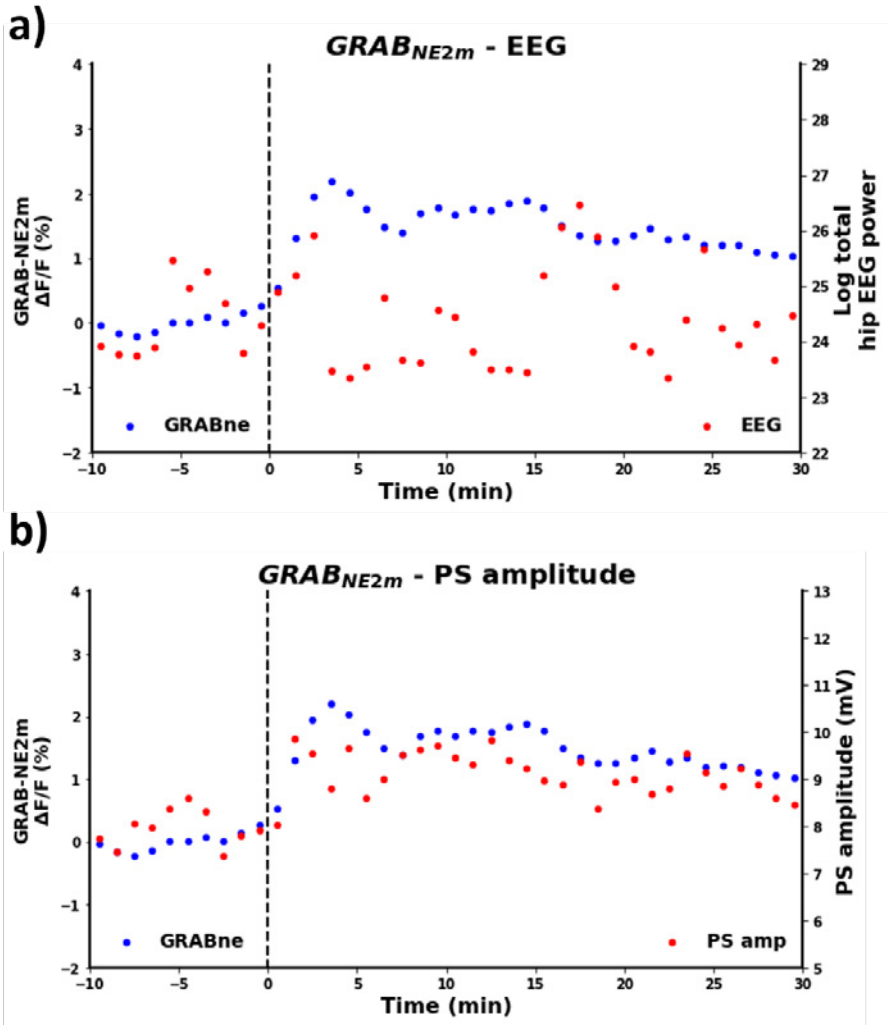

Figure 1: Injection of DCZ resulted in a pronounced increase in GRAB$_{NE2m}$ fluorescence, a decrease in EEG power and an increase in the amplitude of the population spike of the dentate gyrus evoked potential. a) example of 1 min bins of the total power of the hippocampal EEG (red), plotted against the change in GRAB-NE fluorescence signal (blue). b) example of 1 mins of the population spike amplitude increase (red), plotted against the change in GRAB-NE signal.

With this study we are the first to assess the effect of chemogenetic activation of the LC on noradrenaline signaling in the hippocampus with GRAB-sensor technology, providing unprecedented temporal resolution. By means of cell-type specific modulation of LC neurons, we were able to confirm previous findings of pharmacological studies with superior precision and specificity. A research paper on this study is foreseen in the next coming months.

Changes in hippocampal noradrenergic transmission in relation to spontaneous seizures in chronically epileptic mice

In order to investigate changes in noradrenergic transmission in relation to spontaneous seizures, we opted to study the intrahippocampal kainic acid model in mice. This model is increasingly gaining popularity, due to a high frequency of seizures which makes it possible to capture many seizures within a short period of time. In the 4Brain lab, we have extensive experience with this model. After initial intrahippocampal injection of kainic acid, we waited at least two weeks before further injecting with a viral vector for expression of the GRAB-NE fluorescent biosensor

in the hippocampus. The animals were further instrumented with hippocampal EEG electrodes to capture seizures and with an optical fiber over the hippocampus for fiber photometry to capture changes in GRAB-NE fluorescence. The preliminary data shown in the following is from one animal only but shows a clear correlation between hippocampal seizures and changes in GRAB-NE fluorescence. However, rather than an increase in noradrenergic transmission as seen during acute seizures, spontaneous seizures in chronically epileptic mice are observed to lead to a consistent decrease in noradrenergic transmission (**Figure 2**).

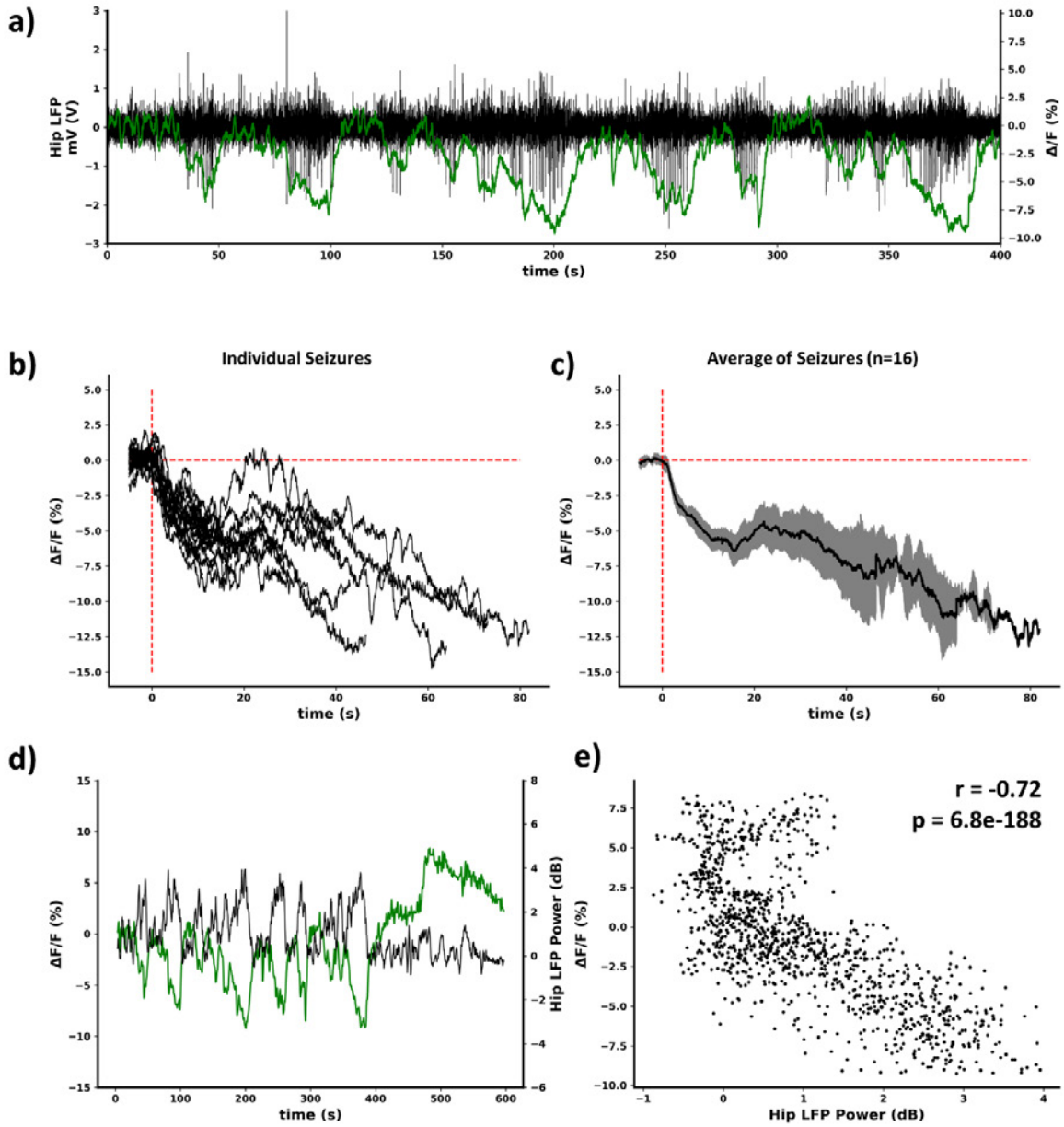

Figure 2: Spontaneous hippocampal seizures lead to a consistent drop in noradrenergic transmission in the hippocampus (n=1). a) example of the hippocampal EEG (black) plotted against the GRAB-NE fluorescence signal (green). b) changes in GRAB-NE fluorescence for a series of individual seizures, c) average of all seizures ± SEM, d) changes in hippocampal EEG power vs. changes in GRAB-NE fluorescence for 1 second bins, and e) correlation between changes in hippocampal EEG power and GRAB-NE fluorescence.

While the data obtained is from a single mouse, the correlation is so consistent and clear that we expect to see it in additional animals – an experiment which is ongoing in this very moment. After establishing the dynamics of changes in noradrenergic transmission in relation to spontaneous seizures, we aim to modulate LC-noradrenergic transmission in relation to

hippocampal seizures to assess the neuromodulatory impact of changes in noradrenergic transmission in relation seizures. We have access to both DREADDs and optogenetics for modulation of the LC at different time scales.

3. Status and future directions

One manuscript has already been finalized with the support of GSKE. The preliminary data presented in this report is further expected to lead to at least two additional high quality publications with the continued support of the GSKE.

Geneeskundige Stichting Koningin Elisabeth
Fondation Médicale Reine Elisabeth
Königin-Elisabeth-Stiftung für Medizin
Queen Elisabeth Medical Foundation

Progress report of the research project of the young researcher

Dr. Delfien Syx
Universiteit Gent (UGent)

Delfien Syx, PhD (UGent)
Department of Biomolecular Medicine
Center for Medical Genetics Ghent (CMGG)
Ghent University Hospital
Medical Research Building I (MRB I) – Ingang 34
C. Heymanslaan 10
B-9000 Ghent
Belgium
T +32 9 33 2 1346
Delfien.Syx@ugent.be
www.cmgg.be
www.ugent.be/ge/biomolecular-medicine

Zebrafish as a model to study pain in Ehlers-Danlos syndromes

1. Background

Chronic pain affects up to 20% of the global population and represents a socio-economical health challenge. [1,2] The etiology of chronic pain is complex, and the underlying mechanisms are poorly understood. Consequently, treatment options are limited and often associated with considerable side effects and serious health risks. [3–5]

Over the years, a role for the extracellular matrix (ECM) in the development and persistence of pain has emerged. The ECM is a complex three-dimensional network that supports and maintains tissue and organ structure. The ECM consists of collagens, glycoproteins, proteoglycans, and secreted factors, which, together with the cells that produce them (e.g., fibroblasts), forms the connective tissue that is found throughout the body (e.g., in skin, bone, tendon and ligaments). [6] An ECM network also surrounds and functionally supports neuronal and non-neuronal cells (including nociceptors) in the peripheral and central nervous systems (PNS/CNS). [7,8] Furthermore, painful peripheral injuries were shown to cause acute and chronic ECM remodeling and/or alter ECM modifying enzymes. [8–10]

The link between the ECM and pain is further reinforced by the presence of chronic widespread pain in several monogenic heritable connective tissue disorders, caused by genetic defects affecting individual ECM components. [11–14] One of these disorders are the Ehlers-Danlos syndromes (EDS), a heterogeneous group of conditions hallmarked by joint hypermobility, soft and hyperextensible skin, abnormal wound healing and generalized tissue fragility. [15] To date, 13 distinct EDS types are recognized, of which 12 are molecularly elucidated and caused by defects in 20 different genes, mainly affecting collagens, proteoglycans and glycoproteins. [15,16] All these EDS-related defects compromise ECM architecture, often visible as ultrastructural changes in the organization and/or structure of collagen fibrils. [17] Chronic widespread pain occurs in 90% of EDS patients and is often one of the main reasons patients seek medical care. [12,18] Despite its high prevalence, little is known about the precise origins and mechanisms contributing to EDS-related pain and the pain is usually inadequately controlled by currently used treatments. An important reason for this is the lack of studies investigating the existing knowledge gaps.

Zebrafish (*Danio rerio*) has emerged as a promising animal model to reliably study pain-related behavior and associated mechanisms since their nervous system shows great similarity to humans. [19–23] We created *b4galt7*$^{-/-}$ and *b3galt6*$^{-/-}$ zebrafish, models of spondylodysplastic EDS (spEDS) [25,26] and *chst14*$^{-/-}$ zebrafish, a model of musculocontractural EDS (mcEDS) (unpublished). Both spEDS and mcEDS result from genetic defects in enzymes involved in proteoglycan biosynthesis. In addition, a zebrafish model with defective collagen biosynthesis was previously investigated: *col1a2*$^{-/-}$ zebrafish, a model of cardiac-valvular EDS (cvEDS). [24]

My research aims to assess the contribution of the abnormal ECM and untangle the specific mechanisms that induce pain and peripheral nervous system changes using EDS zebrafish as a model.

2. Preliminary results

2.1. Evaluating pain-related behavior in EDS zebrafish

Potentially painful events lead to behavioral and physiological changes in zebrafish. [19] Studies have demonstrated that healthy zebrafish are usually swimming constantly, using mid-water and all areas of their tank. In contrast, zebrafish subjected to potentially painful treatment showed increased use of the bottom of the tank (diving behavior) and reduce swimming and activity. [23,27]

To analyze the general swimming behavior of young wild-type zebrafish of 5 days post fertilization (dpf), several experimental setups were tested, including the use of different container sizes (e.g., zebrafish individually placed in 6, 12, 24 or 48 well plates) and several setups with different duration in light and dark conditions. Following this initial exploratory phase in wild-type zebrafish, we opted to use 12-well plates to accommodate 5 dpf zebrafish for subsequent testing since this gave the most consistent results and still allows for a relatively high throughput during testing. The first 10 minutes of the experiment were considered an acclimatization period and were not used for analyses. During the experiment, the temperature was kept constant at 28°C using a Temperature Control Unit (Noldus, The Netherlands). Locomotor activity was analyzed using the DanioVision Observation Chamber (Noldus, The Netherlands) equipped with a Basler GenICam camera capturing 30 frames/second for image acquisition. Data was recorded and analyzed using the EthoVision XT 15 software (Noldus, The Netherlands). For each zebrafish, center-point detection was used. Movement was expressed as cumulative time spent moving (%). Following behavioral analysis, all zebrafish were genotyped. For each EDS zebrafish line, wild-type (+/+), heterozygotes (+/-), and knockout (-/-) animals were examined.

We confirmed decreased movement of 5 dpf wild-type zebrafish following addition of 0.25% acetic acid to the water (Figure 1A), which mimics published findings [23]0.1% and 0.25% and indicates that our experimental setup and conditions can pick up altered swimming behavior in response to a known stimulus.

Analysis of the behavior of 5 dpf *chst14*$^{-/-}$, *b3galt6*$^{-/-}$ and *col1a2*$^{-/-}$ zebrafish, models for mcEDS-*CHST14,* spEDS-*B3GALT6* and cvEDS, respectively, did not show differences in movement compared to wild-type siblings (Figure 1B, 1C and 1E). No differences could be observed between the knockout zebrafish or wild-type and heterozygous zebrafish from the same clutch (Figure 1C and 1E), except for the *chst14* line where wild-type siblings moved less compared to heterozygous siblings (Figure 1B).

When studying locomotor activity of 5 dpf *b4galt7*$^{-/-}$ zebrafish, a model for spEDS-*B4GALT7*, we found that *b4galt7*$^{-/-}$ zebrafish moved significantly less compared to wild-type and *b4galt7*$^{+/-}$ zebrafish (Figure 1D). This finding is similar to what is seen when treating 5dpf zebrafish with a painful stimulus (Figure 1A). Given the observed variability in behavior between wild-type 5 dpf zebrafish and the fact that different clutches (= offspring from one breeding) can show differences in severity of the phenotype, the behavior experiments were repeated two times starting from independent clutches, which resulted in comparable results.

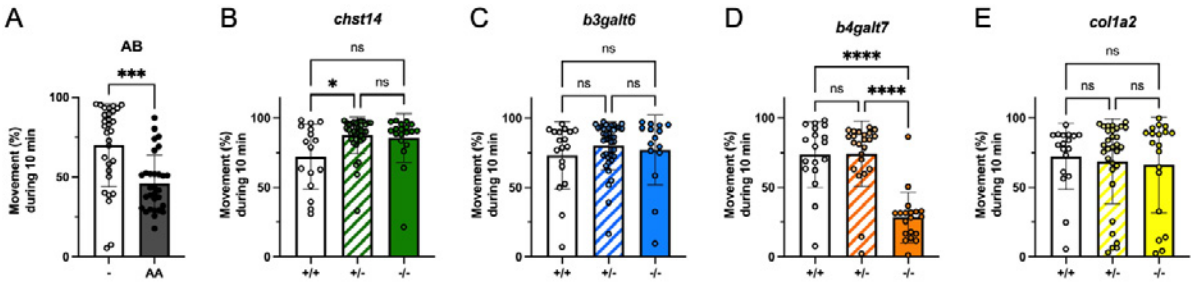

Figure 1 | Behavioral analysis of 5 dpf zebrafish. Movement (in %) during 10 minutes tracking in light conditions. **(A)** Positive control without (-) or with (AA) addition of 0.25% acetic acid in the water of wild-type (AB) zebrafish. **(B)** *chst14*$^{-/-}$, **(C)** *b3galt6*$^{-/-}$ **(D)** *b4galt7*$^{-/-}$ and **(E)** *col1a2*$^{-/-}$ zebrafish and their wild-type and heterozygous siblings. Data is presented as mean ± standard deviation. Every dot represents an individual zebrafish. +/+: wild-type, +/-: heterozygous, and -/-: homozygous zebrafish. * p<0.05; *** p<0.001, **** p<0.0001, t-test (A) or one-way ANOVA (B-E).

To confirm that the altered behavior in *b4galt7*$^{-/-}$ zebrafish, corresponds to a pain-related response, we tried to reverse the behavior by addition of analgesics. Several analgesics have been shown to lead to effective pain-relief in zebrafish. [28] Addition of the non-steroidal anti-inflammatory drugs aspirin (0.01 mg/ml) to the water of the *b4galt7* line did not convincingly show amelioration of the phenotype, however only a limited number of homozygous mutants were analyzed, hence this experiment will be repeated.

So far, behavior analysis has only focused on one parameter (movement), but more subtle behavioral changes might also be indicative of pain-related behavior. Therefore, the obtained data will also be investigated for alterations in turn angle, meandering, etc. Alternatively, pain-related behavior can also develop at a later age. Therefore, behavioral analysis will also be performed in adult zebrafish (> 3 months).

2.2. Monitoring neuronal development in EDS zebrafish

To acquire information about the effect of an aberrant ECM on **neuronal development**, EDS zebrafish models will be crossed with the Tg(*neurog1:EGFP*) line (available in our lab), expressing the pro-neural transcription factor neurogenin1 which is a key regulator for dorsal root ganglion (DRG) neuron development. [29] These crossings will be started soon, and will require some time to obtain homozygous zebrafish in the Tg(*neurog1:EGFP*) background.

To introduce a less time-consuming method to evaluate neuronal development, we started optimizing the NeuroTracer DiI tissue-labeling paste (Thermo Fisher Scientific) that serves as an alternative staining to visualize the nervous system. Several pilot experiments did not yet result in proper visualization of the nervous system. Hence further efforts are required to obtain a suitable protocol.

2.3. Generation and phenotypic characterization of col5a1+/- zebrafish

Our group previously demonstrated the presence of pain in patients with classical EDS (cEDS), caused by genetic defects in the *COL5A1* and *COL5A2* genes. [30] In addition, we showed the presence of pain-related behavior and concomitant alterations in the dermal nociceptive innervation in *Col5a1*$^{+/-}$ mice, a validated model of cEDS. [31] In view of these findings, we aimed to create a zebrafish counterpart that mimics the human cEDS phenotype to assess pain-related behaviors as a proof-of-concept. Since young zebrafish are well-suited for large-scale drug/compound screenings, these EDS zebrafish would open opportunities to start exploring potential therapeutic options.

CRISPR/Cas9-based genome editing was used to generate mutant *col5a1* zebrafish lines (Figure 2). The aim is to obtain zebrafish carrying a premature termination codon, predicted to result in *col5a1* haploinsufficiency, the most common molecular defect observed in cEDS patients and similar to the defect in *Col5a1*$^{+/-}$ mice. Two different models were generated to account for possible off-target effects.

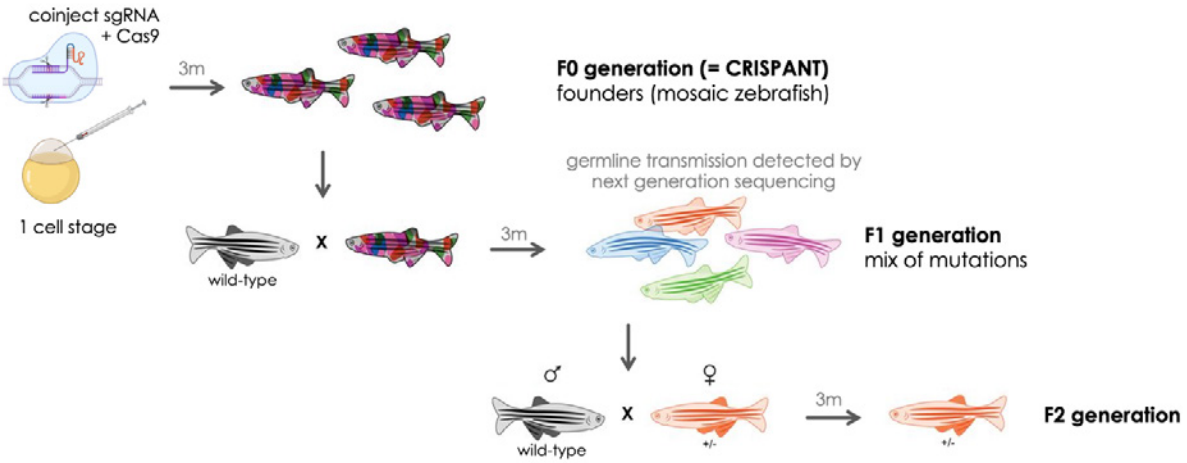

Figure 2 | Schematic overview of the generation of the *col5a1* zebrafish lines using CRISPR/Cas9 genome editing. Adapted from Varshney *et al.* Genome Research, 2015. [32]we present a high-throughput targeted mutagenesis pipeline using CRISPR/Cas9 technology in zebrafish that will make possible both saturation mutagenesis of the genome and large-scale phenotyping efforts. We describe a cloningfree single-guide RNA (sgRNA

Two sgRNAs were designed that target either exon 8 or exon 10 of the zebrafish *col5a1* gene and were individually injected with Cas9 protein into one-cell stage zebrafish eggs. This resulted in an overall indel efficiency of 86,6% for exon 8 and 95,4% for exon 10. Overall, there was a high mortality of injected zebrafish. The surviving zebrafish represent the F0 generation, also called crispants, and are mosaic for different genetic alterations in the *col5a1* gene. These crispants were grown till 3 months of age, bred with wild-type zebrafish and their offspring was tested for germline transmission of the out-of-frame indel variants. Next, a founder crispant zebrafish which carries a high frequency of out-of-frame variants was selected for each of the targeted exons. These founders were subsequently crossed with a wild-type zebrafish and their offspring was allowed to grow till adulthood. This resulted in a mixture of zebrafish, each carrying a particular mutation. We selected zebrafish with a 5bp deletion in exon 8 (cmg109) and 1bp duplication in exon 10 (cmg111) for further establishing stable mutant zebrafish lines. Currently, F2 generation zebrafish are being bred for subsequent phenotypic characterization, but initial behavior testing of the *col5a1* (cmg109) line has been performed.

Analysis of the behavior of 5 dpf heterozygous *col5a1*$^{+/-}$ zebrafish (the expected model of cEDS) did not show differences in movement compared to wild-type siblings (Figure 3). However, we found that homozygous *col5a1*$^{-/-}$ zebrafish moved significantly less compared to wild-type and *col5a1*$^{+/-}$ zebrafish. This finding resembles what is seen when treating 5 dpf zebrafish with a painful stimulus (Figure 1A) and the altered behavior in *b4galt7*$^{-/-}$ zebrafish (Figure 1D).

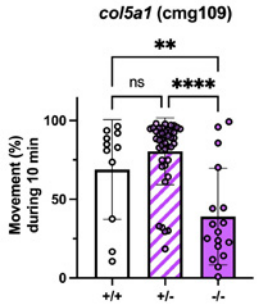

Figure 3 | Behavioral analysis in *col5a1* zebrafish. Movement (in %) during 10 minutes tracking in light conditions. Data is presented as mean ± standard deviation. Every dot represents an individual zebrafish. +/+: wild-type, +/-: heterozygous, and -/-: homozygous zebrafish. ** p<0.01; **** p<0.0001, one-way ANOVA.

Given the reported embryonic lethality of homozygous knockout (*Col5a1*$^{-/-}$) mice, it was initially surprising to notice that homozygous knockout (*col5a1*$^{-/-}$) zebrafish were found at the 5 dpf timepoint when performing genotyping for the zebrafish following behavior analysis. [33]type I collagen accounts for the majority of the collagen mass, and collagen type V, the functions of which are poorly understood, is a minor component. Type V collagen has been implicated in the regulation of fibril diameter, and we reported recently preliminary evidence that type V collagen is required for collagen fibril nucleation (Wenstrup, R. J., Florer, J. B., Cole, W. G., Willing, M. C., and Birk, D. E. (2004 This prompted to evaluate the genotype of for the *col5a1* zebrafish lines over time. This showed that at 1 dpf, the different genotypes approximate the expected Mendelian ratios. This ratio changes during the early stages of development with a clear decrease to absence of homozygous zebrafish at 14 dpf (Figure 4). This indicates that, at least in early developmental stages in zebrafish, the lack of type V collagen is viable, but is associated with behavioral alterations.

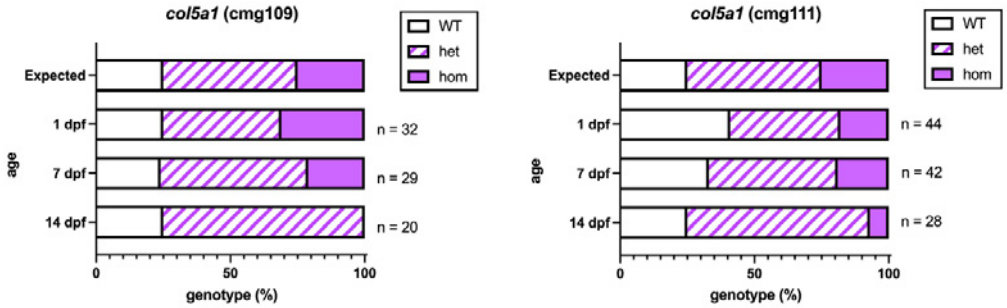

Figure 4 | Genotyping experiment. A clutch of zebrafish offspring from the indicated lines were divided in three equal parts (initial number of zebrafish per part: n = 32 for cmg109 and n = 44 for cmg111) and genotypes were determined after 1, 7 and 14 dpf. The number of surviving animals at each age is indicated next to the bars.

The *col5a1* zebrafish lines will be further phenotypically and molecularly characterized by assessing general body morphology (e.g., length, (kypho)scoliosis, pigmentation), mechanical properties of soft connective tissue specimens as well as ultrastructural analysis to assess collagen architecture in the ECM using transmission electron microscopy, since similar alterations are seen in the human (and murine) counterpart of cEDS. Currently, the study of the effect of the variants on type V collagen quantity (and quality) was hampered by to the lack of a working antibody against type V collagen, a problem that is frequently encountered when working with zebrafish proteins, but different antibodies will be tested to investigate protein levels in more depth.

3. References

1. Goldberg, D.S. and McGee, S.J. (2011) Pain as a global public health priority. *BMC Public Health* 11
2. Breivik, H. *et al.* (2006) Survey of chronic pain in Europe: Prevalence, impact on daily life, and treatment. *Eur. J. Pain* 10, 287
3. Wolfe, M.M. *et al.* (1999) Gastrointestinal toxicity of nonsteroidal antiinflammatory drugs. *N. Engl. J. Med.*
4. Shipton Elspeth E Shipton Ashleigh J Shipton, E.A. (2018) A Review of the Opioid Epidemic: What Do We Do About It? *Pain Ther.* 7, 23–36
5. Skolnick, P. (2018) The Opioid Epidemic: Crisis and Solutions. *Annu. Rev. Pharmacol. Toxicol. Annu. Rev. Pharmacol. Toxicol* 58, 143–59
6. Frantz, C. *et al.* (2010) The extracellular matrix at a glance*Journal of Cell Science*, 1234195–4200
7. Barros, C.S. *et al.* (2011) Extracellular Matrix: Functions in the nervous system. *Cold Spring Harb. Perspect. Biol.* 3, 1–24
8. Tajerian, M. and Clark, J.D. (2015) The role of the extracellular matrix in chronic pain following injury*Pain*, 156Lippincott Williams and Wilkins, 366–370
9. Tajerian, M. and Clark, J.D. (2019) Spinal matrix metalloproteinase 8 regulates pain after peripheral trauma. *J. Pain Res.* 12, 1133–1138
10. Parisien, M. *et al.* (2019) Genetic pathway analysis reveals a major role for extracellular matrix organization in inflammatory and neuropathic pain. *Pain* 160, 932–944
11. Velvin, G. *et al.* (2016) Systematic review of chronic pain in persons with Marfan syndrome*Clinical Genetics*, 89Blackwell Publishing Ltd, 647–658
12. Voermans, N.C. *et al.* (2010) Pain in Ehlers-Danlos Syndrome is common, severe, and associated with functional impairment. *J. Pain Symptom Manage.* 40, 370–378
13. Nghiem, T. *et al.* (2017) Pain Experiences of Children and Adolescents with Osteogenesis Imperfecta: An Integrative Review*Clinical Journal of Pain*, 33Lippincott Williams and Wilkins, 271–280
14. Nghiem, T. *et al.* (2018) Pain experiences of adults with osteogenesis imperfecta: An integrative review. *Can. J. Pain* 2, 9–20
15. Malfait, F. *et al.* (2020) The Ehlers–Danlos syndromes. *Nat. Rev. Dis. Prim.* 6, 64
16. Malfait, F. *et al.* (2017) The 2017 international classification of the Ehlers–Danlos syndromes. *Am. J. Med. Genet. Part C Semin. Med. Genet.* 175, 8–26
17. Malfait, F. *et al.* (2021) Collagens in the Physiopathology of the Ehlers–Danlos Syndromespp. 55–119
18. Sacheti, A. *et al.* (1997) Chronic Pain Is a Manifestation of the Ehlers-Danlos Syndrome. *J. Pain Symptom Manage.* 14, 88–93
19. Sneddon, L.U. (2019) Evolution of nociception and pain: Evidence from fish models*Philosophical Transactions of the Royal Society B: Biological Sciences*, 374Royal Society Publishing
20. Braithwaite, V.A. and Boulcott, P. (2007) Pain perception, aversion and fear in fish. *Dis. Aquat. Organ.* 75, 131–138
21. Costa, F. V. *et al.* (2021) The use of zebrafish as a non-traditional model organism in translational pain research: the knowns and the unknowns. *Curr. Neuropharmacol.* 19
22. Sneddon, L.U. (2015) Pain in aquatic animals*Journal of Experimental Biology*, 218Company of Biologists Ltd, 967–976
23. Lopez-Luna, J. *et al.* (2017) Reduction in activity by noxious chemical stimulation is ameliorated by immersion in analgesic drugs in zebrafish. *J. Exp. Biol.* 220, 1451–1458
24. Gistelinck, C. *et al.* (2018) Zebrafish type I collagen mutants faithfully recapitulate human type I collagenopathies. *Proc. Natl. Acad. Sci. U. S. A.* 115, E8037–E8046
25. Delbaere, S. *et al.* (2020) Hypomorphic zebrafish models mimic the musculoskeletal phenotype of β4GalT7-deficient Ehlers-Danlos syndrome. *Matrix Biol.* 89, 59–75
26. Delbaere, S. *et al.* (2020) b3galt6 Knock-Out Zebrafish Recapitulate β3GalT6-Deficiency Disorders in Human and Reveal a Trisaccharide Proteoglycan Linkage Region. *Front. Cell Dev. Biol.* 8
27. Deakin, A.G. *et al.* (2019) Automated monitoring of behaviour in zebrafish after invasive procedures. *Sci. Rep.* 9
28. Chatigny, F. *et al.* (2018) Updated Review of Fish Analgesia. *J. Am. Assoc. Lab. Anim. Sci.* 57, 5–12
29. McGraw, H.F. *et al.* (2008) Zebrafish dorsal root ganglia neural precursor cells adopt a glial fate in the absence of neurogenin1. *J. Neurosci.* 28, 12558–12569
30. Colman, M. *et al.* (2023) Sensory Profiling in Classical Ehlers-Danlos Syndrome: A Case-Control Study Revealing Pain Characteristics, Somatosensory Changes, and Impaired Pain Modulation. *J. Pain* 24, 2063–2078
31. Syx, D. *et al.* (2020) Pain-related behaviors and abnormal cutaneous innervation in a murine model of classical Ehlers-Danlos syndrome. *Pain* 161, 2274–2283
32. Varshney, G.K. *et al.* (2015) High-throughput gene targeting and phenotyping in zebrafish using CRISPR/Cas9. *Genome Res.* 25, 1030–1042
33. Wenstrup, R.J. *et al.* (2004) Type V collagen controls the initiation of collagen fibril assembly. *J. Biol. Chem.* 279, 53331–53337

Geneeskundige Stichting Koningin Elisabeth
Fondation Médicale Reine Elisabeth
Königin-Elisabeth-Stiftung für Medizin
Queen Elisabeth Medical Foundation

Progress report of the research group of

Dr. Marijne Vandenbergh
Universiteit Antwerpen (UAntwerpen)

Dr. Marijne Vandebergh (UAntwerpen)
Campus Drie Eiken
Center for Molecular Neurology
Universiteitsplein 1
2610 Wilrijk
marijne.vandebergh@uantwerpen.be
Tel. +3232653978

World-wide systematic characterization of TMEM106B and ATXN2 genetic status Towards implementation of genetic testing of modifiers in clinical practice

1. Research Summary

Frontotemporal lobar degeneration (FTLD) is a quickly progressing debilitating neurodegenerative disease and one of the leading causes of young-onset dementia. There are no treatments available that delay the onset or slow down disease progression. The most common form causes changes in behavior and personality, hence FTLD imposes a dramatic impact on social life. In about 30% of patients, a strong family history is present. Autosomal dominant mutations in the chromosome 9 open reading frame 72 (*C9orf72*) gene, the microtubule-associated protein tau (*MAPT*) gene and the progranulin (*GRN*) gene are the most common causes of genetic frontotemporal dementia (FTD). FTD is characterized by variability in age at onset and clinical presentation, even within families. This variability remains poorly understood. Previous studies suggest the transmembrane protein 106 B (*TMEM106B*) and ataxin 2 (*ATXN2*) loci as genetic modifiers of disease risk, especially in patients who already carry dominant disease mutations. The discovery of these loci is exciting; however, studies have been limited in sample size and detailed characterization of the patient cohorts.
In this project, the aims are to:
Characterize the *TMEM106B* protective haplotype and *ATXN2* intermediate repeat carrier status by systematic genotype screens in well-characterized large FTD cohorts and within families
Investigate whether the *TMEM106B* protective haplotype and *ATXN2* intermediate repeats correlate with progression of disease by linking genetic data with detailed longitudinally collected clinical, neurophysiological and imaging data

2. Progress Report

2.1. Characterization of the TMEM106B protective haplotype and ATXN2 intermediate repeat carrier status in large FTD cohorts

Over the past year, the distribution of the *TMEM106B* protective haplotype and *ATXN2* intermediate repeat carrier status was determined in the ARTFL/LEFFTDS Longitudinal Frontotemporal Lobar Degeneration study (ALLFTD, NCT04363684). ALLFTD is a consortium with 27 centers across the US and Canada. For this study, participants were enrolled between 2015 and 2023.

In a cohort of 1789 individuals, we genotyped the *TMEM106B* rs1990622 single nucleotide variant (SNV) and determined the repeat length of *ATXN2* (**Table 1**). A repeat length of at least 27 was defined as intermediate repeat.

	Non-mutation carriers	C9orf72	GRN	MAPT
Total number	1275	254	118	124
***TMEM106B* rs1990622**				
A/A	405	97	54	47
A/G	626	120	56	60
G/G	244 (19%)	37 (15 %)	8 (7%)	17 (14%)
ATXN2				
Repeat length ≥ 27	2.8 %	8.8%	1.5%	2.4%

Table 1. Distribution of TMEM106B rs1990622 and ATXN2 intermediate repeats in ALLFTD

TMEM106B rs1990622 is a common variant, with a minor allele frequency of ~ 40 % in the European non-Finnish population (gnomAD v4.0). Comparing the genetic groups, there is a lower percentage of *TMEM106B* rs1990622*G/G carriers in the *GRN* group. The distribution of the rs1990622 genotype is significantly lower in *GRN* mutation carriers than in participants not carrying a pathogenic mutation in any of the known FTD genes and *C9orf72* mutation carriers (Fisher exact test $p < 0.05$, adjusted for multiple pairwise comparisons with the false-discovery rate method). The *TMEM106B* locus was identified as a genetic modifier of disease risk in individuals with *GRN* mutations, with carriers of the protective haplotype (rs1990622*G) having a 50% lower odds to develop disease symptoms compared to *TMEM106B* non-protective haplotype carriers with *GRN* mutations[1]. Furthermore, our group has shown that *TMEM106B* alters the penetrance of *GRN* mutation. A patient in their 50s presented in the clinic with symptoms of behavioral variant FTD, and genetic testing revealed a pathogenic *GRN* mutation. The patient's asymptomatic parent who was in their 80s was also found to carry the *GRN* mutation, but also carried two copies of the protective *TMEM106B* allele[2]. Hence, we believe that that *GRN* mutation carriers with TMEM106B rs1990622*GG are seen less often in the clinic as they remain without symptoms, and are hence not enrolled in research studies. This would explain the lower proportion of *TMEM106B* rs1990622*GG carriers across *GRN* mutation carriers. We are currently collecting clinical data of *GRN* mutation carriers with the *TMEM106B* protective haplotype beyond ALLFTD, to further demonstrate that these individuals remain healthy at a relatively old age.

In the ALLFTD study, intermediate length repeats in *ATXN2* are more frequent in *C9orf72* mutation carriers than in participants not carrying a pathogenic mutation in any of the known FTD genes (Fisher exact test $p < 0.05$, adjusted for multiple pairwise comparisons with the false-discovery rate method). Interestingly, upon comparison of the clinical phenotypes of C9orf72 carriers with *ATXN2* intermediate repeats, we observed that there are two *C9orf72* mutation carriers in ALLFTD with the progressive supranuclear palsy (PSP) phenotype, a phenotype only rarely associated with C9orf72, and both individuals carry an intermediate *ATXN2* repeat (**Figure 1**). Currently, I am collecting DNA samples of other rare published cases with a *C9orf72* mutation and a PSP phenotype to conduct screenings for *ATXN2*, to investigate whether *ATXN2* is acting as a modifier of the PSP phenotype in *C9orf72* mutation carriers.

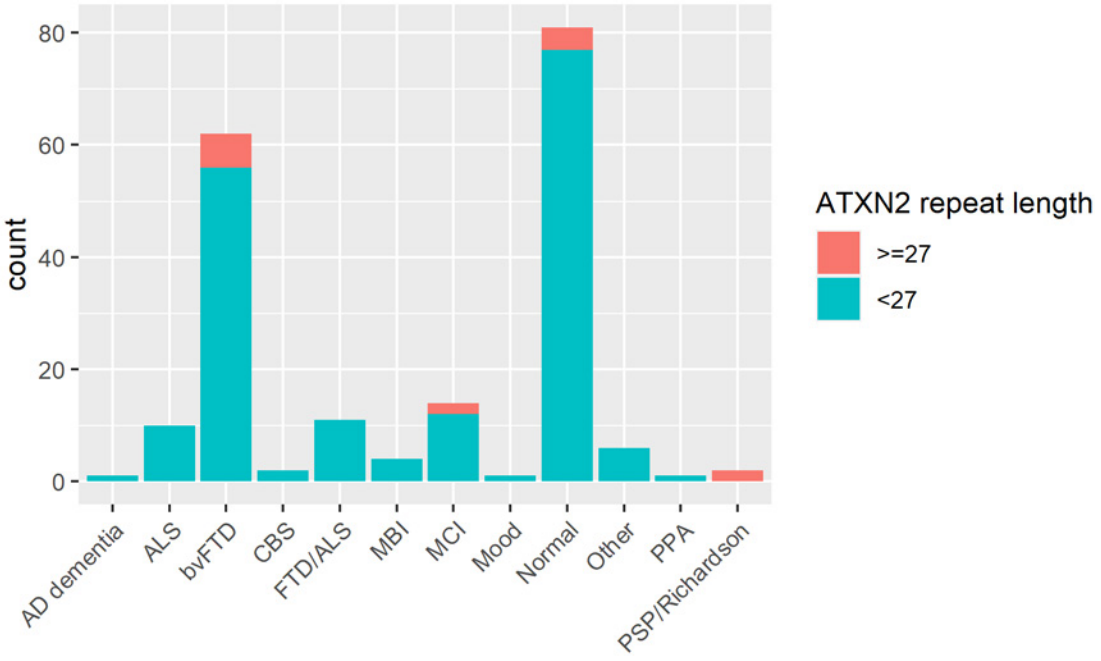

Figure 1. The distribution of ATXN2 intermediate repeats across the clinical phenotypes of C9orf72 mutation carriers in ALLFTD.

2.2. Investigation whether the TMEM106B protective haplotype and ATXN2 intermediate repeats correlate with progression of disease

In ALLFTD participants, I have investigated the effect of *TMEM106B* on disease development. Looking at changes in volumetric gray matter measures, *GRN* carriers homozygous for the protective allele (rs1990622*GG) had significantly greater total gray matter volumes than *GRN* mutation carriers without or with only one protective allele (linear mixed model with years of education, sex, age at visit and the CDR+NACC-FTLD sum of boxes as covariate and with pedigree as random effect, = 3.25 [0.37,6.19], p = 0.034). Looking at individual (sub)cortical regions of interest, the left thalamic region was the top individual region of interest (p = 0.006). Currently, we are conducting association analyses with other clinical measures including cognitive scores, to further map the modifying effect of *TMEM106B* (Vandebergh et al., manuscript in preparation). Likewise, analyses are being conducted to investigate the modifying effect of *ATXN2*.

3. References

1. Pottier C, Zhou X, Perkerson RB, 3rd, et al. Potential genetic modifiers of disease risk and age at onset in patients with frontotemporal lobar degeneration and GRN mutations: a genome-wide association study. *Lancet Neurol* 2018; **17**(6): 548-58.
2. Perneel J, Manoochehri M, Huey ED, Rademakers R, Goldman J. Case report: TMEM106B haplotype alters penetrance of GRN mutation in frontotemporal dementia family. *Front Neurol* 2023; **14**: 1160248.

Geneeskundige Stichting Koningin Elisabeth
Fondation Médicale Reine Elisabeth
Königin-Elisabeth-Stiftung für Medizin
Queen Elisabeth Medical Foundation

Progress report of the research project of the young researcher

Dr. Barbara M.P. Willekens
Universiteit Antwerpen (UAntwerpen)

Prof. dr. Barbara Willekens (UAntwerpen)
Neurologist | MS & CNS Neuroimmune Disorders
T +32 3 821 34 23
Barbara.willekens@uza.be

Department of Neurology
UZA, Drie Eikenstraat 655, 2650 Edegem
T +32 3 821 30 00
www.uza.be/neurologie

University of Antwerp
Translational Neurosciences Research Group
Laboratory of Experimental Hematology, Vaccine & Infectious Disease Institute (VAXINFECTIO)
Faculty of Medicine and Health Sciences
Universiteitsplein 1, 2610 Antwerp, Belgium
Barbara.willekens@uantwerpen.be

Unravelling the role of antigen-specific T cells in NMOSD and MOGAD: first progress report

1. Project summary

Neuromyelitis Optica Spectrum Disorders (NMOSD) and Myelin Oligodendrocyte Glycoprotein Antibody Associated Disease (MOGAD) are rare autoimmune diseases of the central nervous system (CNS) that are distinct from multiple sclerosis (MS), a more prevalent CNS autoimmune disease [1, 2]. Disease pathogenesis is clearly different: the autoantigens are well-defined in Aquaporin-4 positive (AQP4+) NMOSD and MOGAD, in contrast with MS [3]. Despite the fact that there is evidence for a key role of T cells in the pathogenesis of NMOSD and MOGAD, the focus of research has been directed more towards unravelling the role of auto-antibodies. However, improved understanding of antigen-specific T cell functions could be a first step on the road towards development of more targeted therapies, such as antigen-specific cell based treatments [4]. The importance of T cells in the pathogenesis of NMOSD and MOGAD is supported by (i) pathological features in human tissue, (ii) T cell help is needed for blood-brain-barrier breakdown and pathogenicity of auto-antibodies, (iii) Th1 and Th17 pro-inflammatory cytokine profile. However, detection of antigen-specific T cells in the peripheral blood of people with AQP4+ NMOSD and even more so in MOGAD, has been challenging so far [5]. Detection and functional characterisation of antigen-specific autoreactive T cells in the peripheral blood is a necessary step to demonstrate and strengthen the evidence for the pivotal role of T cells in the pathogenesis of NMOSD and MOGAD and may pave the way towards future development of antigen-specific T cell modulatory treatments [3, 4].

2. Research hypothesis and objectives

It is the aim of the applicant to unravel the role of antigen-specific T cells in AQP4+ NMOSD and MOGAD. This knowledge will aid in paving the road towards development of antigen-specific tolerance inducing cell-based treatments for NMOSD and MOGAD [4]. Previous research of our group in the field of MS has demonstrated that longitudinal analysis of myelin-specific T cells with IFN- ELISPOT assay in a cohort of MS patients treated with natalizumab showed a high variability over time [6]. Hence, low frequencies of MOG-specific T cells when measured in a cross-sectional setting could be another explanation for the previous failure of Hofer et al. to detect MOG-specific T cells in a small cohort of MOGAD patients [5]. The primary hypothesis is that T cell responses are detectable in at least 50% of participants with MOGAD and AQP4+ NMOSD [5] and are variable over time in affected individuals. The second hypothesis is that antigen-specific T cells are functionally different between NMOSD and MOGAD patients versus healthy controls.

The objectives are:

1. To identify MOG specific and AQP4 specific T cells in patients with MOGAD and AQP4+ NMOSD.
2. To characterize the functional phenotype of antigen-specific T cells in patients with MOGAD and AQP4+ NMOSD
   - To investigate the secretion of the cytokines in frozen cell culture supernatants.
   - To identify brain-homing potential of antigen-specific CD4+ T cells expression of CXCR3, CCR4 and CCR6.

3. Methodology

Work package 1: Preparation of experiments
Study protocol and informed consent document preparation and writing
Obtain approval from ethical committee (G1)
Register project in biobank
Optimize experimental set-up and test IFN- and IL-6 ELISPOT assay
Work package 2: Experiments
Work package 3: Data analysis
Work package 4: Dissemination

4. Workplan

	Year 1				Year 2				Year 3			
	Q1	**Q2**	**Q3**	**Q4**	**Q1**	**Q2**	**Q3**	**Q4**	**Q1**	**Q2**	**Q3**	**Q4**
WP1		*G1*	**G1**									
WP2				*M2*	**M2**			M3	**M3**			
WP3						M4	**M4**				**M6**	
WP4	**M1**					M5	**M5**		**M5**			**M7**

G1=EC approval, M1=communication on obtaining of funding, M2=all patients included for cross-sectional analysis, M3=all patients included in longitudinal analysis, M4=interim results of cross-sectional analysis , M5=conference presentation, M6=study report finalized, M7=manuscript

5. Current status of the project

5.1. Milestone 1 communication on obtaining of funding: reached on time

Obtaining of the funding was announced by the University of Antwerp and the Antwerp University Hospital, on the Faculty of Medicine and Health Sciences internal newsletter, on my personal webpage of the University of Antwerp, and on the personal LinkedIn account of the applicant, reaching 8346 impressions, 266 reactions, 29 commentaries and 1 repost, providing visibility for the Queen Elisabeth Medical Foundation.

5.2. Work package 1 preparation of experiments

- Study protocol and informed consent document preparation and writing: this has been finalized, study protocol and informed consent documents are in place.
- Obtain approval from ethical committee (G1)
  Final EC approval was obtained on July 24, 2023. This part had a delay of around 3 months, as it took several months in the start of the year to organize the administration of the grant at the University (settled in March 2023).
- Register project in biobank. For this, contracts between University Hospital Antwerp and the University of Antwerp needed to be put in place. This took longer than expected and all necessary documents and contracts were finalized in December 2023.
- Optimize experimental set-up and test IFN- and IL-6 ELISPOT assay: starting February 2024
  Due to these delays, the workplan has been adapted accordingly (see workplan, rescheduled milestones colored in orange). The finalization of the project remains feasible within the timelines.

5.3. The following work packages will start in 2024 and 2025

Work package 2: Experiments (2024)
Work package 3: Data analysis (2025)
Work package 4: Dissemination (2024-2025)

6. Research output with QEMF acknowledgement

No publications yet with QEMF support.
Applicant published one case report on MOGAD

- Daems F, Derdelinckx J, Ceyssens S, Vanden Bossche S, Reynders T, **Willekens B**. Improved detection of MOG antibody-associated transverse myelitis with 18F-FDG-PET: a case report. Acta Neurol Belg. 2023 Apr;123(2):735-738.)
- An abstract for the 2024 Annual Meeting of the American Academy of Neurology was accepted for an oral talk (Etiologies of Myelopathy in Uganda Based On Neuroimaging, Autoantibodies, and Next Generation Sequencing; Kisekka Musubire Abdu , Kristoffer Leon , Eoin Flanagan , David Meya , David Boulware , Paul Bohjanen , Patrick Cras , **Barbara Willekens** , Sean Pittock , Michael Wilson)

7. Other relevant impact

Applicant was promoted to assistant professor of neurology with a focus on multiple sclerosis and neuroimmune disorders of the central nervous system at the Faculty of Medicine and Health Sciences of the University of Antwerp (10% appointment), per November 1st, 2023. She was invited speaker on MS mimics at the Belgian MS Symposium 2023 of the Belgian Society for Radiology. Applicant has been able to expand her international network on NMOSD and MOGAD and was invited to an international MOGAD meeting in Boston, and is involved in international MOGAD meetings and European MEDEN consortium. A MOGAD consortium meeting is planned in January 2025 in Philadelphia, and applicant aims to present results of this research during that meeting. Abstract submission to international conferences, will depend on the results, late breaking submission for ECTRIMS 2024 is being considered. Finally, applicant has been invited as speaker to a meeting on tolerance in Münster, to speak on the potential of tolDC in MOGAD, planned in March 2024.

8. References

1. Marignier, R., et al., *Myelin-oligodendrocyte glycoprotein antibody-associated disease.* Lancet Neurol, 2021. **20**(9): p. 762-772.
2. Wingerchuk, D.M., et al., *International consensus diagnostic criteria for neuromyelitis optica spectrum disorders.* Neurology, 2015. **85**(2): p. 177-89.
3. Lopez, J.A., et al., *Pathogenesis of autoimmune demyelination: from multiple sclerosis to neuromyelitis optica spectrum disorders and myelin oligodendrocyte glycoprotein antibody-associated disease.* Clin Transl Immunology, 2021. **10**(7): p. e1316.
4. Derdelinckx, J., et al., *Cells to the Rescue: Emerging Cell-Based Treatment Approaches for NMOSD and MOGAD.* Int J Mol Sci, 2021. **22**(15).
5. Hofer, L.S., et al., *Comparative Analysis of T-Cell Responses to Aquaporin-4 and Myelin Oligodendrocyte Glycoprotein in Inflammatory Demyelinating Central Nervous System Diseases.* Front Immunol, 2020. **11**: p. 1188.
6. Willekens, B., et al. *Longitudinal analysis of autoreactive T cells in a cohort of multiple sclerosis patients treated with natalizumab*. in *MULTIPLE SCLEROSIS JOURNAL*. 2021. SAGE PUBLICATIONS LTD 1 OLIVERS YARD, 55 CITY ROAD, LONDON EC1Y 1SP, ENGLAND.

Geneeskundige Stichting Koningin Elisabeth
Fondation Médicale Reine Elisabeth
Königin-Elisabeth-Stiftung für Medizin
Queen Elisabeth Medical Foundation

Progress report of the research project of the young researcher

Dr. Wouter Peelaerts
Katholieke Universiteit Leuven (KU Leuven)

Prof. Dr. Wouter Peelaerts (KU Leuven)
Department of Neurosciences
Laboratory for Neurobiology and Gene Therapy
Department of Pharmacy and farmacaceutical
O&N5b-Herestraat 49 box 1023
3000 Leuven
Belgium

Peripheral infections as a trigger of multiple system atrophy

1. Summary of project rationale and hypothesis

Multiple system atrophy (MSA) is a progressive and fatal neurodegenerative disease. The clinical presentation of MSA is heterogeneous as the disease affects a variety of central and peripheral autonomic functions. Although it is believed that MSA risk can be influenced by genetic or environmental factors no risk factors have been identified to date. In the absence of crucial insights into the molecular etiopathogenesis there are no available biomarkers for the early detection of early disease-related changes which limits efficient treatment options.
The hypothesis of this project is that MSA can be triggered by an infectious pathogen. We recently proposed that a trigger can occur before or during advanced disease stages and elicit a local or systemic host response[1]. Infections are prominent in MSA also during the prodrome, and manifest months or years before MSA diagnosis[2–4]. Our overarching goal is study both viral and bacterial infections in MSA and identify those pathogens that might have a significant impact in the development of neuropathology.

Infections manifest frequently in MSA but can go unnoticed because of autonomic failure, lower body temperature, desensitisation of the peripheral pain response or anhidrosis which can mask sudden changes, and which would otherwise warrant for signs of infection. Peripheral symptoms can mask ongoing infection and worsen disease progression. During advanced stages, infections can lead to neuropsychiatric effects[5,6] and sepsis[7]. Yet, and even though infections are common, it is not known if there is a causal link between infections and MSA.

This project focuses on the role of urinary tract infections in MSA. We discovered that urinary tract infections (UTIs) are strongly associated with MSA diagnosis when the infection occurs prior to disease onset. To the best of our knowledge, this is the first significant risk factor identified for MSA to date.

Our lab is currently investigating the contribution of several types of infections in MSA, including viral infections, but these studies are currently more exploratory whereas the focus of this project is on the role of UTIs in MSA. The link between UTIs and MSA is currently better established[8]. Our scientific goals build on these links with new methodological tools and animal models that recapitulate the complexity of genetic and environmental risk in MSA.

2. Scientific goals

Even though infections are thus common in MSA, it is not yet known if there is a direct or causal link between infections and MSA and/or if infections can influence disease progression. The neuroinflammatory response during UTIs has not been examined in MSA and it is also not known if infections in the lower urinary tract could influence central effects related to glial or neuronal health.

For our experimental approach, we use uropathogenic E. coli (UPEC) which is commonly used to experimentally model lower urinary tract infections as this pathogen leads to robust inflammatory responses in mouse.

To examine how peripheral infections influence αSyn pathology and trigger central changes, we have defined the following three aims:
① establish a direct link between peripheral infections and αSyn function
② identify neuroinflammatory triggers in response to peripheral infection
③ examine the influence of peripheral infection on MSA disease progression

The main objective of this project is to identify pathogen-related triggers of MSA and investigate how disease triggers contribute to disease progression in MSA. We will focus on the specific mechanisms underlying UTI-related disease triggers.

3. Research results

Below we have summarized the progress of this project in according to the three proposed work packages (WPs):

3.1. WP1. Determine the role of αSyn in innate immune cells during UTI

This WP focuses on identifying immune cells and subsets of immune cells that express αSyn. To this aim, mouse immune cells from αSyn WT and αSyn KO animals were used from blood and from infected urinary bladders. Via flow cytometry a panel of immune cell markers was optimized to distinguish eosinophils, neutrophils, infiltrating monocytes, inflammatory monocytes, macrophages, dendritic cells, T- and B cells (**Fig. 1**).

We have optimized the isolation and staining of different immune populations in mouse bladder after UTI (**Fig. 1**). As a proof of concept, we find that in mice that have no expression of αSyn, the composition of the populations of neutrophils (and other cells) is significantly altered. This shows that it is feasible to detect significant changes in mouse urinary bladder of UTIs and that αSyn has a potential role in the immune response. Using these methods, we will now further investigate the mechanisms behind these effects and study if these altered populations have a functional impact during UTIs.

A second goal was to develop a method that simultaneously allows to detect αSyn in immune cells. However, we found that during fixation and permeabilization of immune cells there is significant contamination αSyn from erythrocytes, an abundant source of αSyn. Therefore, it is not feasible to further investigate the presence of αSyn in different immune populations.

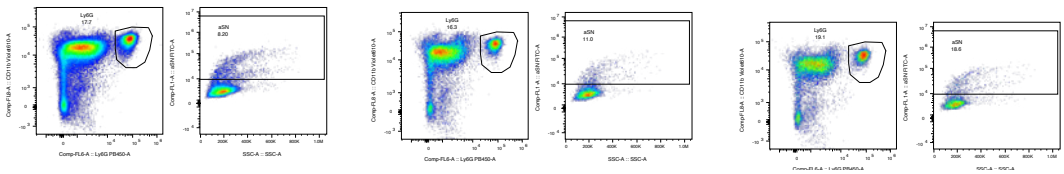

Figure 1. Flow cytometry of neutrophils cells in the urinary bladder after UTI. Flow cytometry results are shown for αSyn $^{+/+}$(WT), αSyn$^{+/-}$ (het), and αSyn$^{-/-}$ (KO) mice. Mice knock out for αSyn have a higher percentage of innate immune cells.

3.2. WP2. Detection of secreted bacterial exosomes to the CNS during UTI

Although peripheral UTIs can trigger a systemic response via inflammatory cytokines it is not known how they can modulate central responses. UTIs mostly trigger neuropsychiatric effects, including dementia and delirium[6,9]delirium is widely viewed as a consequence of and, therefore, a reason to initiate workup for urinary tract infection (UTI. Furthermore, existing neurological disorders can be precipitated because of UTIs[10] and subclinical conditions can develop into

persistent functional impairment suggesting a bidirectional contribution from one condition to the other[11,12]. One possibility is that bacterial extracellular vesicles, carrying LPS and other biomolecules, travel to the CNS where they can potentially cause damage to vulnerable cell populations[13]. The work in this WP is currently ongoing and we hope to provide an update during next progress report.

3.3. WP3. Study the impact of repeated UTIs on MSA progression

Central to MSA is αSyn that deposits throughout the central nervous system in oligodendroglial cells leading to demyelination and neurodegeneration[14]. The pathognomonic feature of MSA is the presence of deposits of the protein α-synuclein (αSyn) in oligodendroglial cells. Accumulation of αSyn results in progressive pathology in oligodendroglia with demyelination and cellular dysfunction. We and others have shown that aggregated αSyn can spread between cells and convert endogenous αSyn into its pathogenic form and which is reminiscent of prions[15]. Glial immune activation is often found in areas with high αSyn burden[16,17]. Considerable experimental and clinical evidence suggests that interactions between αSyn and the immune system occur physiologically[18–20]

To further study the impact in infections in MSA pathogenesis, our lab has recently characterized a humanized αSyn model to examine infectious disease triggers (**Fig. 2a**). These humanized mice ((Snca$^{-/-}$; PAC-Tg(SNCA^{WT}), Jackson #010710) express human αSyn instead of mouse αSyn under control of the endogenous human αSyn promoter. To examine the link between UTIs and MSA disease progression we now examined the effect of repeated infections (chronic UTIs) and if infections can aggravate αSyn pathology in transgenic humanized αSyn mice. To this aim, we superinfected humanized αSyn mice four times with UPEC over a course of 8 months. A superinfection is performed by infecting the animals twice, first with 10^8 CFU of UPEC, followed 24 hours later with 10^7 CFU of UPEC. PBS injected mice serve as a control. After 4 weeks of every superinfection animals received antibiotics to mimic normal clinical practices and to prevent the development of chronic infections or nephritis[21].

Animal's body weight was recorded periodically, and infection outcome was monitored from urine obtained by gentle suprapubic pressure and serially diluted and plated to quantify the colony forming units (CFU). We found that after repeated infections, rUTI treated animals developed chronic infections (**Fig. 2b-d**). Several of these mice had to be treated with antibiotics to remove the infection.

After completing their last round of antibiotics treatment, animals underwent motor performance testing using the CatWalk XT automated gait analysis system (Noldus Information Technology). This system employs a glass-floor walkway with fluorescence light beaming in the glass to track the animal's paws. It can detect natural gait, speed, coordination, and weight distribution. Animals were acclimated to the walkway over two days, with one session per day and were tested until they completed six compliant runs. We observed that animals with rUTIs had persisten behavioral changes (**Fig. 2e-k**), even several weeks after the last antibiotic treatment.

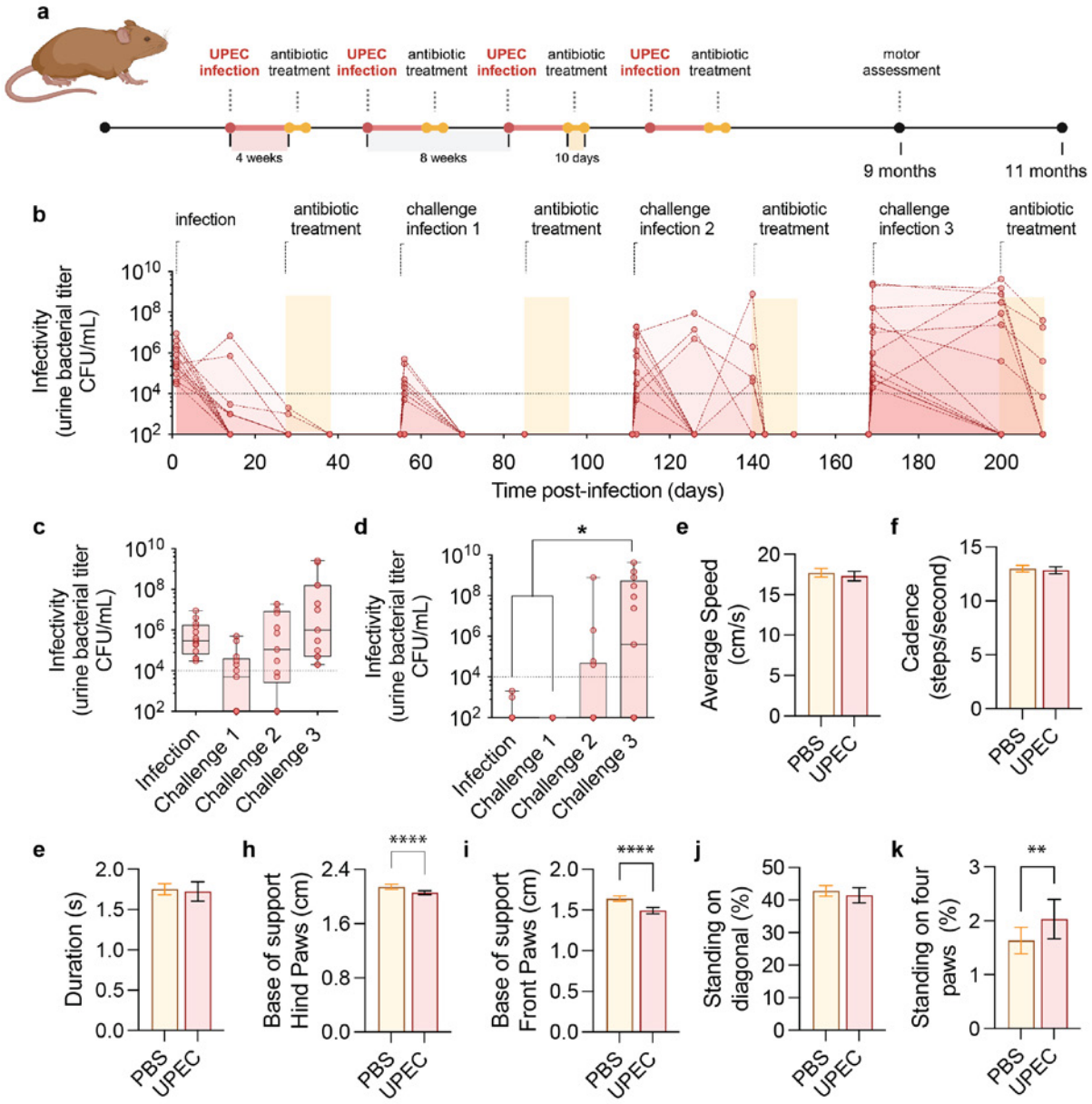

Figure 2. Repeated urinary tract infections in transgenic humanized synuclein mice.

Following rUTIs at 9 months post infection, the urinary bladders of were analyzed for inflammatory markers. The urinary bladder of animals infected with UPEC showed significant hypertrophy (**Fig. 3a**). Both bladder weight as well as bladder size were significantly increased in infected animals (**Fig. 3a-c**). To assess ongoing inflammation, urinary bladders were examined via immunohistochemistry for the markers CD45+ and MPO+ to visualize leukocytes and neutrophils, respectively. We observe that after repeated infection in humanized synuclein mice there is persistent inflammation. In line with this finding, we further find GFP-positive UPEC bacteria (**Fig. 3g**). This shows that after antibiotic treatment, UPEC bacteria are still detectable in the urinary bladder of infected mice.

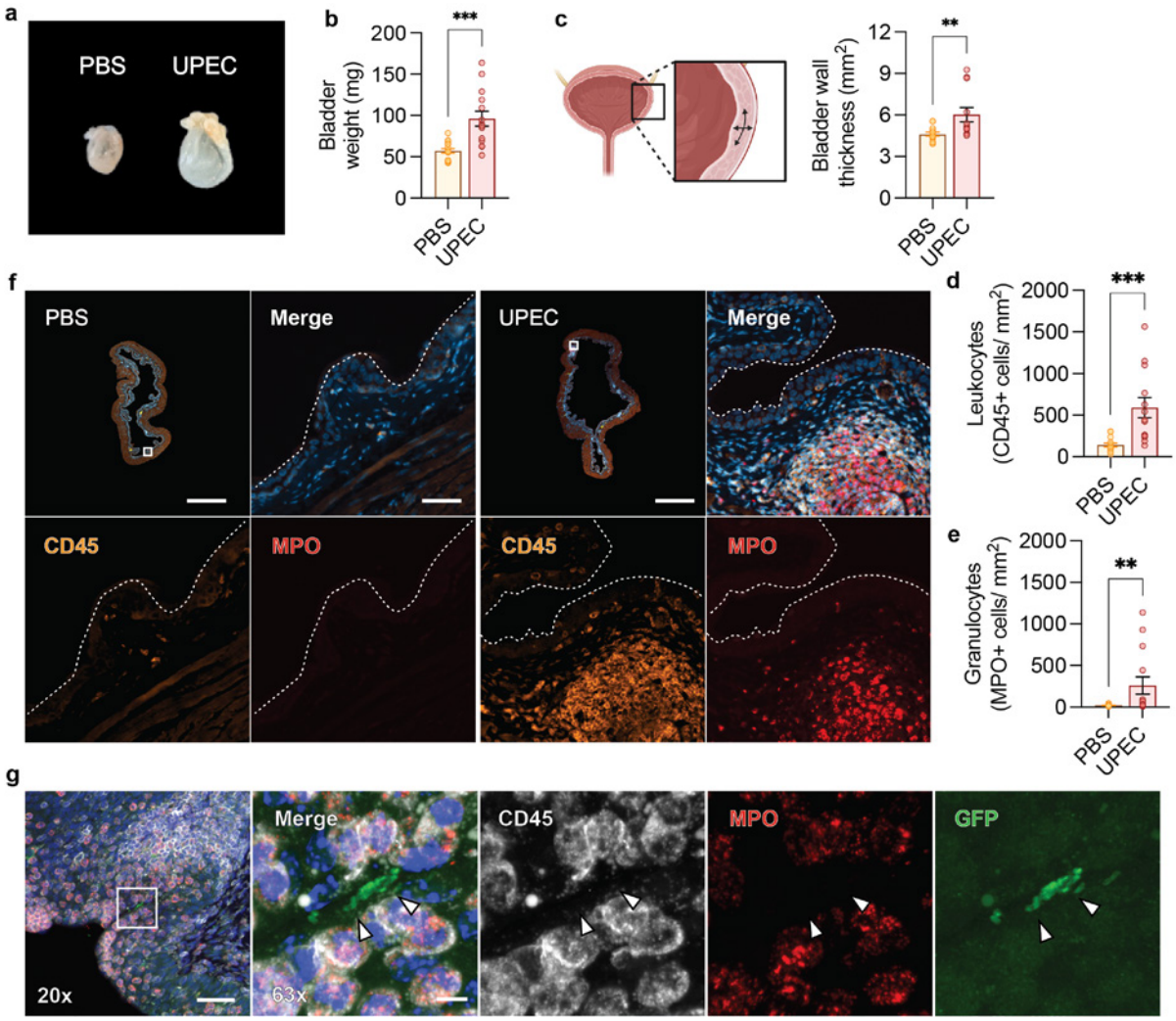

Figure 3. Persistent infections and inflammation in animals with rUTIs.

Peripheral infections can have lasting effects on the brain and further precipitate existing neurological conditions. To examine the effect of repeated UTIs on mouse brain, we examined the microglial response in whole after rUTIs. To perform an unbiased analysis of multiple brain regions, we developed in AI-based via slide scanning and deep learning (Aiforia image analysis) to recognize brain regions and the microglial cells within those regions activation[22]. The AI model does not require overlay with existing brain atlases but recognizes the brain regions autonomously (**Fig. 4a**). The model is trained to recognize Iba-1^{+} microglia and performs both object recognition and instance segmentation, which allows for the count of microglia and the analysis of their morphology at the same time. We found changes in microglial cell numbers in the medulla and cerebellar nuclei, which are areas that are associated with MSA-C (**Fig. 4c)**. In addition, in addition to an increase in microglial numbers, we find reactive microglial cells in the cingulate cortex (**Fig. 4d)**. This suggest that peripheral UTIs can impact central pathology with persistent neuroinflammatory changes.

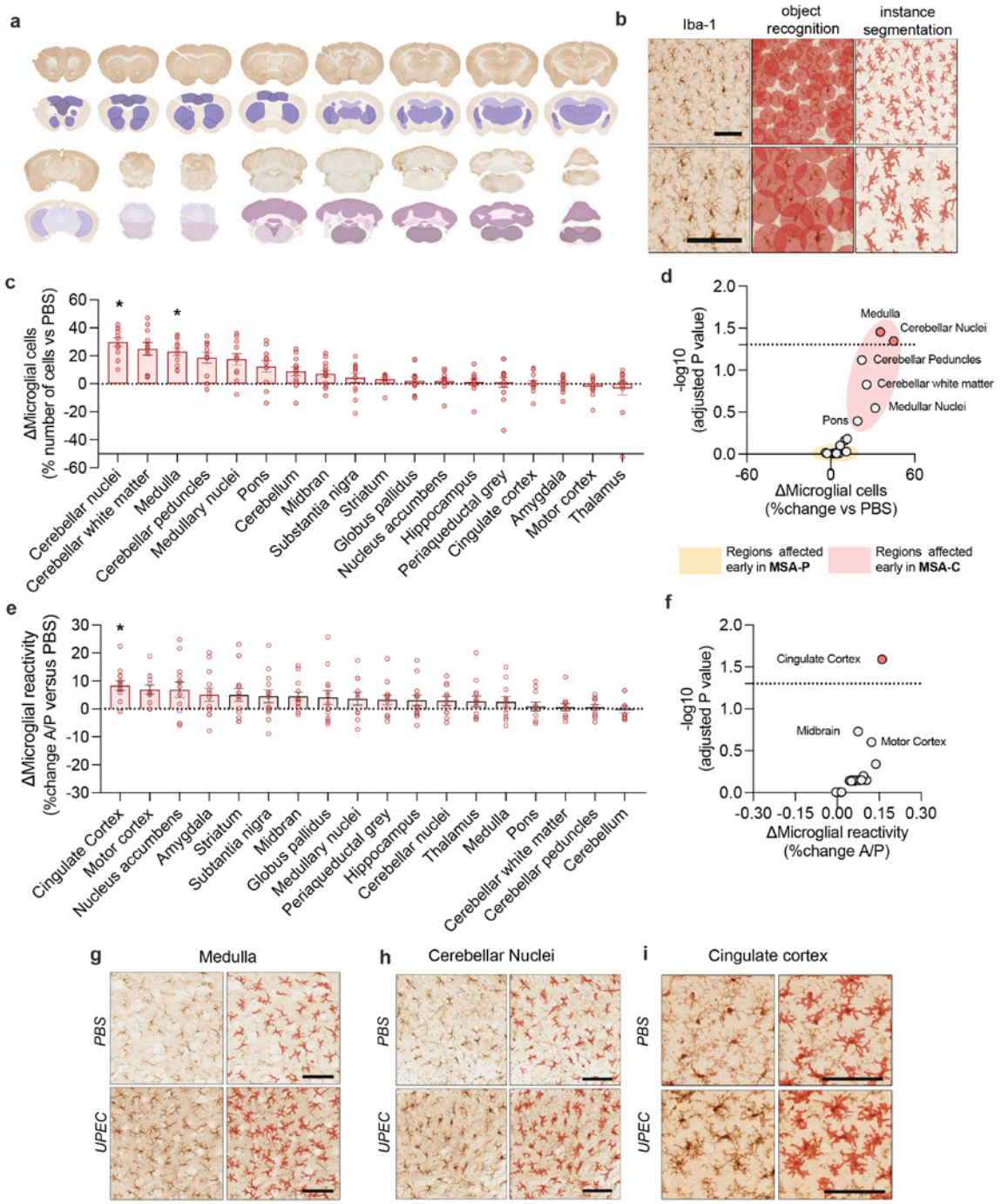

Figure 4. AI model for recognition and quantification of neuroinflammation in whole brain.

In a recent study we have shown that UTIs can influence αSyn *in vivo*. To further examine if UTIs can cause changes in synucleinopathy, aside from neuroinflammatory changes, we performed immunohistochemical staining for phosphorylated αSyn, a conventional marker of pathological αSyn, in the central nervous system. This analysis is based on an in-house developed AI-trained model to detect phosphorylated αSyn inclusions. Similar to our previous AI-model, this model recognizes different brain areas and the pathology within these areas (**Fig. 5a, b**). After performing the analysis in whole brain, we detect no significant changes in phosphorylated αSyn after correction for multiple testing (**Fig. 5c-f**). To study the relationship between phosphorylated αSyn and microglial reactivity we tested the correlation between phosphorylated αSyn and microglial reactivity in the cingulate cortex (**Fig. 5g**). This shows that in the cingulate cortex ad increase in microglial reactivity is significantly correlated with increasing levels of phosphorylated αSyn.

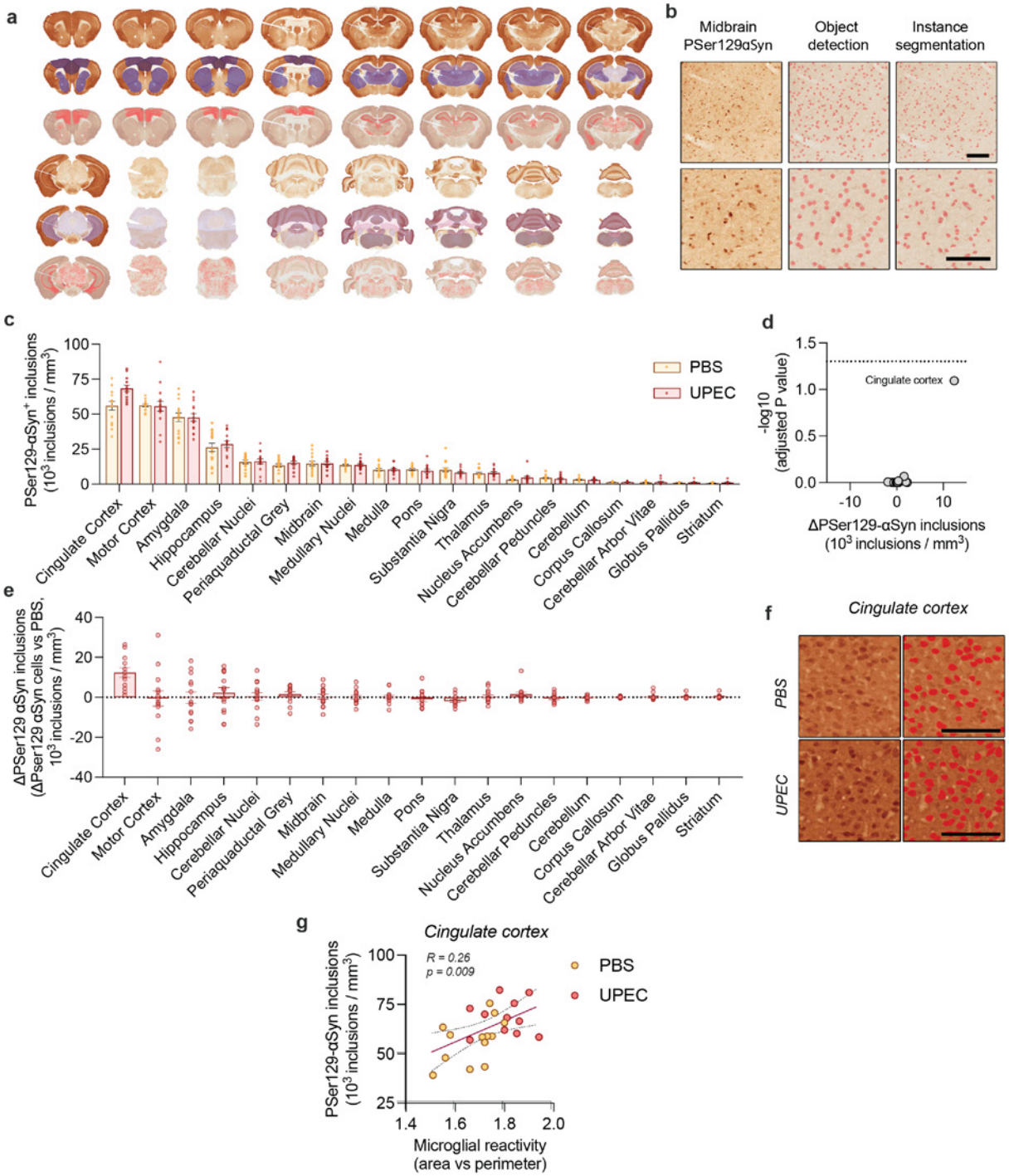

Figure 5. AI model for recognition and quantification of pathological synuclein in whole brain.

These findings of an ongoing unresolved infection together with the behavioral changes but in the absence of any overt neuropathology indicates that these behavioral changes could have caused by persistent UTIs instead of neurological symptoms.

4. Summary

With our epidemiological data and our experimental models[8], this shows that a link between infections, peripheral aggregation and central pathology might exist. With this work we therefore link bacterial infections with synucleinopathy and show that a host response to environmental triggers can result in αSyn pathology that bears semblance to MSA.

After the acceptance of this GSKE grant, our first study on the role of UTIs in MSA was published in a high impact paper:

- Peelaerts *et al*., Urinary tract infections trigger synucleinopathy via the innate immune response. Acta Neuropathol. 2023

With the help of GSKE, we are now preparing a second publication that will follow on our initial work to further describe how UTIs can trigger neuroinflammatory changes in the CNS. Our goal is to disseminate these results to a wider audience including scientific conferences, patient organization meetings (Defeat MSA, MSA Coalition, de Vlaamse Parkinson Liga) and discuss the role of bacterial or viral infections in synucleinopathies.

5. References

1. Tulisiak, C. T., Mercado, G., Peelaerts, W., Brundin, L. & Brundin, P. Can infections trigger alpha-synucleinopathies? in *Molecular Biology of Neurodegenerative Diseases: Visions for the Future, Part A* 299–322 (Elsevier, 2019). doi:10.1016/bs.pmbts.2019.06.002.
2. Kirchhof, K., Apostolidis, A. N., Mathias, C. J. & Fowler, C. J. Erectile and urinary dysfunction may be the presenting features in patients with multiple system atrophy: a retrospective study. *Int. J. Impot. Res.* **15**, 293–298 (2003).
3. Panicker, J. N. *et al.* Early presentation of urinary retention in multiple system atrophy: can the disease begin in the sacral spinal cord? *J. Neurol.* **267**, 659–664 (2019).
4. Sakakibara, R. *et al.* Urinary dysfunction and orthostatic hypotension in multiple system atrophy: which is the more common and earlier manifestation? *J Neurol Neurosurg Psychiatry* **68**, 65–69 (2000).
5. Rashid, M. H. *et al.* Interleukin-6 mediates delirium-like phenotypes in a murine model of urinary tract infection. *J. Neuroinflammation* **18**, 1–16 (2021).
6. Balogun, S. A. & Philbrick, J. T. Delirium, a symptom of UTI in the elderly: fact or fable? A Systematic Review. *Can Geriatr J* **17**, 22–26 (2013).
7. Papapetropoulos, S. *et al.* Causes of death in multiple system atrophy . *J. Neurol. Neurosurg. Psychiatry* **78**, 327 (2006).
8. Wouter Peelaerts, Gabriela Mercado, Sonia George, Marie Villumsen, Alysa Kasen, P. B. Urinary tract infections trigger synucleinopathy via the innate immune response. *Acta Neuropathol.* (2023).
9. Eriksson, I., Gustafson, Y., Fagerström, L. & Olofsson, B. Urinary tract infection in very old women is associated with delirium. *Int. Psychogeriatrics* **23**, 496–502 (2011).
10. Jennifer Chae, J. H. & Miller, B. J. Beyond urinary tract infections (UTIs) and delirium: A systematic review of UTIs and neuropsychiatric disorders. *J. Psychiatr. Pract.* **21**, 402–411 (2015).
11. Caljouw, M. A. A., den Elzen, W. P. J., Cools, H. J. M. & Gussekloo, J. Predictive factors of urinary tract infections among the oldest old in the general population. A population-based prospective follow-up study. *BMC Med.* **9**, 1–8 (2011).
12. Eriksson, I., Gustafson, Y., Fagerström, L. & Olofsson, B. Prevalence and factors associated with urinary tract infections (UTIs) in very old women. *Arch. Gerontol. Geriatr.* **50**, 132–135 (2010).
13. Bittel, M. *et al.* Visualizing transfer of microbial biomolecules by outer membrane vesicles in microbe-host-communication in vivo. *J. Extracell. Vesicles* **10**, e12159 (2021).
14. Grazia Spillantini, M. *et al.* Filamentous -synuclein inclusions link multiple system atrophy with Parkinson's disease and dementia with Lewy bodies. *Neurosci. Lett.* (1998) doi:10.1016/S0304-3940(98)00504-7.
15. Peelaerts, W. & Baekelandt, V. -Synuclein strains and the variable pathologies of synucleinopathies. *J. Neurochem.* 256–274 (2016) doi:10.1111/(ISSN)1471-4159/homepage/special_issues.htm.

16. Hoffmann, A. *et al.* Oligodendroglial synucleinopathydriven neuroinflammation in multiple system atrophy. *Brain Pathol.* **29**, 380 (2019).
17. Ishizawa, K. *et al.* Microglial Activation Parallels System Degeneration in Multiple System Atrophy. *J. Neuropathol. Exp. Neurol.* **63**, 43–52 (2004).
18. Grozdanov, V. & Danzer, K. M. Intracellular Alpha-Synuclein and Immune Cell Function. *Frontiers in Cell and Developmental Biology* (2020) doi:10.3389/fcell.2020.562692.
19. Labrie, V. & Brundin, P. Alpha-Synuclein to the Rescue: Immune Cell Recruitment by Alpha-Synuclein during Gastrointestinal Infection. *J. Innate Immun.* **9**, 437–440 (2017).
20. Reish, H. E. A. & Standaert, D. G. Role of -synuclein in inducing innate and adaptive immunity in Parkinson disease. *J. Parkinsons. Dis.* **5**, 1 (2015).
21. Schwartz, D. J., Conover, M. S., Hannan, T. J. & Hultgren, S. J. Uropathogenic Escherichia coli Superinfection Enhances the Severity of Mouse Bladder Infection. *PLoS Pathog.* **11**, e1004599--12 (2015).
22. Lucas, S. *et al.* A novel automated morphological analysis of microglia activation 1 using a deep learning assisted model 2 3. doi:10.1101/2022.03.11.483994.

Geneeskundige Stichting Koningin Elisabeth
Fondation Médicale Reine Elisabeth
Königin-Elisabeth-Stiftung für Medizin
Queen Elisabeth Medical Foundation

Progress report of the research project of the young researcher

Dr. Sarah van Veen
Katholieke Universiteit Leuven (KU Leuven)

Dr. Sarah van Veen, PhD (KU Leuven)
FWO postdoctoral fellow

Laboratory of Cellular Transport Systems
KU Leuven, Department of Cellular and Molecular Medicine
ON Ibis Herestraat 49, box 802 – 3000 Leuven (Belgium)

T +32 (0)16 32 90 55
sarah.vanveen@kuleuven.be

The impact of ATP13A4-mediated polyamine transport in astrocytes on synaptogenesis and neurodevelopmental disorders

I am very grateful to the GSKE for their generous support of my research. The funding provided by the Foundation in 2023 has offered me invaluable support, and with this progress report, I provide a summary of my major accomplishments and my future goals.

1. Research summary

Polyamines, such as spermidine and spermine, are low-molecular-weight polycations that are highly abundant in the brain and crucial for normal brain function. In the brain, polyamines preferentially accumulate in astrocytes from which they can be released to regulate neuronal synaptic activity. How polyamines are taken up by or released from glial cells is still an important outstanding question. I identified ATP13A4 as a major component of the polyamine transport system in astrocytes. ATP13A4 is a virtually unstudied gene that has been associated with neurodevelopmental disorders (NDD) like specific language impairment, autism and psychiatric diseases. Furthermore, in 2023, I established a connection between ATP13A4 and cancer, by identifying ATP13A4 as a novel polyamine transporter controlling polyamine uptake of breast cancer cells[1]. Within the framework of the project funded by GSKE, I found that ATP13A4 is mainly expressed by astrocytes in the brain and functions as a polyamine transporter that impacts cellular polyamine homeostasis. Of interest, autism-associated ATP13A4 mutations exhibit a loss-of-function phenotype. In addition, my preliminary findings show a novel role for polyamines in astrocyte morphogenesis and synaptogenesis. Understanding the physiological role of ATP13A4 in astrocytes and in the brain may validate ATP13A4 as a candidate therapeutic target for NDD.

2. Major accomplishments

2.1. Learning methods to assess astrocyte function and interactions with neurons

in 2023 I worked for six months, as a visiting scholar, in the renowned laboratory of Prof. Cagla Eroglu (HHMI investigator; Duke University, NC, USA), a leading expert in the field of astrocyte biology and astrocyte-synapse interactions. Here, I acquired state-of-the-art techniques and skills for evaluating astrocyte and neuron function *in vitro* and *in vivo*:

1. I successfully **learned how to generate primary astrocyte and neuron mono-cultures** from rat cortical tissue (postnatal day 1, PND1) via the classical 'shake-off' method (in which shaking is used to remove neurons, oligodendrocyte precursors and microglia during the culture procedure) and immunopanning, respectively[2]. I also learned how to establish and maintain primary astrocyte-neuron co-cultures[2].
2. I **learned sophisticated methods to assess astrocyte morphology** in a primary cortical neuron and astrocyte co-culture system[2]. I learned how to evaluate and quantify morphological complexity via confocal microscopy and Sholl analysis, respectively.
3. I **learned how to assess synapse numbers *in vitro*** via pre- and post-synaptic marker double staining. Excitatory and inhibitory synapses appear as punctae that are double-positive for both presynaptic Bassoon and postsynaptic Homer1 or Gephyrin, respectively. I also learned how to quantify synapses using the ImageJ-based software SynBot[3].

4. **I developed novel tools to study ATP13A4 in astrocytes.** To investigate the putative role of ATP13A4 in astrocytes, I designed and constructed multiple shRNA vectors to knockdown ATP13A4 *in vitro* and *in vivo*.
5. To assess the impact of Atp13a4 deficiency on astrocyte morphology *in vivo*, I **learned the technique of postnatal astrocyte labelling by electroporation (PALE)**[2]. To this end, shRNAs against Atp13a4 were cloned into a PiggyBac transposon system expressing a membrane-targeted mCherry (mCherry-CAAX). Plasmids were then injected into the lateral ventricle of CD1 mice and introduced into radial glial stem cells at late PND0 via PALE, resulting in a sparse knockdown and labelling of cortical astrocytes. Brains were collected at PND21, *i.e.* after the completion of astrocyte morphological maturation. To analyse astrocyte complexity and territory, whole astrocytes were imaged by confocal microscopy and reconstructed using the Imaris filament tracing tool (Bitplane). Astrocyte morphology is quantified in two ways: morphological complexity measured by 3D Sholl analysis and astrocyte territory volume analysed by convex hull analysis. In addition, I learned how to quantify the density of excitatory synapses within PALE KD astrocytes, based on the colocalization of Bassoon (presynaptic marker) and PSD95 (postsynaptic marker)[2]. The analysis of the PALE images is ongoing.

Currently, I am setting up these techniques in my host institution. During my stay at the Eroglu lab I already obtained exciting preliminary data showing that Atp13a4 and polyamines impact astrocyte morphogenesis and neuronal synaptogenesis *in vitro* and *in vivo*. I aim to finalize these datasets in 2024.

2.2. Atp13a4 is a major component of the polyamine transport system in astrocytes

Single-cell transcriptome atlases indicate strong enrichment of ATP13A4 in astrocytes[4-6]. I now confirmed these findings using qPCR and found **significantly higher expression of Atp13a4 in rat primary cortical astrocytes compared to neurons**. This *in vitro* dataset will now be validated *in vivo* by using fluorescent in situ hybridization (FISH) to look for *Atp13a4* mRNA in cortical sections of Aldh1L1-EGFP BAC-transgenic mice, in which all astrocytes express EGF[2]. In addition, I will assess Atp13a4 protein levels via western blotting and immunohistochemistry in primary cultures and mouse cortex.

My exciting preliminary data in immortalized mouse astrocyte cells (C8-D1A) with stable Atp13a4 knockdown demonstrated reduced endogenous polyamine levels compared to control cells, whereas flow cytometry data showed reduced BODIPY-polyamine uptake in Atp13a4 deficient cells. Furthermore, decreased Atp13a4 expression reduced sensitivity to polyamine toxicity. **Here, I confirmed that knockdown of Atp13a4 significantly decreases cellular uptake of BODIPY-labelled polyamines in primary rat cortical astrocytes, in line with my hypothesis that Atp13a4 is a major component of the polyamine transport system in astrocytes.** On the other hand, the reduced sensitivity to polyamine toxicity following Atp13a4 knockdown in C8-D1A cells was not observed in primary cultures. In contrast, primary astrocytes with reduced Atp13a4 expression demonstrated slightly higher polyamine cytotoxicity. Finally, metabolomics experiments will be conducted in 2024 to assess the impact of Atp13a4 knockdown on cellular polyamine levels in primary astrocytes.

3. Ongoing work and future outlook

3.1. Impact of Atp13a4 deficiency on mouse behaviour

Due to the genetic link between ATP13A4 and NDD, I will assess the role of Atp13a4 in disease susceptibility *in vivo*. Therefore, we will subject full-body *Atp13a4* KO mice (C57BL/6NJ-*Atp13a4*$^{em1(IMPC)Bay}$/Mmnc) to thorough behavioural phenotyping at the mouse phenotyping core facility to screen for neurodevelopmental phenotypes (mINT, Dr. CallaertsVegh, KU Leuven). **These experiments will be initiated in February 2024.** In a blinded approach, both male and female mice between 8–12 weeks of age will be used for the experiments. We will turn to several methods to evaluate cognition (maze learning, conditioning, recognition) and motor function (coordination, locomotion, strength). Due to ATP13A4's link with autism and schizophrenia, we will also assess social interaction (social exploration, social preference, nesting behaviour) and "schizophrenic" emotionality. For the latter, we will measure pre-pulse inhibition of startle (ability of a non-startling "pre-pulse" to inhibit responding to the subsequent startling stimulus or "pulse"[7]) and assess latent inhibition (ability to ignore or suppress biologically irrelevant stimuli). In case no basal behaviour phenotype would be detected in Atp13a4 KO mice, we will challenge the mice with spermidine treatment to increase plasma polyamine levels and evoke polyamine stress. These interventions have been validated in our lab, and changes in plasma polyamine levels have been confirmed via metabolomics.

3.2. Investigating the Atp13a4-Mertk interplay *in vitro* and *in vivo*

Recently, I observed a putative link between ATP13A4 and MERTK. First, they have a similar spatiotemporal expression pattern in the developing brain (r = 0.936; brainspan.org), suggesting ATP13A4 and MERTK may be related in function. In addition, polyamines have been linked to MERTK signalling, promoting phagocytosis via modulating the MERTK-ERK1/2 pathway[8]. My exciting preliminary data support interplay between ATP13A4 and MERTK in glial cells. Spermidine triggered rapid upregulation of MERTK and ERK1/2 phosphorylation in cells overexpressing WT ATP13A4. Furthermore, treatment with the specific MERTK inhibitor UNC569 led to a dose-dependent decrease of BODIPY-spermidine uptake in Atp13a4 expressing astrocytes, to the level observed following Atp13a4 knockdown. My final goal in 2024 is to further investigate the interplay between the polyamine transport function of ATP13A4 and the MERTK phagocytic pathway in primary astrocytes as well as *in vivo*. I hypothesize that loss of Atp13a4-mediated polyamine uptake in astrocytes will lead to decreased Mertk expression and reduced phagocytic capacity.

4. Publications funded by GSKE

- van Veen S., Irala D., Hays K., Ausloos E., Van Asselberghs J., Van den Haute C., Baekelandt V., Eggermont J., Holt M.G., Eroglu C., Vangheluwe P. Connecting polyamine transport in astrocytes to neurodevelopmental disorders via ATP13A4. *Manuscript in preparation.*

5. Publications not funded by GSKE

- van Veen S., Kourti A., Ausloos E., Van Asselberghs J., Van den Haute C., Baekelandt V., Eggermont J., Vangheluwe P. (2023). ATP13A4 upregulation drives the elevated polyamine transport system in the breast cancer cell line MCF7. *Biomolecules.* 13 (6): 918. doi: 10.3390/biom13060918.

6. References

1. van Veen, S. *et al.* ATP13A4 Upregulation Drives the Elevated Polyamine Transport System in the Breast Cancer Cell Line MCF7. *Biomolecules* **13** (2023). https://doi.org:10.3390/biom13060918
2. Stogsdill, J. A. *et al.* Astrocytic neuroligins control astrocyte morphogenesis and synaptogenesis. *Nature* **551**, 192-197 (2017). https://doi.org:10.1038/nature24638
3. Savage, J. T., Ramirez, J., Risher, W. C., Irala, D. & Eroglu, C. SynBot: An open-source image analysis software for automated quantification of synapses. *bioRxiv* (2023). https://doi.org:10.1101/2023.06.26.546578
4. Zhang, Y. *et al.* An RNA-sequencing transcriptome and splicing database of glia, neurons, and vascular cells of the cerebral cortex. *J Neurosci* **34**, 11929-11947 (2014). https://doi.org:10.1523/JNEUROSCI.1860-14.2014
5. Tabula Muris, C. *et al.* Single-cell transcriptomics of 20 mouse organs creates a Tabula Muris. *Nature* **562**, 367-372 (2018). https://doi.org:10.1038/s41586-018-0590-4
6. Batiuk, M. *et al.* Molecularly distinct astrocyte subpopulations spatially pattern the adult mouse brain. *bioRxiv*, 317503 (2018).
7. Powell, S. B., Zhou, X. & Geyer, M. A. Prepulse inhibition and genetic mouse models of schizophrenia. *Behav Brain Res* **204**, 282-294 (2009). https://doi.org:10.1016/j.bbr.2009.04.021
8. Yurdagul, A., Jr. *et al.* ODC (Ornithine Decarboxylase)-Dependent Putrescine Synthesis Maintains MerTK (MER Tyrosine-Protein Kinase) Expression to Drive Resolution. *Arterioscler Thromb Vasc Biol* **41**, e144-e159 (2021). https://doi.org:10.1161/ATVBAHA.120.315622

Geneeskundige Stichting Koningin Elisabeth
Fondation Médicale Reine Elisabeth
Königin-Elisabeth-Stiftung für Medizin
Queen Elisabeth Medical Foundation

Progress report of the research project of the young researcher

Prof. Giulia Liberati
Université Catholique de Louvain (UCLouvain)

Giulia Liberati (UCLouvain)
Université catholique de Louvain Institute of Neuroscience (IoNS)
Avenue Mounier 54
UCL 54.02 B-1200 Brussels
Belgium
T +32 (2) 7645467
giulia.liberati@uclouvain.be

Identifying biomarkers with invasive and non-invasive brain stimulation targeting ongoing neural oscillations

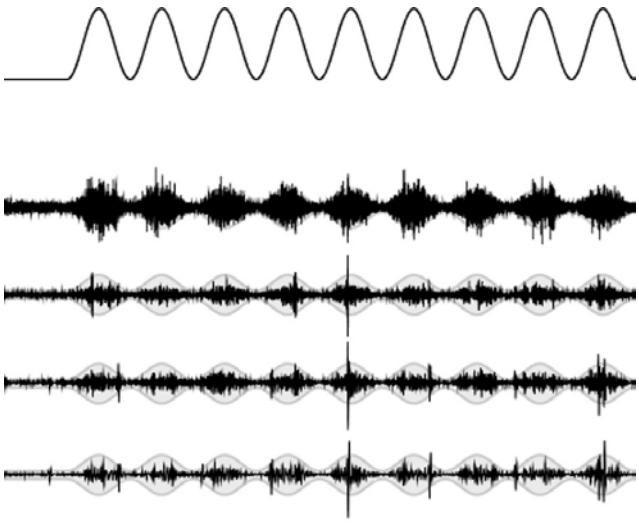

1. Introduction

Around 10% of adults worldwide suffer from chronic pain conditions[1]. The identification of effective neural biomarkers for pain – which would allow improving the stratification of pain conditions, predicting responses to treatment, and offering personalized interventions – is of major importance[2]. In recent years, works from our group[3,4] and others[5,6] have strongly suggested that pain perception may arise from the modulation of ongoing neural oscillations within different frequency bands. However, despite these encouraging findings, there is still disagreement on the degree to which these modulations of neural oscillations are actually related to pain, or whether they are merely an epiphenomenon.

My project, STIM-WAVES, remedies this gap by directly assessing the causal relationship between ongoing neural oscillations and pain perception, combining both scalp electroencephalography (**EEG**) and intracerebral electroencephalography (**iEEG**) with **invasive and non-invasive brain stimulation**, with the aim of (i) better characterizing pain-related modulations of ongoing neural oscillations, and (ii) understanding whether disrupting these modulations through brain stimulation would also affect pain perception.

The project is structured in two WPs. Throughout the WPs, pain-related modulations of ongoing oscillations are investigated employing **sustained periodic nociceptive and non-nociceptive stimuli,** as well as a newly developed approach, **frequency tagging of ongoing oscillations (FT-OO)**[3], an extension of the more established frequency tagging approach. FT-OO can be used to characterize the selective modulation of ongoing oscillations exerted by sustained thermonociceptive stimuli delivered at a given frequency. In an iEEG study performed by our group, we have shown that thermonociceptive stimuli elicit a selective modulation of insular ongoing oscillations in the theta (4-8 Hz) and alpha (8-12 Hz) frequency bands, suggesting that these oscillations could be related to the perception of pain (**Fig. 1**). Although encouraging, these findings should be interpreted with caution, as **only by assessing whether directly disrupting these oscillations will lead to an alteration in pain perception would ascertain the causal link between oscillations and pain.**

1 PhD student (Chiara Leu) worked full time on WP1. 1 postdoc researcher (Yaser Fathi Arateh) worked full time on WP2 (starting from October 2023).

1.1. WP1: Characterizing the modulation of pain-related ongoing oscillations exerted by sustained painful stimuli

If ongoing oscillations are related to the pain experience, then cognitive processes that are known to affect pain intensity (e.g. distraction) should also affect these oscillations. Using scalp EEG, Leu et al.[7] recently investigated the effects of a distraction task (i.e. repeatedly subtracting 7 from a 3-digit number) on pain perception and on ongoing neural oscillations in the theta (4-8 Hz), alpha (8-12 Hz), and beta (12-40 Hz) frequency bands. Whereas the intensity of pain perception was significantly reduced by the arithmetic task, no clear effect was observed on ongoing oscillations in any of the frequency bands. Hence, the fact that, unlike pain perception, these oscillations did not appear to be affected by the task suggests that they are dissociable from pain perception. However, two reasons for the lack of pain-related observable effects on neural oscillations could be (i) the lower signal-to-noise ration of scalp EEG compared to other techniques, such as iEEG[3], as well as (ii) the fact that scalp EEG might not be able to sufficiently detect activity in deeper pain-related brain regions such as the insular cortex. To this end, in **WP1.1**, we **used iEEG recorded using depth electrodes implanted in the insula of 7 hospitalized patients** undergoing a presurgical evaluation of focal epilepsy (Leu et al., *in preparation*). The patients had to perform the same task as in Leu et al.[7] (**Fig. 2**), namely repeatedly subtracting 7 from a 3-digit number, while receiving a sustained periodic thermonociceptive stimulation or a frequency matched non-nociceptive vibrotactile stimulation contralaterally to the electrode implanted in the insula. A thermal cutaneous stimulator (TCS II, QST.Lab, Strasbourg, France) was used to deliver sustained periodic thermonociceptive stimuli (0.2 Hz). It has been shown that periodic thermonociceptive stimulation at this frequency predominantly activates unmyelinated C-fibers, generating a reliable periodic response with a high signal-to-noise ratio[4]. Each sustained periodic stimulation comprised 15 stimulation cycles, lasting a total of 75 s per stimulus[3,7,8]. Inter-stimulus intervals were variable and self-paced by the experimenter to allow participants to provide intensity ratings, as well as to give responses to the arithmetic task. The thermode was displaced after each trial to avoid habituation and sensitization. Sustained periodic vibrotactile stimuli were delivered via a recoil-type vibrotactile transducer driven by a standard audio amplifier (Haptuator, Tactile Labs Inc, Canada), positioned between the fingertips of the index and the thumb. The vibrations consisted in a 251 Hz sine wave whose amplitude was periodically modulated at a frequency of 0.2 Hz. We chose this kind of stimulation because, despite being non-nociceptive and non-painful, it is generally perceived as highly intense, which makes it a suitable comparison to investigate whether the observed modulations might be preferential for pain perception. Preliminary results of this study, suggesting that **distraction not only decreases pain perception, but also decreases the amplitude of the modulation of ongoing oscillations in all frequency bands** (**Fig. 3**), have been recently presented at the **Translational Neurobiology of the Pain System Meeting** (Aalborg, November 2023). This study will also be presented at the **Organization for Human Brain Mapping** (Seoul, June 2024).

In **WP1.2** and in **WP1.3** (currently ongoing), we are investigating the effects of **individual expectations** and of the **saliency of stimulation** respectively, on both pain perception and ongoing neural oscillations. Several **pilot studies** have been performed to achieve the optimal stimulation parameters for the different experiments. Both experiments have been pre-registered and received "**in principle acceptation**" (https://osf.io/qbrf2; https://osf.io/y6fb8). This means that the studies will be accepted upon completion, granted that there were no changes in the protocol.

1.2. WP2: Fine-tuning neurostimulation for the modulation of pain-related ongoing oscillations

In September 2023, I hired a postdoctoral researcher with a biomedical engineer background to work on **WP2**, which is centered on **invasive and non-invasive brain stimulation**. A literature review on neuromodulation and pain, as well as an in-depth research of the devices able to perform transcranial alternate current stimulation (tACS) and EEG concomitantly, led us to acquire a cutting-edge system that **integrates electrical stimulation and EEG**, that is able to deliver **highly focal stimulation** (**Fig. 4**, https://www.neuroelectrics.com/solutions/starstim). While all previous research in the pain field analyzed EEG data before and after electrical stimulation, this new device allows the unique feature of concomitant stimulation and recording, including 32 channels for electrical stimulation or EEG. In particular, it allows for high-resolution transcranial electrical stimulation and EEG monitoring in real time, with high-definition montages that enables a higher focal stimulation compared to standard tACS protocols. This feature, together with the high time resolution of the EEG, will provide us with a better understanding of the mechanisms of how tACS works in interaction with ongoing neural oscillations. The device also allows for a double-blind protocol in which neither the participant nor the experimenter can identify which type of stimulation (active or sham) is delivered, therefore reducing the effect of bias on the experiment results.

Ethical approval was obtained to perform **tACS** on healthy participants and **intracerebral periodic current stimulation (iPCS)** on patients undergoing a presurgical evaluation of focal epilepsy with depth electrodes implanted in the insula and in other pain-related brain regions. Pilot studies are currently being conducted for optimizing stimulation parameters using tACS. In particular, we aim to stimulate the sensorimotor cortex in the alpha frequency with the aim of both affecting alpha oscillations and pain perception**. By recording and analyzing EEG data before, during, and after tACS, we intend to identify how different oscillatory activities contribute to the experience of pain.**

In **WP2.1** we aim to test the hypothesis that **tACS can modulate pain perception in terms of quality and intensity by modulating EEG ongoing oscillations**. When periodic brain stimulation is applied at a frequency F_1, it is expected not only to increase EEG power at F_1, but also to modulate existing oscillations at the same frequency. Likewise, when a sustained painful stimulus fluctuates periodically at a frequency F_2, it is expected to increase EEG power at F_2 and affect ongoing oscillations at this frequency. Concurrent application of periodic brain stimulation and periodic thermonociceptive stimulation may result in additional peaks in the EEG frequency spectrum, reflecting the interplay between F_1 and F_2, including frequencies like nF_1+mF_2 and their harmonics To determine if the effect of brain stimulation is pain-related, the cross-modulation responses from periodic painful thermonociceptive stimulation will be compared with those from non-nociceptive periodic vibrotactile stimuli. These effects will be further compared to those from a sham stimulation. The sham protocol mimics real stimulation by generating currents at the start and end of the session but maintains either no or very low (around 0.2 mA) stimulation in-between. This approach ensures negligible effective cortical stimulation while preserving similar cutaneous sensations. The stimulation target will be the sensorimotor area of the contralateral side of the dominant hand, based on a meta-analysis and literature review[9].

We performed a **pilot study** in which we recorded EEG signals from **40 healthy participants** during sustained and periodic 0.2 Hz thermonociceptive stimulation (temperature baseline and peak were set at 35°C and 49°C, respectively), and we modulated them with a sine wave generated in MATLAB (**Fig. 5**). We used two different frequencies for the sine wave: 5 Hz and 10 Hz, to simulate theta and alpha stimulation. As a result, the peak of the frequency spectrum

of the EEG signal at 0.2 Hz shifted to around the modulation frequency. Using frequency tagging to examine each frequency band more specifically, we observed that the 0.2 Hz oscillatory activity within each band could either be amplified or diminished, depending on the stimulation frequency (**Fig. 6**). By modulating oscillations using tACS, monitoring these oscillations, and concurrently measuring alterations in pain quality and intensity, we aim to better understand how pain is related to theta and/or alpha frequency bands.

Whereas in WP2.1 the frequency and amplitude of oscillatory activities are of main interest, to better understand the role played by the phase of the oscillations in pain perception, in **WP2.2**, we aim to explore the **relationship of the phase of the oscillations with brain interregional connectivity and pain perception**. Previous studies have reported changes in connectivity between the contralateral parietal operculum (cPO) and the anterior cingulate cortex (ACC) when pain intensity increases[10].

Using the same dataset as in WP2.1, we conducted another **pilot study** in which we computed the **phase lag index (PLI)** values between EEG channels of the left and right sensorimotor cortex, which revealed notable differences in this index between the left and right sensorimotor cortices across various frequency bands (**Fig. 7**). These observations provide a more comprehensive understanding of the neural dynamics underlying pain perception and the potential modulatory effects of tACS on local and interregional connectivity. This experiment is also a preliminary step towards unraveling the contributions and interactions of different brain regions to the sensation and modulation of pain, **leading to more targeted and effective interventions for pain management**.

In **WP2.3**, we plan to test the hypothesis that iPCS can modulate pain perception in terms of quality and intensity, using a similar stimulation protocol as in WP2.1, but targeting the insular cortex.

2. Figures

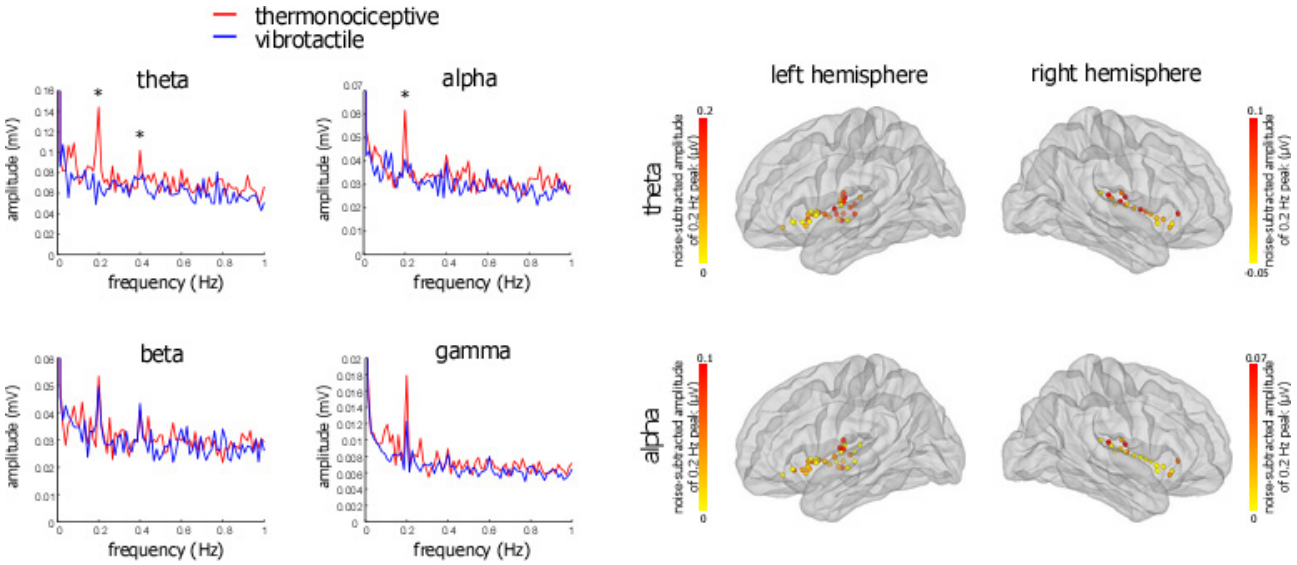

Fig. 1. Frequency tagging of ongoing oscillations (FT-OO). Adapted from Liberati et al[3]. FT-OO is an extension of frequency tagging. Left: To extend frequency tagging to ongoing oscillations, (i) we applied a band-pass filter to retain the EEG signal within different frequency bands (e.g. theta, alpha, beta, and gamma); we performed a Hilbert transform on the filtered EEG data to estimate the envelope of the signal within each frequency band; and (iii) we transformed the signal in the frequency domain, to see how the periodic modulation of the amplitude of the different ongoing oscillations concentrated at the frequency of stimulation and at its harmonics. Left: Differently from standard frequency tagging, FT-OO allowed discriminating between thermonociceptive and vibrotactile responses. Compared to vibrotactile stimuli, thermonociceptive stimuli elicited a greater modulation of ongoing oscillations at 0.2 Hz in the theta (4-8 Hz) and alpha (8-12 Hz) frequency bands (($p<.001$ and $p=.002$, respectively). Right: For both types of oscillations, and for both hemispheres, this modulation was more prominent in the posterior insula compared to the anterior insula.

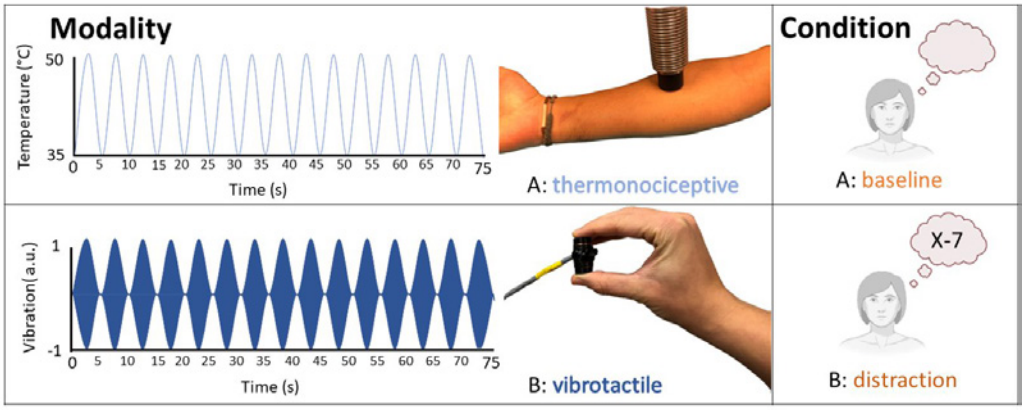

Fig. 2. Investigating the effects of distraction on pain perception and neural oscillations using iEEG. Two stimulation modalities (thermonociceptive and non-nociceptive) and two conditions (baseline and distraction) were used in a 2 X 2 design. During the distraction task, patients had to continuous subtract 7 from a 3-digit number and report their final value at the end of the trial. Answer accuracy was tracked to ensure compliance.

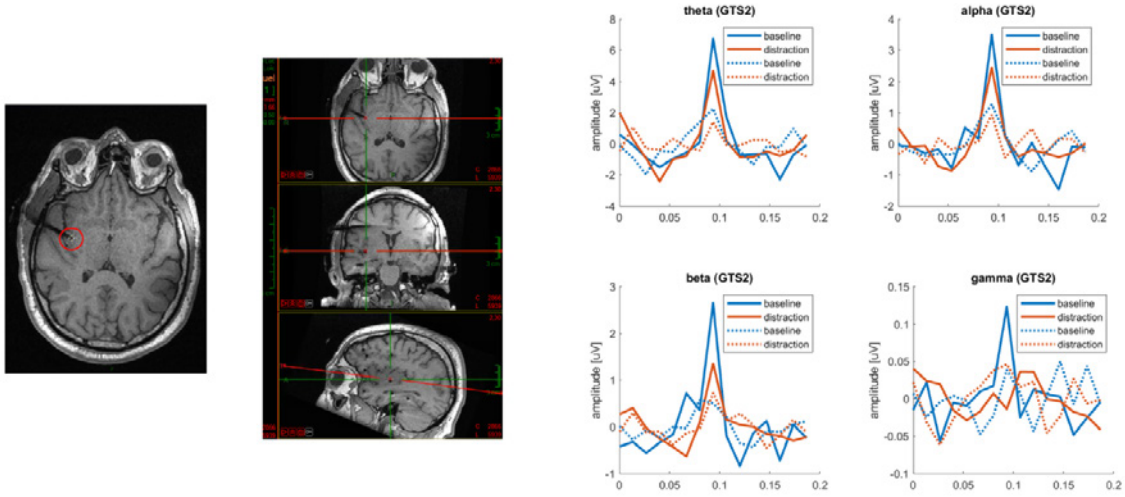

Fig. 3. Investigating the effects of distraction on pain perception and neural oscillations using iEEG: preliminary findings. Distraction not only decreased pain perception, but also decreased the amplitude of the modulation of ongoing oscillations in all frequency bands.

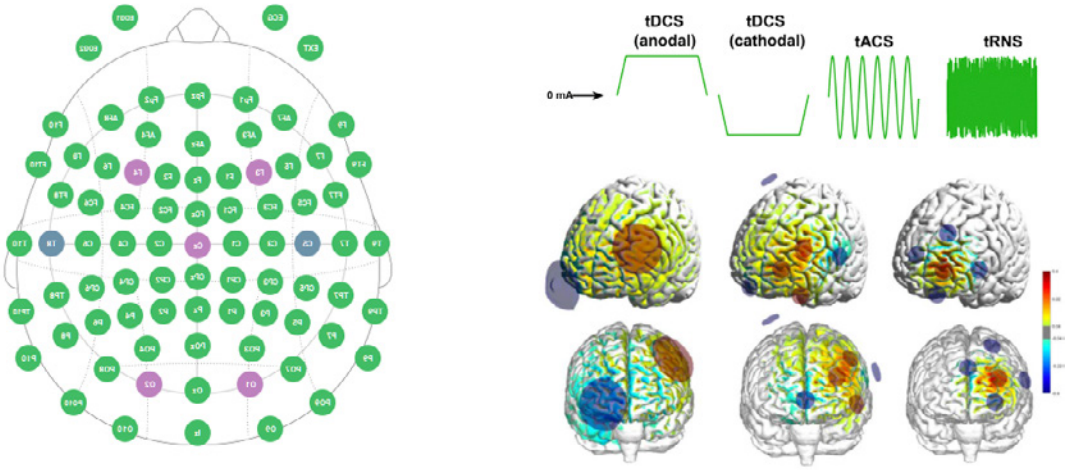

Fig. 4. Concomitant EEG and transcranial electrical stimulation. The newly acquired Starstim device allows for EEG recording during transcranial electrical stimulation and enables us to study the immediate effects of the intervention. It is possible to assign different channels for electrical stimulation (blue) or recording EEG (purple) concomitantly through the software interface of the device. Furthermore, the multichannel stimulation montages provide enhanced focality compared to traditional two-electrode montages.

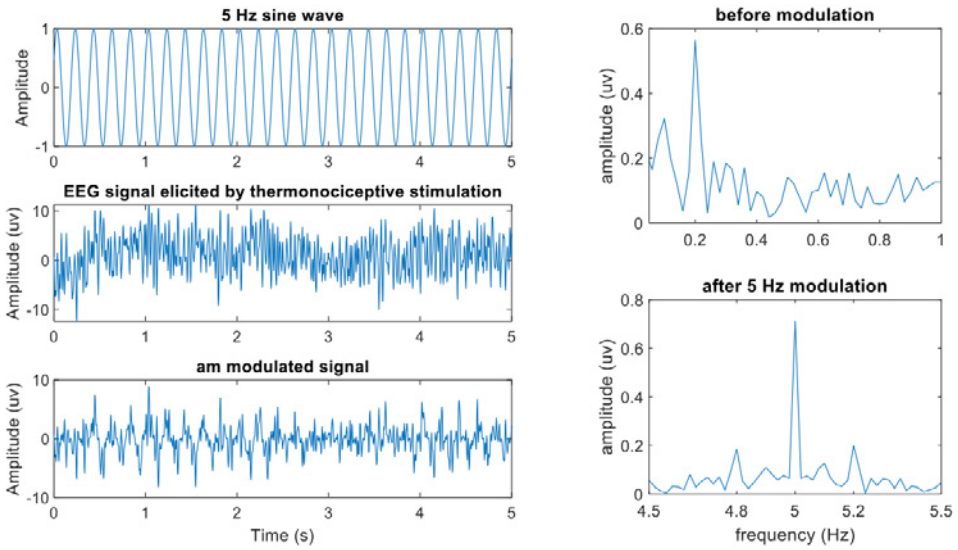

Fig. 5. Amplitude modulation of EEG signal with a sine wave. We recorded scalp EEG signals during sustained periodic thermonociceptive stimulation of the forearm. The stimulation pattern was a sine wave (0.2 Hz) oscillating between 35˚C to 50˚C. To simulate what would happen after tACS neuromodulation, we generated a sine wave in Matlab and modulated it with the EEG signal based on the general amplitude modulation formula ($y_m = (1 + M.y_2).y_1$, where y_1 is the sine wave with frequency f_1, y_2 is EEG signal elicited by 0.2 Hz painful thermal stimulation, y_m is modulated signal, and M is the modulation index). On the right figures the Fast Fourier Transform (FFT) of EEG signal shows a clear peak at the 0.2 Hz frequency. After modulation with the 5 Hz sine wave, new peaks at f_1 and f_1 can be seen.

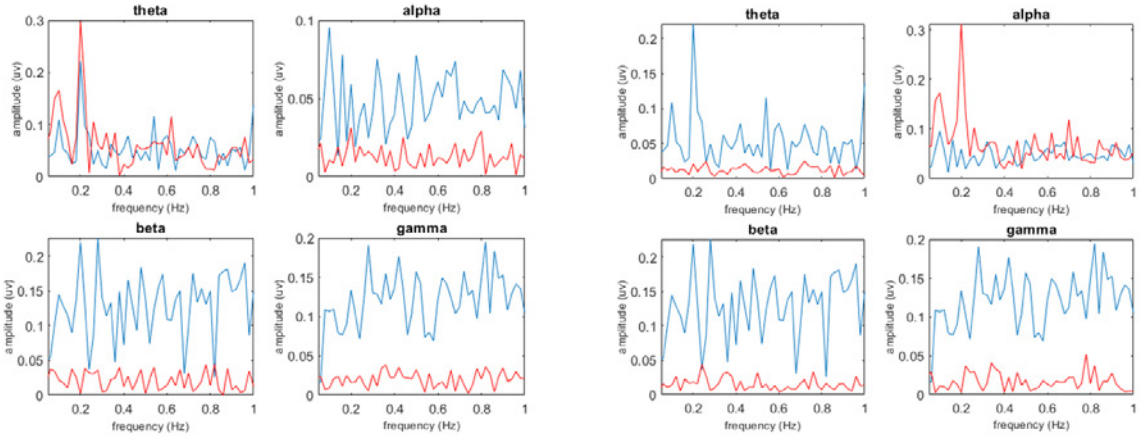

Fig. 6. Frequency tagging analysis on the EEG signal before and after the modulation with different frequencies. We modulated the recorded EEG signals using sine waves at two distinct frequencies: 5Hz and 10Hz. The FT analysis illustrates changes in peak frequency within various frequency bands resulting from the modulation. Specifically, after the 5Hz modulation—within the theta frequency range (4-8 Hz)—there's a noticeable boost in the 0.2 Hz peak within the theta band compared to the pre-modulation state. Conversely, no clear peaks are observed in other bands, and overall oscillations are weakened. After the 10Hz modulation—within the alpha frequency range (8-12 Hz)—enhanced the 0.2 Hz peak in the alpha band while diminishing it in the theta band. The data of this figure is for one representative subject but similar patterns were consistently noted in all 40 participants.

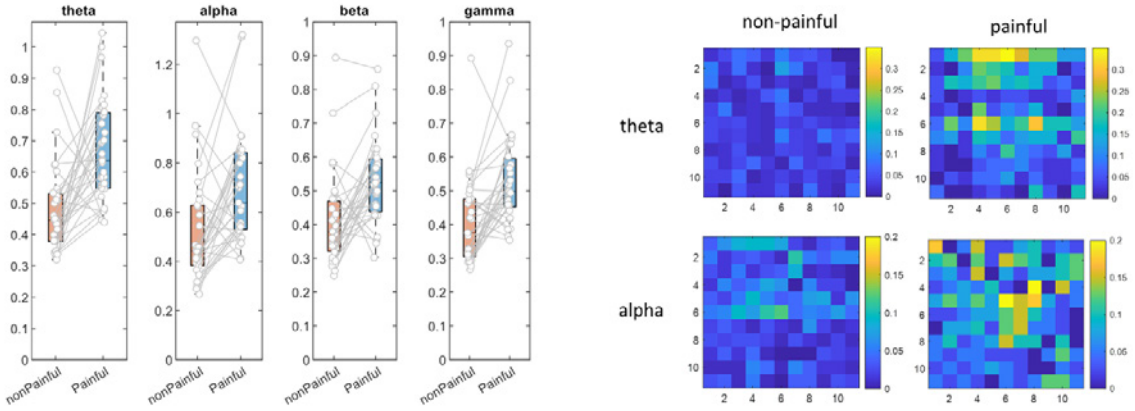

Fig. 7. Connectivity analysis. We calculated the phase lag index (PLI) values between EEG channels of the left and right sensorimotor cortices across painful and non-painful thermonociceptive stimulations. Left: PLI values for 40 participants, which increases significantly iin different frequency bands after delivering painful stimulation. Right: left-right connectivity based on PLI values for the theta (4-8 Hz) and alpha (8-12 Hz) frequency bands.

1. Andrews, P., Steultjens, M. & Riskowski, J. Chronic widespread pain prevalence in the general population: A systematic review. *Eur. J. Pain* **22**, 5–18 (2018).
2. Mouraux, A. & Iannetti, G. D. The search for pain biomarkers in the human brain. *Brain* **141**, 3290–3307 (2018).
3. Liberati, G. *et al.* Tonic thermonociceptive stimulation selectively modulates ongoing neural oscillations in the human posterior insula: Evidence from intracerebral EEG. *Neuroimage* **188**, 70–83 (2019).
4. Colon, E., Liberati, G. & Mouraux, A. EEG frequency tagging using ultra-slow periodic heat stimulation of the skin reveals cortical activity specifically related to C fiber thermonociceptors. *Neuroimage* **146**, 266–274 (2016).
5. Ploner, M., Sorg, C. & Gross, J. Brain rhythms of pain. *Trends Cogn Sci (Regul Ed)* **21**, 100–110 (2017).
6. Peng, W. & Tang, D. Pain related cortical oscillations: methodological advances and potential applications. *Front. Comput. Neurosci.* **10**, 9 (2016).
7. Leu, C., Courtin, A., Cussac, C. & Liberati, G. The role of ongoing oscillation in pain perception: Absence of modulation by a concomitant arithmetic task. *Cortex* **168**, 114–129 (2023).
8. Mulders, D. *et al.* Dynamics of the perception and EEG signals triggered by tonic warm and cool stimulation. *PLoS ONE* **15**, e0231698 (2020).
9. Kong, Q., Li, T., Reddy, S., Hodges, S. & Kong, J. Brain stimulation targets for chronic pain: Insights from meta-analysis, functional connectivity and literature review. *Neurotherapeutics* e00297 (2023) doi:10.1016/j.neurot.2023.10.007.
10. Bott, F. S. *et al.* Local brain oscillations and interregional connectivity differentially serve sensory and expectation effects on pain. *Sci. Adv.* **9**, eadd7572 (2023).

Geneeskundige Stichting Koningin Elisabeth
Fondation Médicale Reine Elisabeth
Königin-Elisabeth-Stiftung für Medizin
Queen Elisabeth Medical Foundation

Progress report of the research project of the young researcher

Prof. dr. Jeroen Bogie
Universiteit Hasselt (UHasselt)

Prof. dr. Jeroen Bogie (UHasselt)
Assistant Professor
T +32(0)11 26 92 61
www.uhasselt.be
Universiteit Hasselt - Campus Diepenbeek
Agoralaan Gebouw D - B-3590 Diepenbeek
Kantoor BMO-C107a

Getting a grip on slippery protein modifications in multiple sclerosis

1. State-of-the-art

A major pathological hallmark of neuroinflammatory disorders such as MS is the accumulation of macrophage subsets and T cells within the CNS. Driving these immune cells towards an anti-inflammatory, repair-promoting phenotype is considered a promising therapeutic strategy to halt MS disease progression and promote CNS repair. Emerging evidence indicates that fatty acids control the fate of immune cells in inflammatory disorders such as MS. We and others demonstrated that changes in the desaturation, -oxidation, and synthesis of fatty acids regulate the induction and maintenance of anti-inflammatory and reparative macrophage, microglia, and CD4+ T cell subsets in experimental models of MS. To date, however, the culprit fatty acids and molecular mechanisms that govern their influence on immune cell function and MS pathology remain ill-defined.

The saturated fatty acid palmitate is the most common fatty acid in the human body. It is situated at the heart of fatty acid metabolism, as it is the primary end-product of fatty acid synthesis and represents a major substrate for -oxidation and desaturation. We recently demonstrated that subtle changes in cellular palmitate levels have a major impact on the inflammatory and reparative properties of immune cells *in vitro* and in animal models of MS. Most studies on fatty acids in general, and palmitate in particular, focused on their role in energy metabolism and their effect on membrane composition. Based on our preliminary findings, we propose that S-palm, a posttranslational modification that consists of the reversible addition of palmitate to cysteine residues on proteins, is an important determinant of palmitate function in immune cells and MS pathology. In line with the importance of this modification, palmitoyl-proteome screens indicate that over 10% of the proteome is susceptible to S-palm, and accordingly, a family of 24 zinc finger DHHC-domain containing proteins (zDHHCs) have been identified as palmitoyl-transferases. Ample evidence indicates that S-palm dynamically regulates protein membrane interactions, intracellular sorting, and stability, and in doing so, tightly controls cellular function in health and disease

Our understanding of the role of S-palm in immunity is limited. Importantly, no studies have thus far addressed how changes in the S-palm landscape and machinery impact the polarization of primary macrophage, microglia, and T cell subsets, and to what extent these alterations can be harnessed to reduce neuroinflammation and promote CNS repair. Our preliminary data show that pharmacological inhibition of S-palm suppresses the induction of disease-associated macrophages (DAMs) and boosts that of repair-associated macrophages (RAMs) *in vitro*. Furthermore, they demonstrate that S-palm inhibition completely prevents disease severity in an in vivo autoimmune-induced neuroinflammation model, which was associated with an increase in regulatory T cells at the expense of Th17 cells. Finally, we found that S-palm inhibition enhances remyelination in ex vivo and in vivo toxin-induced demyelination models. All in all, these findings provide convincing evidence that S-palm represents a hub and driver of MS pathology as well as macrophage and CD4+ T cell physiology.

The short-term goal of this project is to address the role of S-palm in the induction of disease- and repair-associated immune cell subsets in MS. The long-term goal of this project is to identify S-palm as a novel therapeutic target to suppress neuroinflammation and promote CNS repair in MS.

Based on preliminary results, we hypothesize that S-palm drives the inflammatory and reparative properties of macrophage and T cell subsets in MS.

2. New findings

2.1. Active MS lesions show a markedly altered palmitoyl-proteome.

Employing the acyl-biotin exchange (ABE) assay, an innovative "cysteine-centric" proteomic tool to assess the protein S-acetylation landscape, we discovered that actively demyelinating human MS lesions, harboring abundant immune cells, exhibit a significantly altered palmitoyl-proteome (A). Of interest, we observed heightened lesional S-palm of proteins implicated in endocytosis, notably including caveolin 1 (CAV1) and fatty acid binding protein 5 (FABP5), providing a potential molecular rationale for incessant uptake of myelin and the induction of disease-promoting lesional foamy phagocytes in MS. Noteworthy, MS lesion lysates also underwent processing without hydroxylamine (HA), enabling the exclusion of false positives and establishing the enrichment of putative S-palm proteins (B). Our findings underscore the marked absence of proteins in active MS lesion lysates not subjected to HA, in contrast to lysates exposed to HA, which revealed enrichment of diverse established S-palm proteins. These findings validate the efficacy of the ABE in quantifying the palmitoyl-proteome of human brain tissue. In future experiments, we will extent the ABE analysis to other lesion subtypes and circulating immune cells of MS patients.

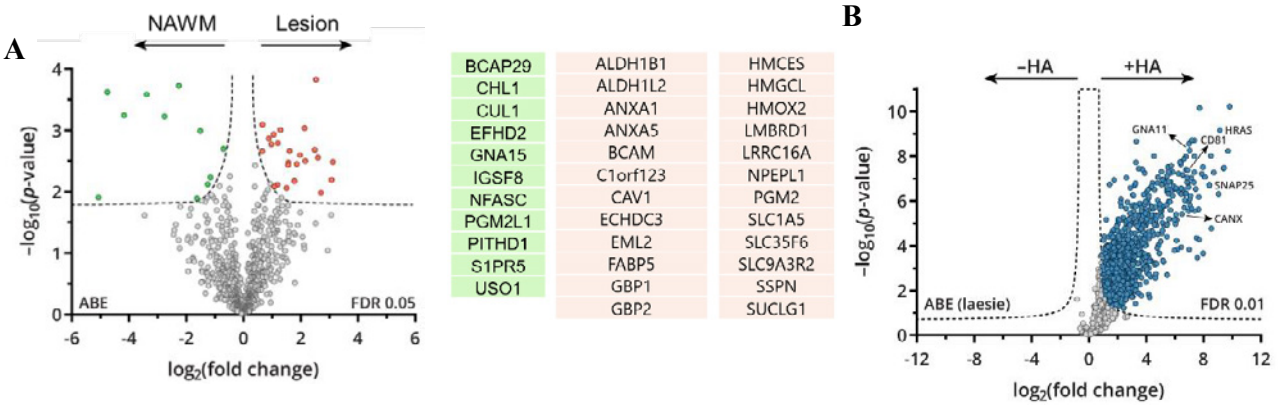

2.2. Inhibition of de-palmitoylation by APT-1 worsens remyelination

While S-palm is catalyzed by 24 acyltransferases, two acyl-protein thioesterases control the process of de-palmitoylation (APT-1 and APT-2). Of interest, our recent findings highlight that APT1 inhibition, but not APT2 inhibition, affects remyelination in contrasting ways compared to the S-palm inhibitor. Specifically, APT-1 (ML349 and PALM-B), and not APT-2 (ML-349) inhibition suppresses remyelination in ex vivo cerebellar brain slices (A) and the in vivo cuprizone model (B). The discovered insights unveil the intricate molecular mechanisms underlying S-palm dynamics in remyelination, offering compelling evidence that underscores the detrimental influence of S-palm on the remyelination process.

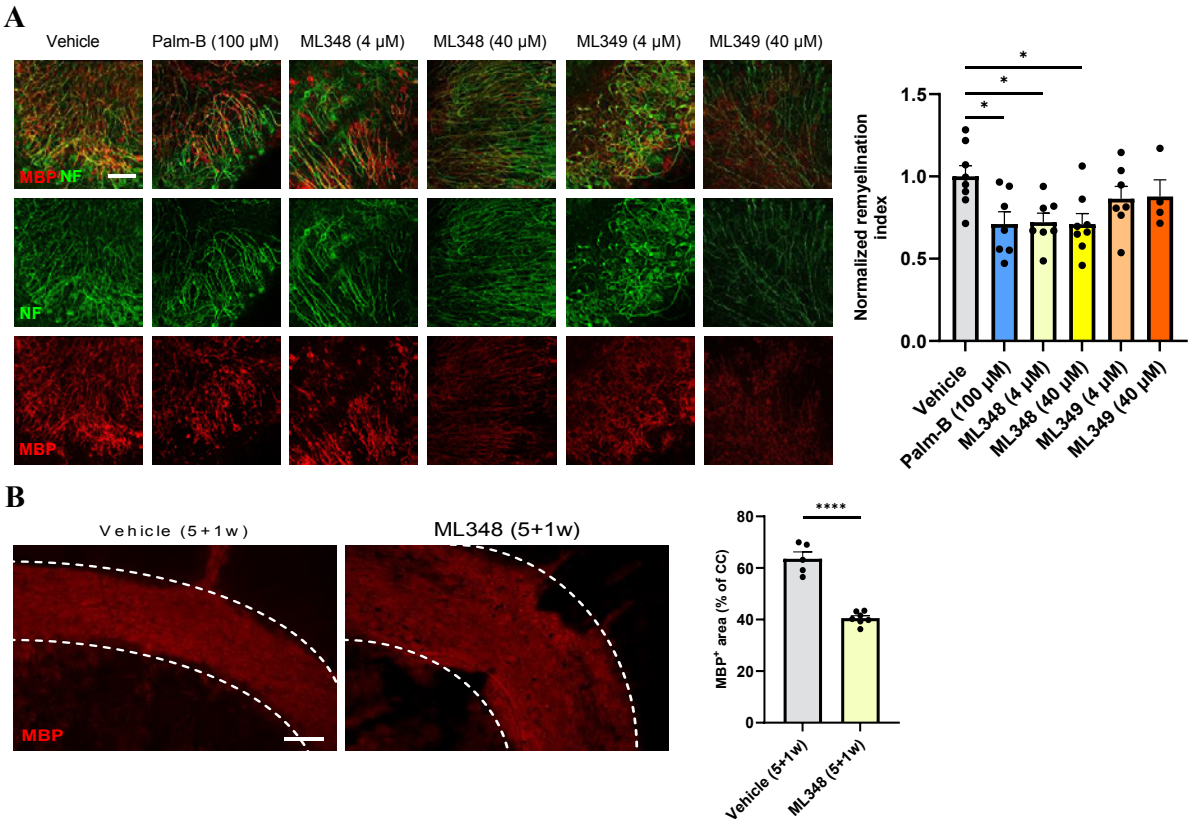

2.3. zDHHC5/18 are associated with the inflammatory phagocyte formation and demyelination

Despite promising preliminary findings showing that S-palm inhibition suppresses neuro-inflammation and promotes remyelination, the intricate regulation of S-palm by 24 zDHHC enzymes raises concerns about the potential for unforeseen side effects with broad inhibition. To address this, we conducted a transcriptomic screening to pinpoint specific zDHHCs linked to inflammatory phagocytes and active demyelination in experimental models and MS lesions. Analysis of bulk RNAseq datasets reveals a positive correlation between zDHHC5/18 and the induction of harmful macrophage subsets (foamy BMDMs, LAMs; LPS/IFN-stimulated BMDM, DAMs), as well as with active demyelination in the cuprizone model and human active MS lesions (A). Consistent with these findings, immunofluorescent stains demonstrated an increased protein abundance of these acyltransferases in $CD68^{+}$ phagocytes in MS lesions (B). Based on these findings, we hypothesize that inhibition of these acyl-transferases underpin the benign impact of the pan S-palm inhibitor on remyelination. To study the importance of zDHHC5/18 in driving phagocyte physiology, we will in the next year perform several key experiments. First, lentiviral vectors will be used to silence and overexpress zDHHC5/18 in macrophages and microglia, after which functional experiments will be performed. Our preliminary findings already indicate that lentiviral knockdown of zDHHC5 impacts the metabolic properties of myelin-containing "foamy" macrophages in a similar way as the pan-inhibitor of S-palm (2-BP) (C). Second, $LysM^{Cre}zDHHC5^{fl/fl}$ mice will be used to study the impact of phagocyte-specific zDHHC5 deficiency on remyelination in vivo. To this end, a research visit (3 months, March-May 2024) is planned by Jeroen Guns to the lab of Prof. dr. Neculai (Zhejiang University, China). Finally, a recent study has introduced a compelling repositioning of the FDA-approved drug lomitapide, identifying it as an inhibitor of zDHHC. In this context, our research endeavors in the next year encompass the administration of lomitapide to EAE and cuprizone mice to evaluate its potential in suppressing neuroinflammation and remyelination.

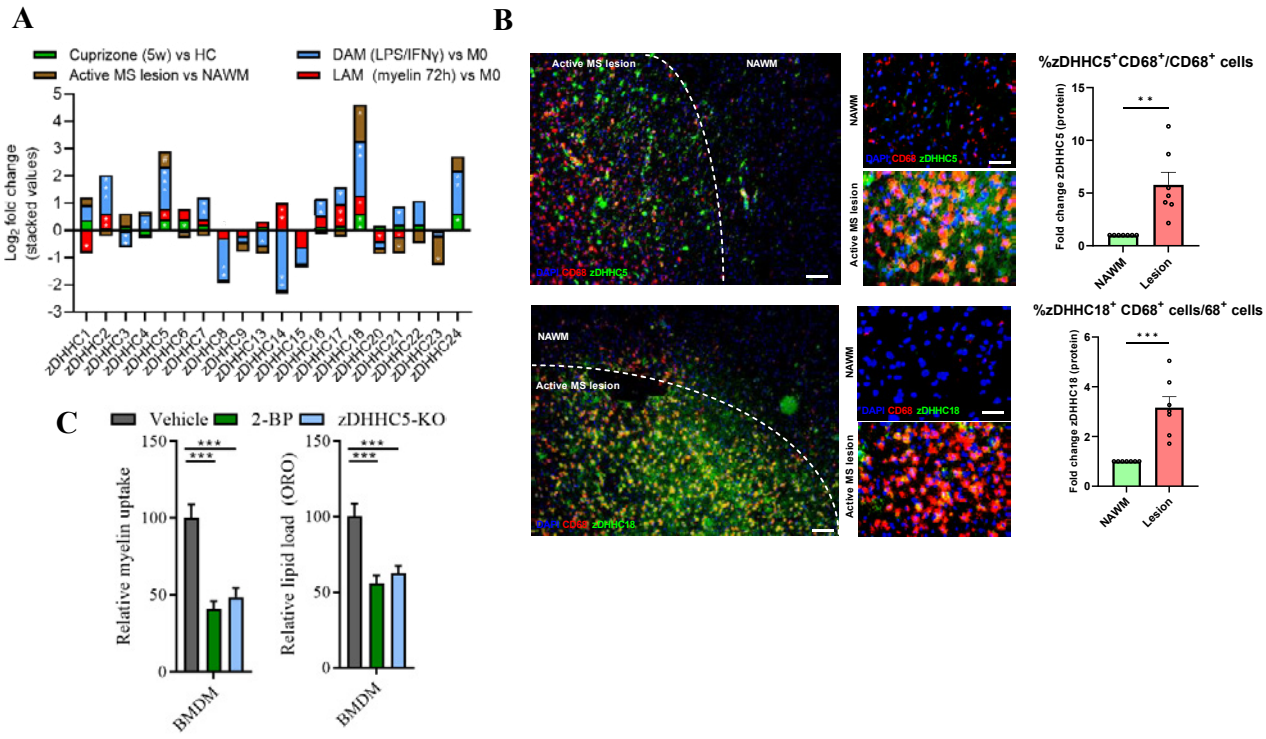

2.4. S-palm inhibition prevents DC maturation in vitro

Our preliminary data argue for early changes in T cell physiology in secondary lymph nodes underpinning the impact of pan-inhibition of S-palm on EAE disease. To dissect the cellular and molecular mechanisms and interactions driving the impact of broad S-palm inhibition on EAE disease, single cell RNAseq (scRNAseq) will be performed in the upcoming months on inguinal and cervical lymph nodes of EAE mice treated with 2-BP. This approach is necessary as the impact of S-palm on T cells could involve both direct and indirect effects. Notably, while lymphocytic proteins crucial for Tan and Treg differentiation are susceptible to S-palm (e.g. mTOR, LCK, and LAT), aberrant S-palm of co-stimulatory proteins and immunogenic peptides (PLP) in antigen-presenting cells might underlie alterations in Tan and Treg cells as well. In support of the latter, our recent data indicate that pan-inhibition of S-palm prevents the increase of CD80 and CD86 associated with dendritic cell maturation *in vitro*.

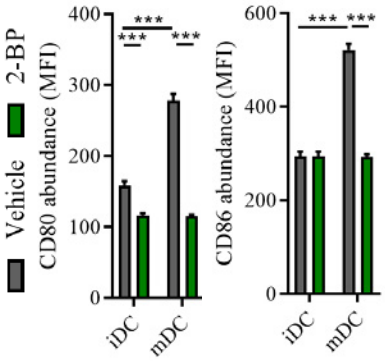

Geneeskundige Stichting Koningin Elisabeth
Fondation Médicale Reine Elisabeth
Königin-Elisabeth-Stiftung für Medizin
Queen Elisabeth Medical Foundation

Progress report of the research group of

Prof. dr. Bieke Broux
Universiteit Hasselt (UHasselt)

Bieke Broux, PhD (she, her) (UHasselt)

Assistant Professor Immunology
Chronic inflammation and Blood brain barrier disruption in Neurodegeneration (CBN)

Neuroimmune Connections & Repair (NIC&R) lab
Hasselt University – Biomedical Research Institute
Agoralaan, building C – B-3590 Diepenbeek
T +32 11 26 92 54
T +32 468 14 30 54

High salt diet causes blood-brain barrier disturbances in multiple sclerosis: involvement of the renin-angiotensin-aldosterone system

1. State of the art

Multiple sclerosis (MS) is a chronic neurodegenerative disorder that affects 2.8 million people worldwide[1]. In MS brain lesions, disturbances of the blood brain barrier (BBB) allow migration of immune cells into the brain parenchyma, causing demyelination and neurodegeneration. This leads to irreversible pathology resulting in physical and cognitive deterioration[2,3]. **Although several genetic and environmental factors have been shown to play an important role in MS pathogenesis, its etiology remains unclear, hindering the quest for a cure.**

In healthy conditions, the BBB protects the neuronal micro-environment by serving as a physical barrier between the periphery and the brain[4]. Specialized endothelial cells (ECs), together with astrocytic endfeet, limit paracellular migration of molecules and cells[5]. My research and that of others has pinpointed several immune-derived factors that regulate BBB integrity[6-8]. **However, the complex interplay between immune cells, the BBB and extrinsic (e.g. dietary) factors, remains elusive.**

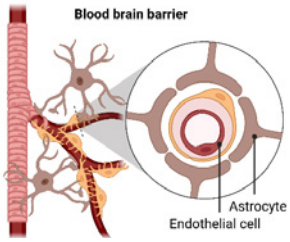

Dietary factors have been shown to play an important role in MS pathogenesis. My collaborator Prof. Dr. Markus Kleinewietfeld (VIB-UHasselt) identified high salt diet (HSD) as an important driver of T cell pathogenicity and loss of peripheral T cell tolerance[9,10], suggesting that HSD is a risk factor for MS[11]. Indeed, HSD, independently of blood pressure, exacerbates clinical and pathological measures of experimental autoimmune encephalomyelitis (EAE), a preclinical model for MS[9,12-14]. Interestingly, a study by Krementsov *et al.* suggested that EAE mice on HSD show enhanced leakage of the BBB[13]. In contrast, Na *et al.* recently reported that HSD suppresses spontaneous autoimmune demyelination, due to tightening of the murine BBB[15]. These contradictory findings need to be elucidated, and **the direct effect of high salt concentrations on the human BBB, and on the interplay between different NVU cells, has not been investigated yet.**

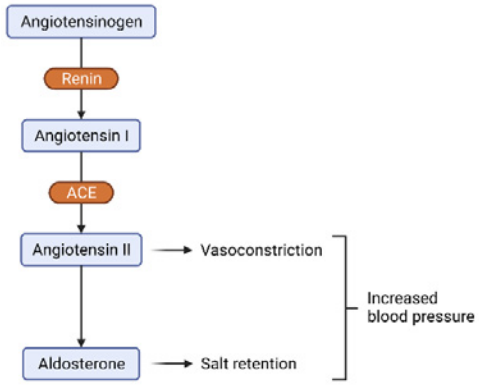

In MS patients and related animal models, increased salt loading in the skin was recently found[16], which is a sign of heightened salt sensitivity[17]. In addition, several groups have reported an involvement of the RAAS in animal models of MS, shown by reduced severity of disease after RAAS inhibition[18-20]. These reports suggest that in MS, salt sensitivity and/or RAAS homeostasis are disturbed. At the molecular level, RAAS activation increases Angiotensin II (AngII), produced from AngI by angiotensin converting enzyme I (ACEI), which then acts on the AngII receptor type 1 (AT_1R) on ECs. In the CNS, AngII was shown to be produced by astrocytes[21], and to act on AT_1R expressed on BBB-ECs. This modulates BBB integrity, although reports are contradictory[21,22]. Interestingly, some studies report that expression of AT_1R and AT_2R are regulated by salt[23-26]. Also, RAAS inhibition was found to reduce BBB permeability in rats, thereby improving salt-induced cognitive impairment, independent of changes in blood pressure[27,28]. However**, the impact of salt on RAAS homeostasis within the human NVU, in the context of neuro-inflammation, is not known.**

In this project, I propose a novel concept of dietary influence on disease: **I hypothesize that HSD, directly or through dysregulation of RAAS homeostasis in the NVU, leads to enhanced BBB disruption and exacerbation of neuro-inflammatory processes in MS.**

2. Milestones

Results from this project will reveal whether high salt concentrations have a direct effect on human BBB activation and integrity (**M1**). Detailed protein expression and RAAS fingerprint datasets are generated to assess effects of salt in presence or absence of inflammation in BBB-ECs and astrocytes (**M2**). These datasets can be additionally mined for future research projects. Salt-induced RAAS-mediated effects on human BBB integrity are identified (**M3**), as well as the impact of newly identified protein interactions between BBB-ECs and astrocytes, in inflammatory and high-salt conditions (**M4**). Finally, first correlations between salt sensitivity, RAAS homeostasis and BBB impairment are made in MS patients (**M5**). Together, this study will generate novel, highly informative knowledge on dietary influence on disease, in particular HSD in MS. In addition, the therapeutic potential of pathways and molecules involved will be explored, giving this project additional translational value.

3. Results

To get a first view of the effect of high salt concentrations on the BBB, hCMEC/D3 cells (a validated human cerebromicrovascular EC line[29-31]) were treated with 0 (control/CTL), 10, 40 or 80mM NaCl for 48h. First, when investigating BBB integrity (intercellular junctional stability), we found that high salt concentrations (not cytotoxic, data not shown), induced downregulation of the tight junction molecule Claudin-5 (Figure 1a). This was reflected in a decreased transendothelial electrical resistance (TEER), a surrogate marker of BBB integrity (Figure 1b). Second, when evaluating BBB activation (upregulation of cell adhesion molecules and chemokines), we found that VCAM-1 was significantly increased on BBB-ECs in high salt concentrations, and ICAM-1 showed a trend towards increase (Figure 1c-d). In addition, mRNA expression of chemokines CCL2 and CXCL10 was increased (Figure 1e-f). This suggests that high salt concentrations increase BBB permeability and activation, which together could lead to increased immune cell infiltration. In addition, we wished to get an initial understanding about the effect of high salt concentrations on RAAS-components in BBB-ECs. Using the same conditions as above, gene expression of renin, angiotensinogen (AGT) and AT_1R were determined. Interestingly, all genes were downregulated in low salt conditions, and were comparable to CTL levels in higher concentrations (Figure 1g-i). This suggests a dose-dependent salt-induced regulation of RAAS homeostasis in BBB-ECs.

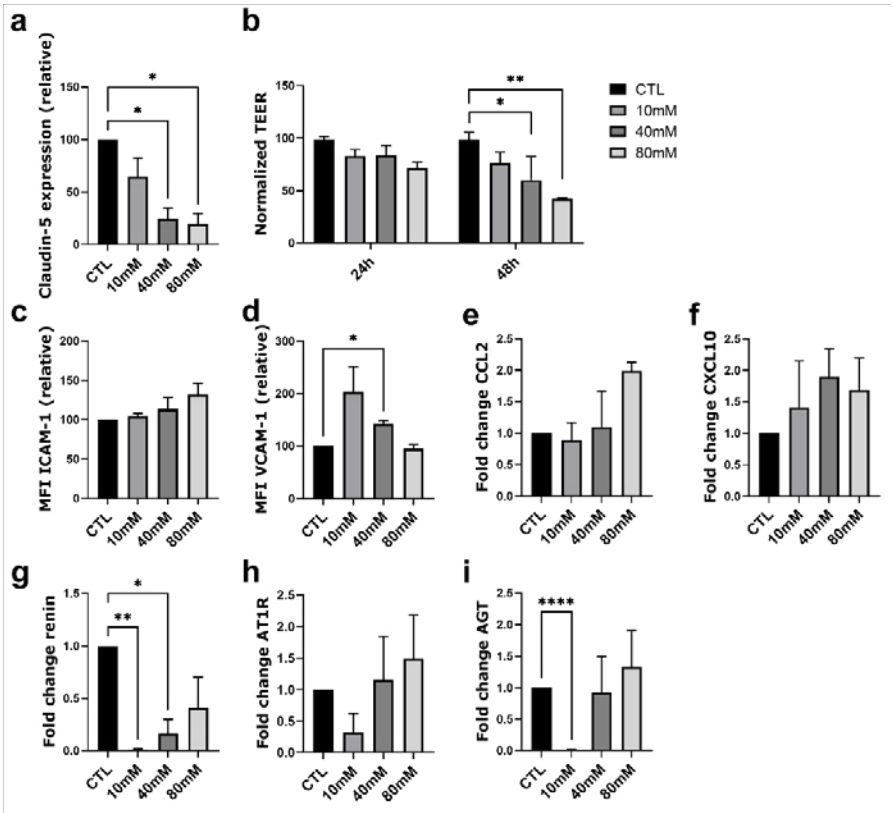

Figure 1. High salt concentration affects integrity, activation and RAAS homeostasis in human BBB-ECs. *The human cell line hCMEC/D3 was cultured until confluent, and treated with 0, 10, 40 or 80mM NaCl for 48h (n=2-4).* ***a)*** *Claudin-5 expression was measured by western blotting.* ***b)*** *TEER was measured in real-time using an in house designed device (in collaboration with Prof. Dr. Ronald Thoelen, IMO-IMOMEC, UHasselt). Measurements at 24 and 48h are shown.* ***c-d)*** *Protein expression of ICAM-1 and VCAM-1 was measured using flow cytometry.* ***e-i)*** *mRNA expression of CCL2, CXCL10, renin, AT_1R and AGT was measured using qPCR.*

Next, we aimed to evaluate whether high salt concentrations affected human BBB integrity **(M1)**. Previously optimized protocols for measuring real time TEER made use of the hCMEC/D3 cell line. Here we already showed in a preliminary experiment that after 48h both 40mM and 80 mM NaCl addition resulted in a decrease of TEER values (Figure 2). However, although the hCMEC/D3 is considered a reliable cell line to study functional BBB aspects such as immune cell migration, there are limitations in regards to the TEER values. Therefore, we have purchased the more stable hBEC5i cell line which has been reported to reach higher TEER values compared to the hCMEC/D3 cell line. After several optimization procedures we were able to reproduce the reported reliability of the TEER values in this cell line. Moreover, the cells were more susceptible to inflammatory cytokines and showed less variation (Figure 2). Next steps with this cell line will be to execute the real time TEER with addition of the salt conditions to unravel whether there is also an effect seen at 24 hours.

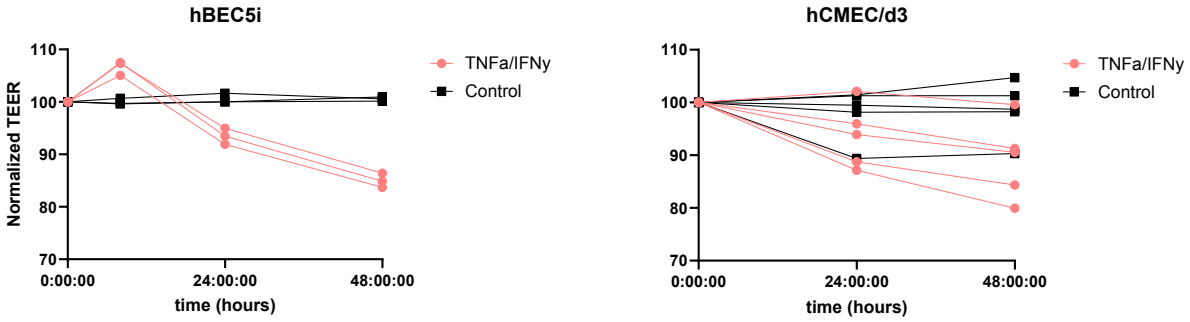

Figure 2. Reduction in TEER measured over time after adding inflammatory cytokines. *hBEC5i or hCMEC/D3 cells were cultured and grown till confluency. At day of confluency as measured by a plateau in TEER cells were treated with 10 ng/ul TNF/IFN (time point 0) or left untreated. RT-TEER was measure for a period of 48 hours after treatment.*

Further, hBEC5i cells will also be used in co-culture with astrocytes for diffusion assays. In order to optimize the protocol and determine the day of confluency on the inserts, manual TEER has to be measured each day. A new EVOM™ (manual TEER measurement device) has been purchased to ensure reliable and reproducible readings. Diffusion assays using hCMEC/D3 cells have previously been optimized in our lab with great success however the higher TEER values and less variation seen in hBEC5i cells warrants us to perform diffusion assays as such.

In addition, first experiments of transwell migration assays using a monolayer of hCMEC/D3 were performed. When the monolayer was formed, confluency measured with manual TEER, BBB-EC were treated with either inflammation or different salt concentrations for 24h. Next, lymphocytes were isolated from healthy donors and allowed to migrated over the monolayer. Using flow cytometry on collected lymphocytes, the % of migrated cells was calculated from live cells (Figure 3). Migration over an inflamed monolayer was increased compared to control conditions, suggesting a more permeable barrier as expected. Indeed, migration over NaCl treated monolayers was also enhanced, suggesting that salt can directly affect barrier integrity.

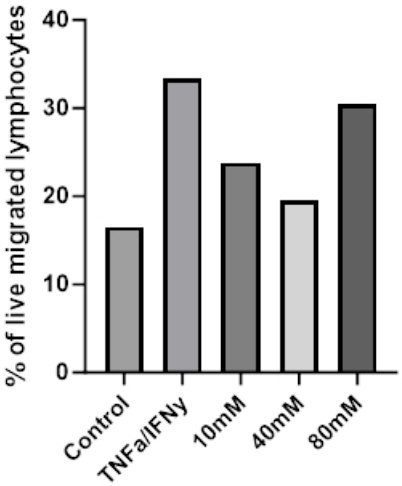

Figure 3. % of live migrated lymphocytes collected after 24h migration over hCMEC/D3 monolayer. *Results show increased migration in all experimental conditions when compared with the control (untouched) monolayer. Number of live lymphocytes were determined using a viability dye and flowcytometry.*

4. Future plans

There are still many questions remaining in this project that need to be investigated. Therefore, a new PhD student has been enrolled to work on the remainder of this project. Xue Zhong is a medically trained professional with knowledge about the RAAS system and clinical classifications making her a perfect candidate to reach the desired output in **M5.** While working on that data collection and analysis, drs. Zhong will also be trained in all BBB models required to bring this project to the finish line. Finally, she will implement a new BBB model in the lab in the coming year, using iPSC-derived BBB-endothelial cells. Doing so, this project, as well as all other projects in the lab, will take a step further in the translational value of our *in vitro* models.

5. Reference list

Publications of the applicant are highlighted in bold

1. Walton, C. *et al.* Rising prevalence of multiple sclerosis worldwide: Insights from the Atlas of MS, third edition. *Mult Scler* **26**, 1816-1821 (2020). https://doi.org/10.1177/1352458520970841
2. Ransohoff, R. M., Hafler, D. A. & Lucchinetti, C. F. Multiple sclerosis-a quiet revolution. *Nat Rev Neurol* **11**, 134-142 (2015). https://doi.org/10.1038/nrneurol.2015.14
3. Mundt, S., Greter, M., Flugel, A. & Becher, B. The CNS Immune Landscape from the Viewpoint of a T Cell. *Trends Neurosci* (2019). https://doi.org/10.1016/j.tins.2019.07.008
4. Correale, J. & Villa, A. The blood-brain-barrier in multiple sclerosis: functional roles and therapeutic targeting. *Autoimmunity* **40**, 148-160 (2007). https://doi.org/10.1080/08916930601183522
5. **Broux, B., Gowing, E. & Prat, A. Glial regulation of the blood-brain barrier in health and disease. *Semin Immunopathol* 37, 577-590 (2015). https://doi.org/10.1007/s00281-015-0516-2**
6. **Broux, B. *et al.* Interleukin-26, preferentially produced by TH17 lymphocytes, regulates CNS barrier function. *Neurol Neuroimmunol Neuroinflamm* 7 (2020). https://doi.org/10.1212/NXI.0000000000000870**
7. Kebir, H. *et al.* Human TH17 lymphocytes promote blood-brain barrier disruption and central nervous system inflammation. *Nat Med* **13**, 1173-1175 (2007). https://doi.org/10.1038/nm1651
8. **Hermans, D. *et al.* Oncostatin M triggers brain inflammation by compromising blood-brain barrier integrity. *Acta Neuropathol* (2022). https://doi.org/10.1007/s00401-022-02445-0**
9. Kleinewietfeld, M. *et al.* Sodium chloride drives autoimmune disease by the induction of pathogenic TH17 cells. *Nature* **496**, 518-522 (2013). https://doi.org/10.1038/nature11868
10. Hernandez, A. L. *et al.* Sodium chloride inhibits the suppressive function of FOXP3+ regulatory T cells. *J Clin Invest* **125**, 4212-4222 (2015). https://doi.org/10.1172/JCI81151
11. Muller, D. N., Wilck, N., Haase, S., Kleinewietfeld, M. & Linker, R. A. Sodium in the microenvironment regulates immune responses and tissue homeostasis. *Nat Rev Immunol* **19**, 243-254 (2019). https://doi.org/10.1038/s41577-018-0113-4
12. Wu, C. *et al.* Induction of pathogenic TH17 cells by inducible salt-sensing kinase SGK1. *Nature* **496**, 513-517 (2013). https://doi.org/10.1038/nature11984
13. Krementsov, D. N., Case, L. K., Hickey, W. F. & Teuscher, C. Exacerbation of autoimmune neuroinflammation by dietary sodium is genetically controlled and sex specific. *FASEB J* **29**, 3446-3457 (2015). https://doi.org/10.1096/fj.15-272542
14. Wilck, N. *et al.* Salt-responsive gut commensal modulates TH17 axis and disease. *Nature* **551**, 585-589 (2017). https://doi.org/10.1038/nature24628
15. Na, S. Y., Janakiraman, M., Leliavski, A. & Krishnamoorthy, G. High-salt diet suppresses autoimmune demyelination by regulating the blood-brain barrier permeability. *Proc Natl Acad Sci U S A* **118** (2021). https://doi.org/10.1073/pnas.2025944118
16. Huhn, K. *et al.* Skin sodium is increased in male patients with multiple sclerosis and related animal models. *Proc Natl Acad Sci U S A* **118** (2021). https://doi.org/10.1073/pnas.2102549118
17. Selvarajah, V., Connolly, K., McEniery, C. & Wilkinson, I. Skin Sodium and Hypertension: a Paradigm Shift? *Curr Hypertens Rep* **20**, 94 (2018). https://doi.org/10.1007/s11906-018-0892-9
18. Stegbauer, J. *et al.* Role of the renin-angiotensin system in autoimmune inflammation of the central nervous system. *Proc Natl Acad Sci U S A* **106**, 14942-14947 (2009). https://doi.org/10.1073/pnas.0903602106

19. Platten, M. *et al.* Blocking angiotensin-converting enzyme induces potent regulatory T cells and modulates TH1- and TH17-mediated autoimmunity. *Proc Natl Acad Sci U S A* **106**, 14948-14953 (2009). https://doi.org/10.1073/pnas.0903958106
20. Timmermans, S. *et al.* High fat diet exacerbates neuroinflammation in an animal model of multiple sclerosis by activation of the Renin Angiotensin system. *J Neuroimmune Pharmacol* **9**, 209-217 (2014). https://doi.org/10.1007/s11481-013-9502-4
21. Wosik, K. *et al.* Angiotensin II controls occludin function and is required for blood brain barrier maintenance: relevance to multiple sclerosis. *J Neurosci* **27**, 9032-9042 (2007). https://doi.org/10.1523/JNEUROSCI.2088-07.2007
22. Fleegal-DeMotta, M. A., Doghu, S. & Banks, W. A. Angiotensin II modulates BBB permeability via activation of the AT(1) receptor in brain endothelial cells. *J Cereb Blood Flow Metab* **29**, 640-647 (2009). https://doi.org/10.1038/jcbfm.2008.158
23. Nickenig, G. *et al.* Salt induces vascular AT1 receptor overexpression *in vitro* and in vivo. *Hypertension* **31**, 1272-1277 (1998). https://doi.org/10.1161/01.hyp.31.6.1272
24. Wang, D. H. & Du, Y. Regulation of vascular type 1 angiotensin II receptor in hypertension and sodium loading: role of angiotensin II. *J Hypertens* **16**, 467-475 (1998). https://doi.org/10.1097/00004872-199816040-00008
25. Gonzalez, M. *et al.* High-salt diet inhibits expression of angiotensin type 2 receptor in resistance arteries. *Hypertension* **45**, 853-859 (2005). https://doi.org/10.1161/01.HYP.0000161990.98383.ad
26. Foulquier, S. *et al.* High salt intake abolishes AT(2)-mediated vasodilation of pial arterioles in rats. *J Hypertens* **29**, 1392-1399 (2011). https://doi.org/10.1097/HJH.0b013e328347050e
27. Pelisch, N. *et al.* Blockade of AT1 receptors protects the blood-brain barrier and improves cognition in Dahl salt-sensitive hypertensive rats. *Am J Hypertens* **24**, 362-368 (2011). https://doi.org/10.1038/ajh.2010.241
28. Pelisch, N., Hosomi, N., Mori, H., Masaki, T. & Nishiyama, A. RAS inhibition attenuates cognitive impairment by reducing blood- brain barrier permeability in hypertensive subjects. *Curr Hypertens Rev* **9**, 93-98 (2013). https://doi.org/10.2174/1573402113099990003
29. Weksler, B., Romero, I. A. & Couraud, P. O. The hCMEC/D3 cell line as a model of the human blood brain barrier. *Fluids Barriers CNS* **10**, 16 (2013). https://doi.org/10.1186/2045-8118-10-16
30. **Broux, B. *et al.* IL-15 amplifies the pathogenic properties of CD4+CD28- T cells in multiple sclerosis. *J Immunol* 194, 2099-2109 (2015). https://doi.org/10.4049/jimmunol.1401547**
31. Helms, H. C. *et al.* In vitro models of the blood-brain barrier: An overview of commonly used brain endothelial cell culture models and guidelines for their use. *J Cereb Blood Flow Metab* **36**, 862-890 (2016). https://doi.org/10.1177/0271678X16630991

Geneeskundige Stichting Koningin Elisabeth
Fondation Médicale Reine Elisabeth
Königin-Elisabeth-Stiftung für Medizin
Queen Elisabeth Medical Foundation

Progress report of the research group of

Dr. Sophie Laguesse
Université de Liège (ULiège)

Dr. Sophie Laguesse (ULiège)
Liège University
F.R.S-FNRS Research Associate
Giga-Stem Cells, Giga-Neurosciences
Laboratory of molecular regulation of Neurogenesis – Addiction development
Quartier Hôpital
15, Avenue Hippocrate
B-4000 Liège
Belgium
T +32 4 366.59.51
slaguesse@uliege.be
ORCID 0000-0002-9217-0087

Unveiling the alcohol-dependent alterations in mRNA local translation and its consequences on adolescent prefrontal cortex maturation and function

1. Goals of the research

Alcohol use disorder (AUD) is characterized by an impaired ability to control alcohol use and ranks among the most prevalent mental disorders globally. The neural mechanisms of AUD have remained uncertain, and multiple genetic, psychological and environmental factors are thought to be involved. For decades, AUD has been considered as a pathological condition that develops in adults, but growing evidence suggests that its roots may emerge during adolescence. Indeed, studies have shown that adolescent alcohol exposure (AAE) may interfere with the maturation of some frontal brain regions, including the prefrontal cortex (PFC) and lead to heightened vulnerability to develop AUD and comorbid psychopathology later in life. However, **the precise mechanisms by which alcohol perturbs the maturation of the PFC are not fully understood**. Addiction has been conceptualized as a maladaptive form of memory involving persistent drug-associated memories. In this view, alcohol is thought to usurp the molecular mechanisms underlying memory, including synaptic plasticity which depends on the local translation of mRNAs at synaptic sites. Here, **we hypothesize that AAE interferes with local translation of mRNAs, thereby impairing prefrontal cortex maturation**. The main goals of this research are *(i)* To unveil whether AAE leads to PFC malfunction in mice, *(ii)* To decipher whether AAE modulates the activity of specific local translation regulators in the PFC, *(iii)* To identify the pool of mRNAs whose local translation is modulated by AAE in specific neuronal populations and *(iv)* unveil their involvement in AAE-induced PFC defects, and finally *(v)* To decipher whether AAE differentially impacts male and female PFC.

2. Task 1: Characterizing PFC malfunction induced by adolescent alcohol binge-drinking

By using a modified version of the Drinking in the Dark paradigm, we previously reported that voluntary alcohol binge-drinking in adolescent mice significantly increases anxiety-like, depressive-like behaviors and alcohol consumption, while impairing recognition memory and behavioral flexibility in adulthood, suggesting that AAE compromises long-term PFC function (Van Hees, Didone et al. 2022).

2.1. Uncovering the structural and physiological defects induced by AAE in the PFC

We performed whole cell patch-clamp recordings in layer V glutamatergic neurons of the prelimbic subregion of the PFC in adolescent (P43) and adult (P80) male mice. In late adolescent mice, we showed a significant increase in the frequency of spontaneous excitatory post-synaptic currents in AAE animals as compared to control littermates, without significant change in their amplitude (**Figure 1**).

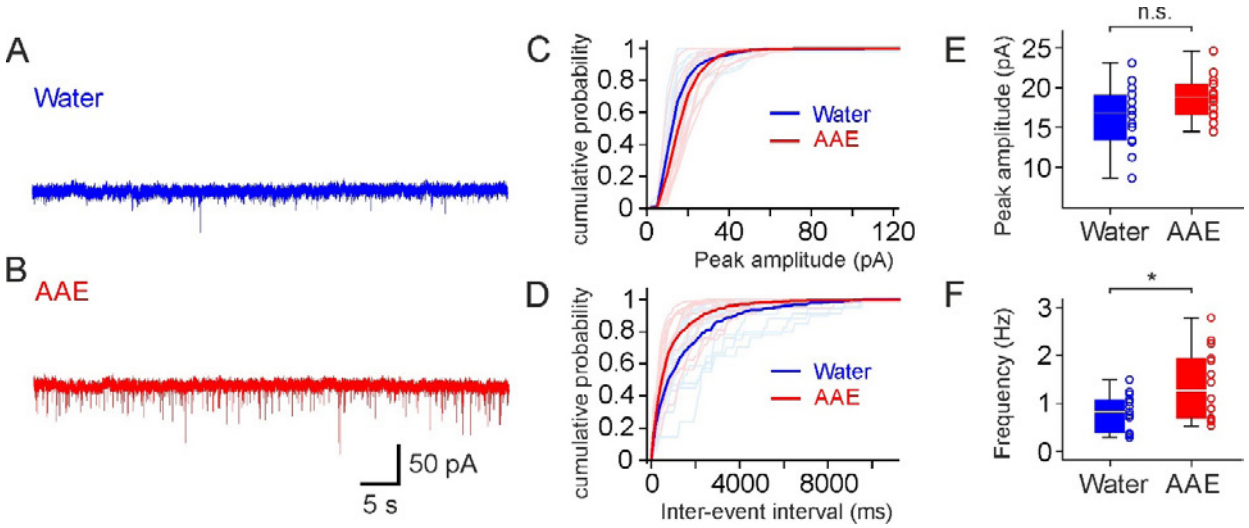

Figure 1. Alcohol consumption increases sEPSC frequency in layer 5 pyramidal neurons of the prelimbic cortex at P43. (**A, B**) Current traces showing spontaneous EPSCs at -60 mV in slices from water-consuming mice (top, blue traces) and from alcohol-consuming mice (bottom, red traces). External solution contained 50 µM picrotoxin to block inhibitory synaptic currents. (**C, D**) Cumulative distributions of spontaneous EPSC amplitude (**C**) and inter-event intervals (**D**). Thick lines are average cumulative distributions from pyramidal neurons in water- (blue) and alcohol-consuming (red) mice, respectively. Thin lines are from individual cells. Data are from 14 and 14 individual neurons, respectively. (**E, F**) Histograms of EPSC peak amplitude (**E**) and frequency (**F**) for water-consuming mice and alcohol-consuming mice. Data are from 14 pyramidal neurons (water) and 14 pyramidal neurons (AAE). * $p<0.05$.

In adulthood, no difference was observed in the frequency or amplitude of sEPSCs between AAE and water animals (**Figure 2**). We are currently performing the same experiment on female mice at P43 and P80 to decipher whether alcohol differentially impact projection neuron transmission in male and female adolescent mice. Moreover, spontaneous and evoked inhibitory post-synaptic currents (sIPSCs and mIPSCs) will be recorded to assess potential AAE-induced changes in inhibitory responses. Finally, layer II-III projection neurons will also be analyzed.

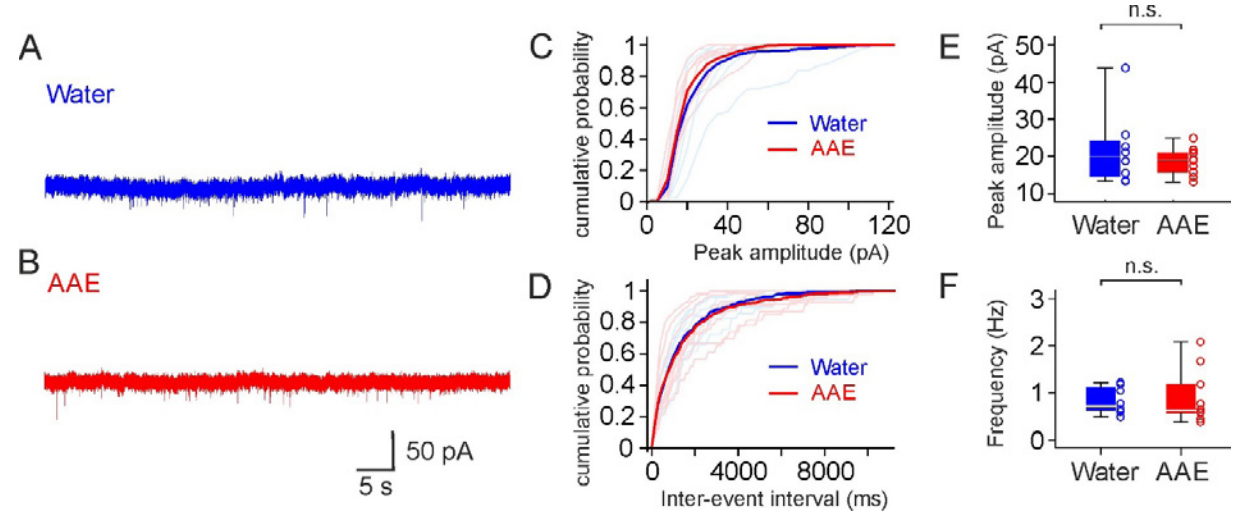

Figure 2. Alcohol consumption does not modify sEPSC frequency in layer 5 pyramidal neurons of the prelimbic cortex at P80. (**A, B**) Current traces showing spontaneous EPSCs at -60 mV in slices from water-consuming mice (top, blue traces) and from alcohol-consuming mice (bottom, red traces). External solution contained 50 µM picrotoxin to block inhibitory synaptic currents. (**C, D**) Cumulative distributions of spontaneous EPSC amplitude (**C**) and inter-event intervals (**D**). Thick lines are average cumulative distributions from pyramidal neurons in water- (blue) and alcohol-consuming (red) mice, respectively. Thin lines are from individual cells. Data are from 8 and 10 individual neurons, respectively. (**E, F**) Histograms of EPSC peak amplitude (**E**) and frequency (**F**) for water-consuming mice and alcohol-consuming mice. Bars represent mean ± SEM; open circles indicate data from individual recordings. Data are from 8 pyramidal neurons (water) and 10 pyramidal neurons (AAE).

Neurons were filled with biocytin for *post hoc* immunohistochemistry, 3D reconstruction and morphological analysis. We did not observe any defect in dendritic arborization of layer V glutamatergic neurons of the prelimbic PFC, neither at P43 or P80 (**Figure 3**).

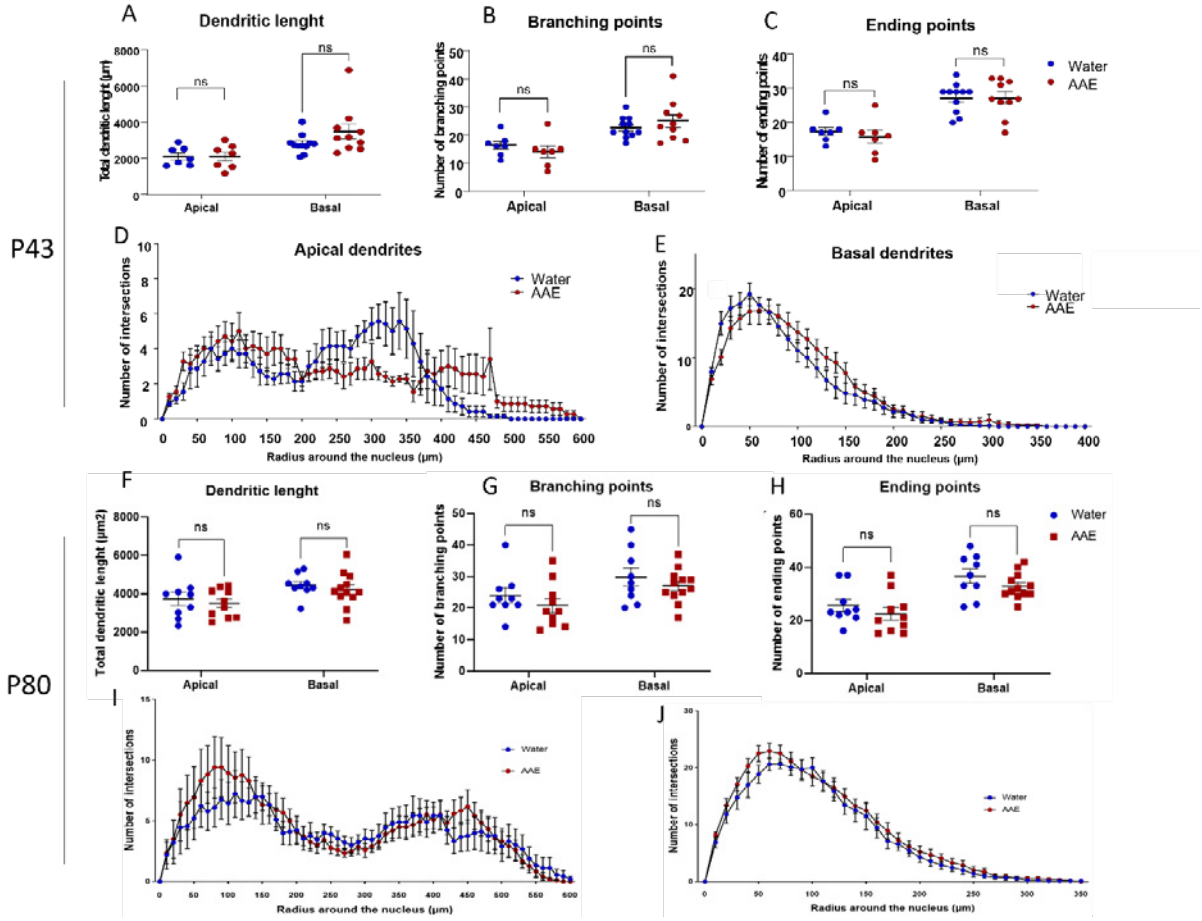

Figure 3: No change in apical and basal dendrites morphometric measurements after AAE in prelimbic layer V projection neurons at P43 or P80. (**A**) Total length of apical (left) and basal (right) dendritic arborizations. Unpaired t test showed no effect of alcohol on apical dendritic length (p=0.9854) nor on basal dendritic length (p=0.1361). (**B-C**) Number of branching and ending points per apical and basal dendritic arborization per neuron. Unpaired t test showed no effect of alcohol on the number of apical (p=0.4114) and basal (p=0.8279) branching points nor on the number of apical (p=0.50) and (p=0.9731) basal ending points. (**D-E**) Sholl analysis of apical (**D**) and basal (**E**) dendrites. Two-way ANOVA showed no effect of AAE (*apical*: p=0.715, $F_{(1,12)}$=0.1403; *basal* p=0.5116, $F_{(1,19)}$=0.4474). *Data are presented as mean ± SEM; for apical dendrites: n=7 water, n=7 AAE; for basal dendrites: n=11 water, n=10 AAE.* (**F**) Total length of apical (left) and basal (right) dendritic arborizations, expressed in µm. Unpaired t test did not show any significant difference in apical (p=0.5773) and basal dendritic length (p=0.5274). (**G-H**) Number of branching and ending points per apical (left) and basal (right) dendritic arborization per neuron. Unpaired t test showed a similar number of apical (p=0.3406) and basal (p=0.3518) branching points and a constant number of apical (p=0.3627) and (p=0.1907) basal ending points between water and AAE mice. (**I-J**) Sholl analysis of apical (**I**) and basal (**J**) dendrites. Two-way ANOVA showed no effect of AAE (*apical*: p=0.5814, $F_{(1,19)}$=0.3146; *basal*: p=0.341, $F_{(1,19)}$=0.9539). *Data are presented as mean ± SEM; for apical dendrites: n=9 water, n=10 AAE; for basal dendrites: n=9 water, n=12 AAE*

However, we identified changes in dendritic spine morphology in late adolescence following AAE, including increased mean spine head size and an increased proportion of mushroom-type spines (**Figure 4**), which were not present anymore in adulthood (**Figure 5**). The same morphological analysis is currently being performed in females and will be also conducted in layer II-III neurons.

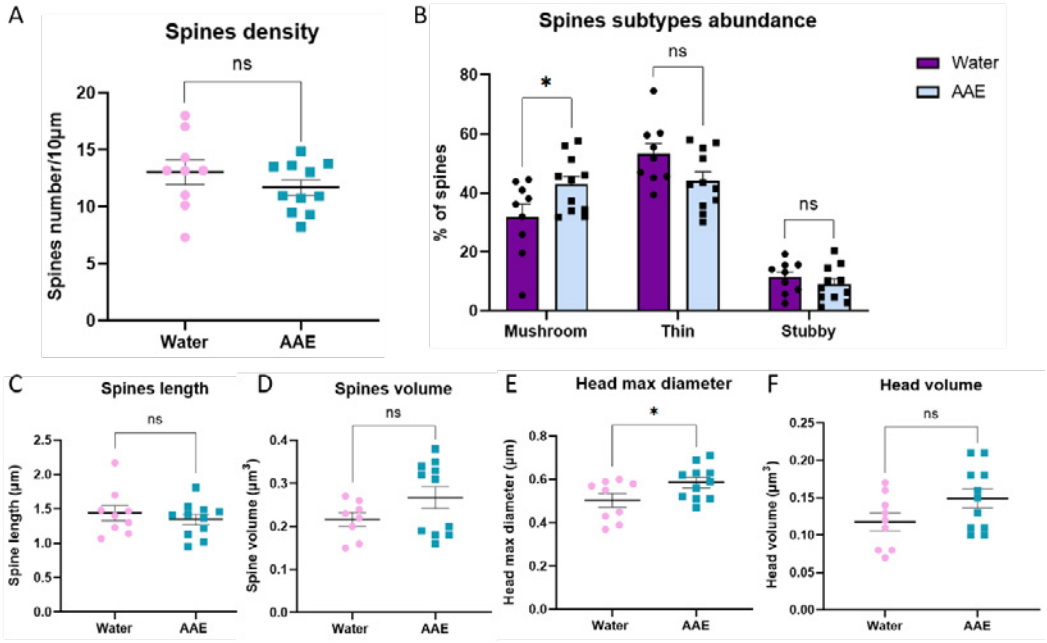

Figure 4: AAE modifies dendritic spines morphology in PFC layer V projection neurons at P43. (**A**) Spine density defined as the number of spines per 10µm of dendrite. Unpaired t test did not show any significant difference in spines density between alcohol and control groups (p=0.2862). (**B**) Percentage of mushroom, thin and stubby-type spines. Percentage is measured as the number of each type of spines on the total number of spines per dendrite*100. Unpaired t test showed a significant effect of AAE on the percentage of mushroom-type spines (p=0.0427), but no main effect on thin- (p=0.663) or stubby-type (p=0.3597) percentage. (**C-F**) Average spine length, volume, head max diameter and head volume of water and AAE mice. Unpaired t test showed a significant increased head max diameter (**E**) (p=0.045) but no significant difference in spine length (**C**) (p=0.4818), spine volume (**D**) (p=0.1367) or head volume (**F**) (p=0.0945). Regarding spine volume analysis, Grubbs' test detected an outlier value in water data (n=8 water), which has been removed. *Data are presented as mean ± SEM; n=9 water, n=11 AAE ;*p<0.05.*

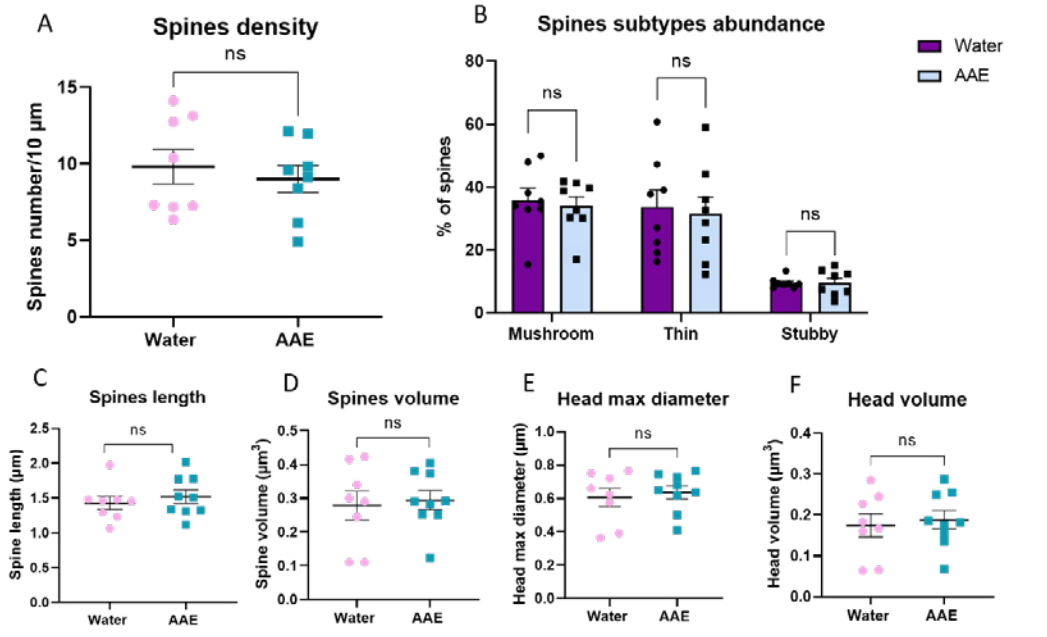

Figure 5: No defect in dendritic spines number or morphology in PFC layer V projection neurons at P80 (**A**) Spines density defined as the number of spines per 10µm of dendrite. Unpaired t test showed no significant difference between alcohol and control groups (p=0.5838). (**B**) Percentage of mushroom, thin and stubby-type spines. Percentage is measured as the number of each type of spines on the total number of spines per dendrite*100. Unpaired t test showed no main effect of AAE on the percentage of mushroom- (p=0.6882), thin- (p=0.77) and stubby-type (p=0.999) spines. (**C-F**) Average spine length, volume, head max diameter and head volume of water and AAE mice. Unpaired t test showed that AAE did not significantly modify spine length (p=0.5098), spine volume (p=0.7667), head max diameter (p=0.6508) and head volume (p=0.711). *Data are presented as mean ± SEM; n=8 water neurons, n=9 AAE neurons.*

3. Task 2: Deciphering whether AAE modulates local translation in the adolescent PFC

3.1. Analysis of mTORC1 activity in the PFC following AAE

By western blot analysis on total PFC extracts, we have reported that AAE increases the phosphorylation levels of S6 Kinase and S6 in the PFC of males and females at P40, suggesting AAE-induced activation of mTORC1 activity following acute alcohol consumption (**Figure 6**).

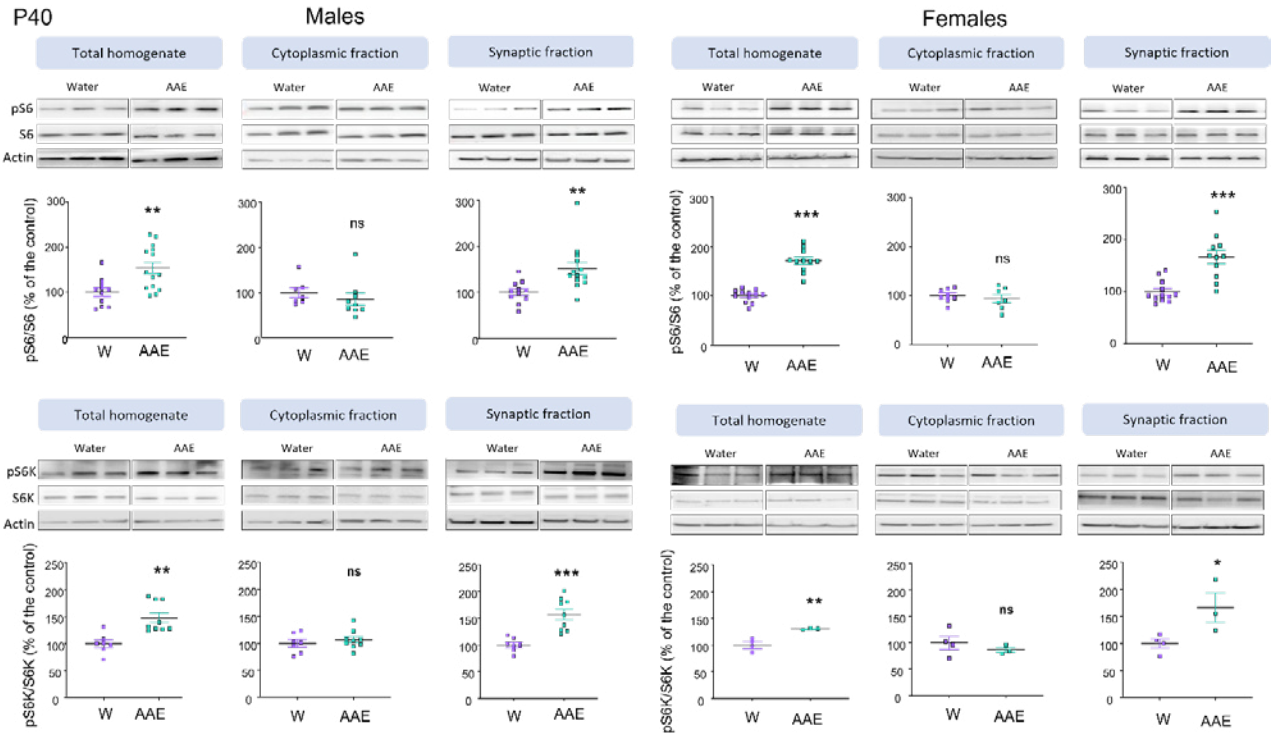

Figure 6. AAE activates mTORC1 in the adolescent PFC. Western blot analysis of phosphorylation levels of ribosomal protein S6 and S6 kinase in the PFC of males and females adolescent mice. Immediately after the last drinking session, PFC samples were dissected and analyzed by western blot. Significant increased phosphorylation of S6 and S6K were observed in the total homogenate and synaptic fraction of PFC extracts, both in males and females. *p<0.05; **p<0.01; ***p<0.001.

Moreover, by performing cytoplasmic and synaptic purification, we demonstrated that this increased mTORC1 activity is specifically found in the synaptic fraction, suggesting that alcohol exposure might specifically modulate the activity of mTORC1 in local translation rather than in global translation in the adolescent PFC (**Figure 6**). Importantly, phosphorylation levels of S6 were not increased in the motor cortex of alcohol-exposed adolescent mice (data not shown), suggesting that the alcohol-induced modulation of local translation might be specific to discrete brain regions including the PFC. We also assessed S6 phosphorylation levels 72 hours after the last drinking session. As shown in **Figure 7**, S6 phosphorylation levels were significantly increased in the PFC of both males and females at P43, suggesting long-lasting activation of mTORC1 following AAE. Finally, when assessed at P80, no change in S6 phosphorylation levels were detected between water and AAE male mice (**Figure 8**). Additional western blot to assess p-S6K and p-4E-BP are currently performed in cytoplasmic and synaptic fractions of the PFC in both sexes at the three time-points.

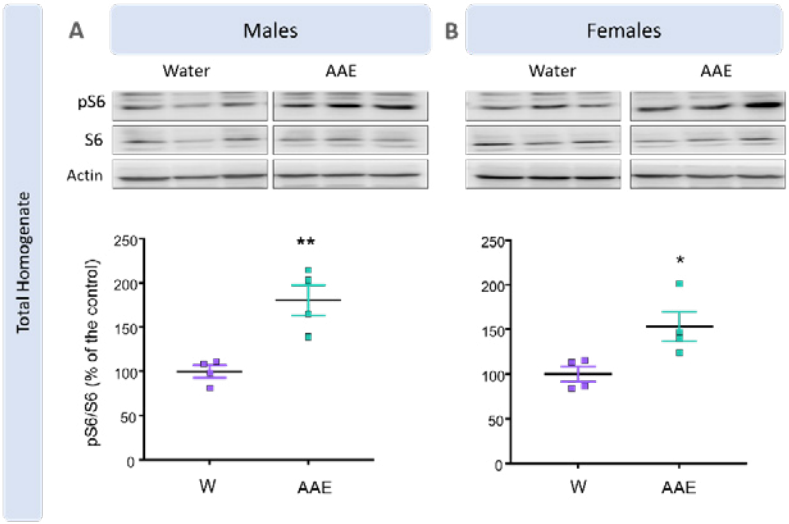

Figure 7. AAE-induced activation of mTORC1 is long-lasting. Western blot analysis of phosphorylation levels of ribosomal protein S6 in the PFC of males and females adolescent mice. Seventy-two hours after the last drinking session, PFC samples were dissected and analyzed by western blot. Significant increased phosphorylation of S6 were observed in the total homogenate of PFC extracts, both in males and females. *p<0.05; **p<0.01.

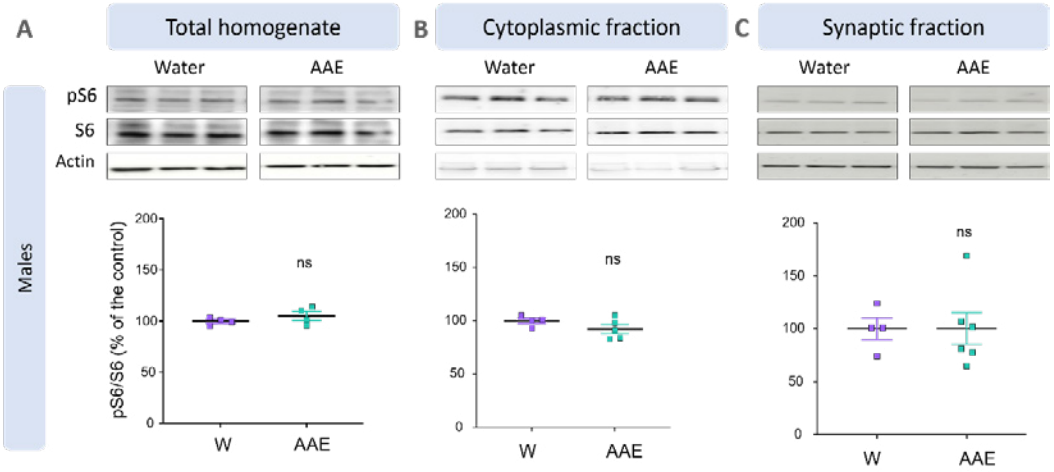

Figure 8. AAE-induced mTORC1 activation in the PFC is no longer present in adulthood. Western blot analysis of phosphorylation levels of ribosomal protein S6 in the PFC of males adult mice. Forty days after the last drinking session, PFC samples were dissected and analyzed by western blot. No significant change in S6 phosphorylation were observed in the total homogenate or synaptic/ cytoplasmic fractions of PFC extracts.

We also assessed mTORC1 activation following AAE by immunofluorescence. As shown in **Figure 9**, we observed a significant increased phosphorylation of S6 in AAE animals at P40, both in males and females, which may specifically localize in the Ctip2+ layer V projection neurons. Additional experiments are currently being conducted with additional neuronal identity markers (SatB2, Tbr1,…), and at later time-points (P43, P80), in both sexes. Furthermore, we will use the Super-resolution Zeiss LSM880 AiryScan Elyra S1 confocal, in order to more specifically study pS6 localization within the neuronal cells. Finally, eIF2 and eEF2 activity will be assessed in the PFC.

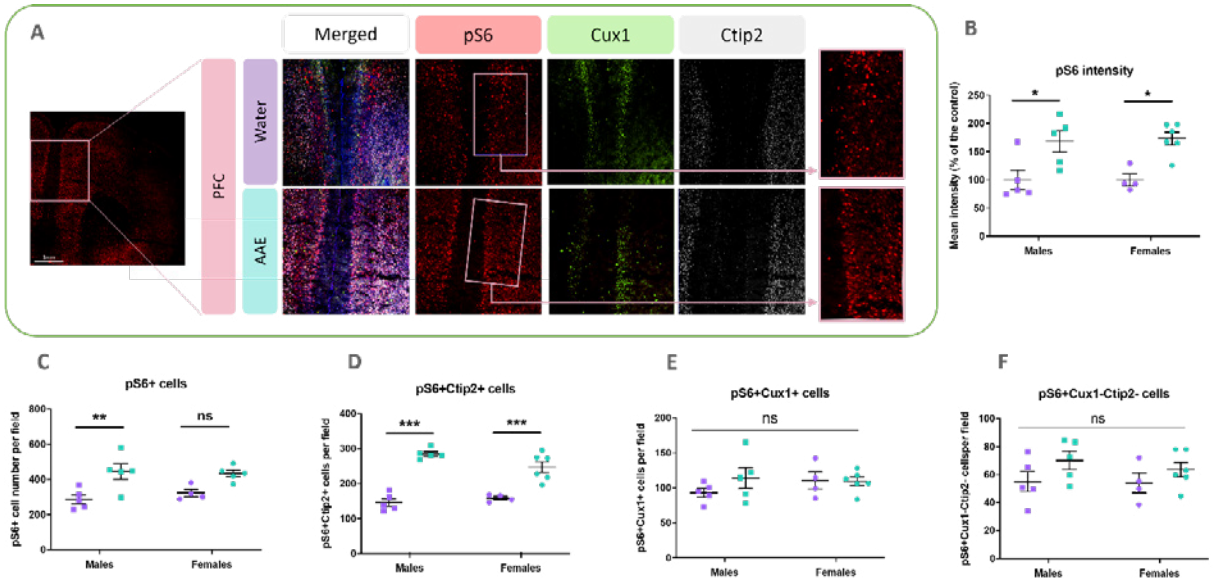

Figure 9. AAE increases S6 phosphorylation levels in PFC layer V neurons. Immunolabeling of the phosphorylated form of the ribosomal protein S6 in the PFC of males and females P40 adolescent mice. Immediately after the last drinking session, brains were dissected, fixed and used for Immunofluorescence. (**A**) pS6 in red, Cux1 in green, Ctip2 in gray. (**B**) Significant increased S6 phosphorylation intensity were observed in AAE animals compared to water controls extracts in both sexes. (**C**) Significant increased number of pS6-positive cells in AAE animals as compared to water controls. (**D-F**) The increased phosphorylation levels of S6 are localized mostly in layer V Ctip2-positive cells. *p<0.05; **p<0.01; ***p<0.001.

Task 2.2 Deciphering whether mTORC1, eIF2 and/or eEF2 mediate the structural and transmission defects induced by AAE in the PFC, as well as behavioral defects

We first conducted a pilot experiment where we inhibited mTORC1 activity by using systemic rapamycin injections, at the end of session 5 and session 10 of the AAE paradigm (**Figure 10**). Such timing of injections was used to avoid decreased alcohol consumption following rapamycin injections (Beckley, Laguesse et al. 2016). As shown in **Figure 10**, rapamycin treatment during adolescence significantly reduced alcohol consumption in adulthood in AAE animals. These findings suggest that counteracting alcohol-dependent activation of mTORC1 during AAE may partially rescue the increased alcohol intake observed in adulthood following AAE.

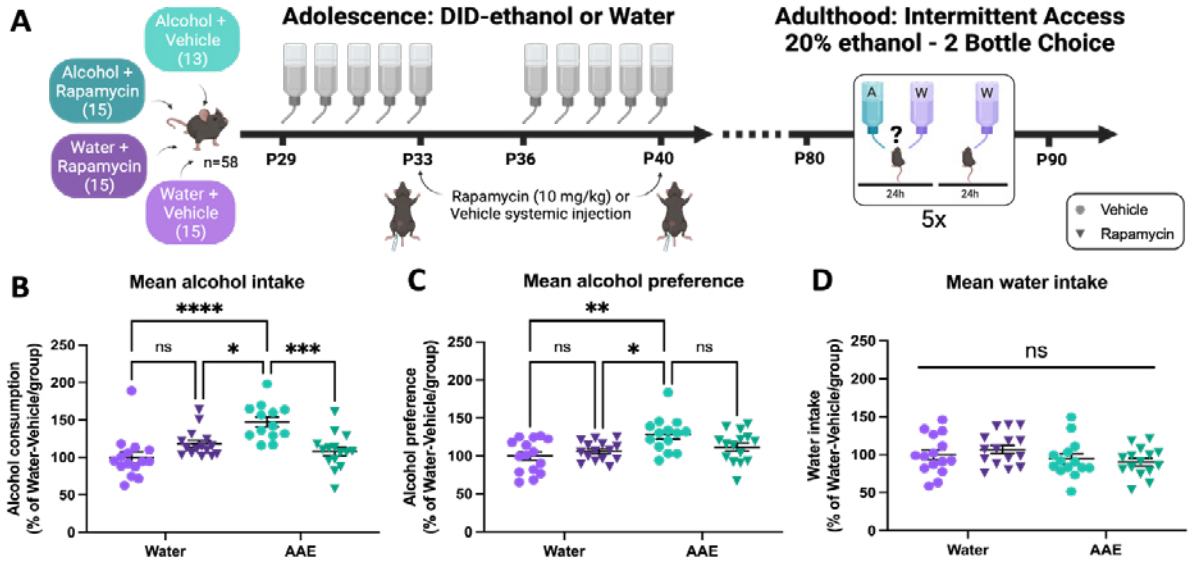

Figure 10. mTORC1 systemic inhibition during adolescent alcohol exposure reduces alcohol consumption and preference in adulthood. 4 groups of mice underwent the DID paradigm between P29 and P40. Rapamycin and Vehicle injections are shown in the scheme. After 40 days of abstinence, adult female mice underwent the Intermittent access to alcohol 20%-two-bottle choice (IA-20%-BC) paradigm for five sessions. **(B)** Mean alcohol consumption. Two-way ANOVA revealed a main effect of AAE (p<0.0001)

and an interaction (p<0.01) but no significant main effect of rapamycin (p=0.10). Post hoc Tukey test showed a significant difference between AAE/Vehicle and Water/Vehicle (p<0.0001) as well as between AAE/Vehicle and AAE/Rapamycin (p<0.001). **(C)** Alcohol preference. Two-way ANOVA showed a main effect of AAE (p<0.01) and an interaction (p<0.05) but no significant main effect of rapamycin. **(D)** Water consumption. Two-way ANOVA showed no significant main effect of AAE or rapamycin and no interaction. *p<0.05; **p<0.01; ***p<0.001; ****p<0.0001.

As we previously reported that AAE leads to increased anxiety levels in adulthood, we tested anxiety levels in adult animals exposed to alcohol or water during adolescence, and which have received rapamycin or vehicle injections on days 5 and 10 (**Figure 11**). Our results confirm that AAE induces anxiety-like disorder in adult animals, and suggest that rapamycin treatment during adolescence inhibits this increased anxiety levels.

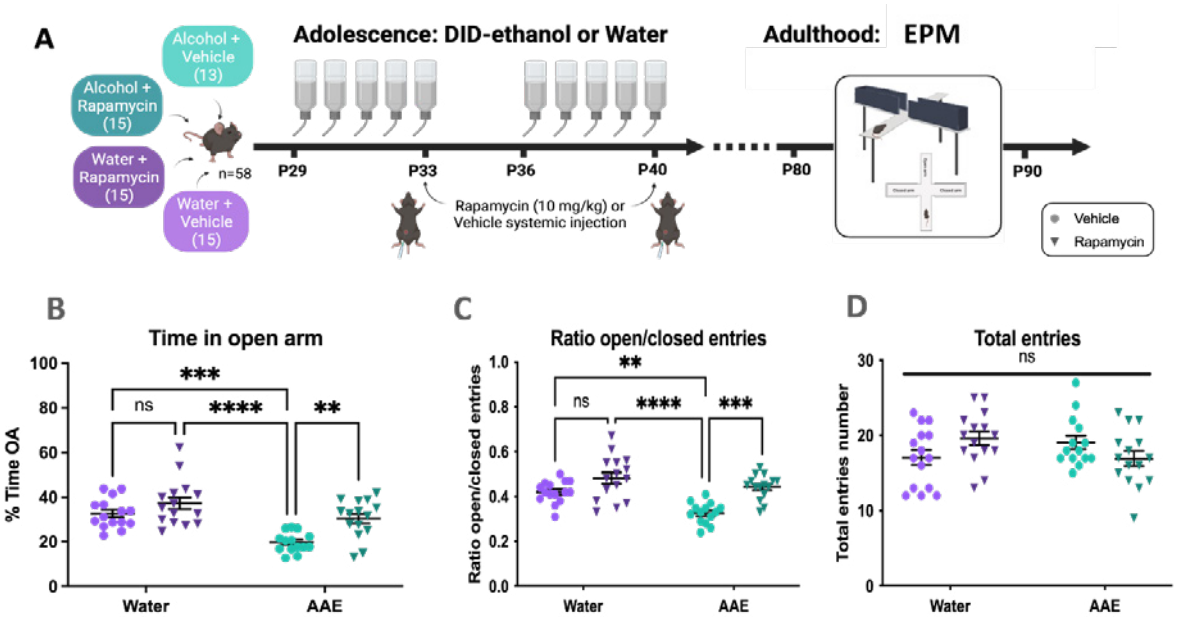

Figure 11. mTORC1 systemic inhibition during adolescent alcohol exposure reduces anxiety-like disorder in adulthood. 4 groups of mice underwent the DID paradigm between P29 and P40. Rapamycin and Vehicle injections are shown in the scheme. After 40 days of abstinence, adult female mice underwent the EPM test. **(B)** Time in open arms. Two-way ANOVA revealed a main effect of AAE (p<0.0001), of rapamycin (p<0.001) but no interaction. Post hoc Tukey test showed a significant difference between AAE/Vehicle and Water/Vehicle (p<0.001) as well as between AAE/Vehicle and AAE/Rapamycin (p<0.01). **(C)** Ratio Open/closed arm entries. Two-way ANOVA showed a main effect of AAE (p<0.001) and rapamycin (p<0.001) an interaction (p<0.05). **(D)** Total entries. Two-way ANOVA showed no significant main effect of AAE or rapamycin and no interaction. *p<0.05; **p<0.01; ***p<0.001; ****p<0.0001.

Those findings are very interesting as they suggest that mTORC1 signaling may be involved in the development of behavioral disorders following AAE. However, for the next steps, we will use intra-PFC AAV-delivery of shRNA against Raptor, which will allow for brain region specificity. Such constructs are under construction, and the set up of stereotaxic coordinates for targeting the PFC at P21 is currently undergoing.

4. Task 3: Global approach: identify the mRNAs whose local translation is modulated by AAE in specific neuronal populations.

Following validation of the Ribotag technology specificity (**Figure 12**), we performed the Ribotag-RNAseq profiling at P43 and P80 on male mice (Rpl22$^{tm1.1Psam}$ mice crossed with VGlut1-cre mice, in order to purify the ribosome-associated mRNA from PFC projection neurons only).

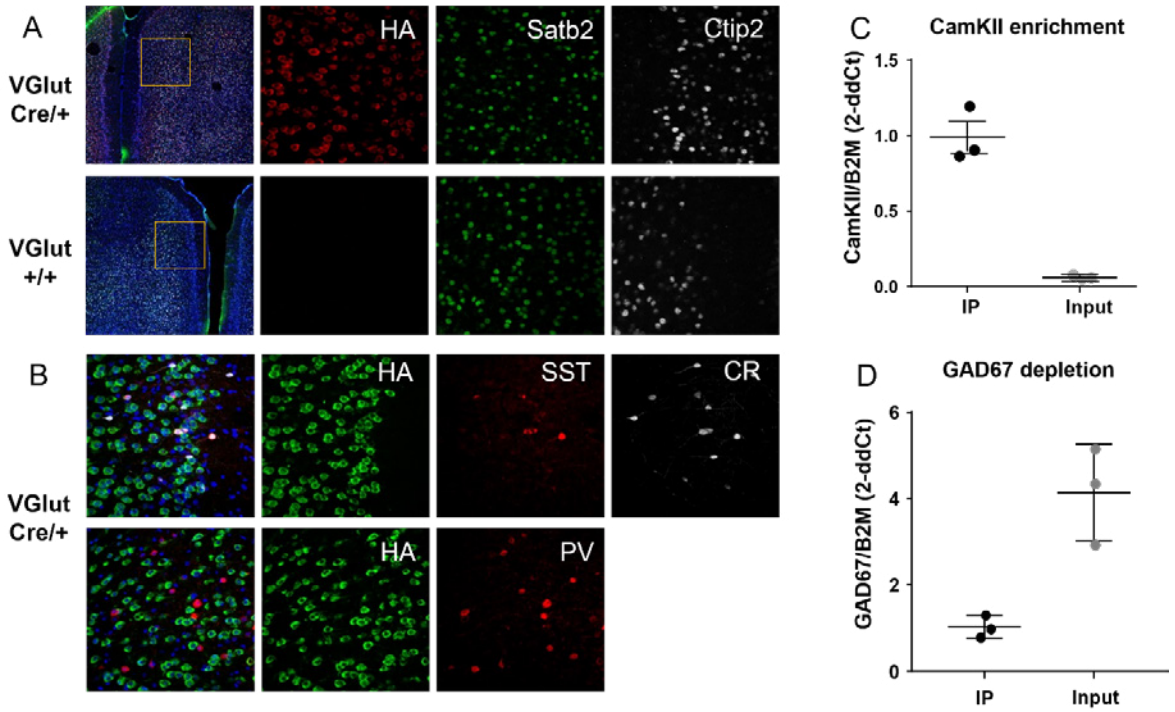

Figure 12: Validation of the specificity of the Ribotag mouse. **(A)** HA (red) co-localizes with glutamatergic markers Satb2 (green) and Ctip2 (grey) in prefrontal cortex of VGlutcre/+ mice, but is not expressed in absence of the Cre driver. **(B)** HA (green) does not co-localize with interneuron markers somatostatin (SST, red), calretinin (CR, grey), or paravalbumin (PV, red) in the PFC of VGlutcre/+ mice. (C, D) qRT-PCR after Ribotag immunoprecipitation shows that CamKII expression is enriched in the immunoprecipitate fraction from PFC of VGlutCre/+ mice as compared to the input (total mRNA) (C), whereas GAD67 expression is depleted (D).

At P43, several ribosome-bound mRNA candidates were differentially expressed within the projection neuron population, including the Acetyl-Coenzyme A acetyltransferase (ACAT3) and the Neuropeptide FF (NPFF), which showed reduced expression in AAE animals as compared to water controls. In order to validate the profiling results, we purified ribosome-bound mRNA from PFC projection neurons and analyzed it by qRT-PCR. Preliminary results suggest AAE-dependent reduced expression of ACAT3 and NPFF in the PFC of P43 animals (but not the motor cortex (data not shown)) (**Figure 13**).

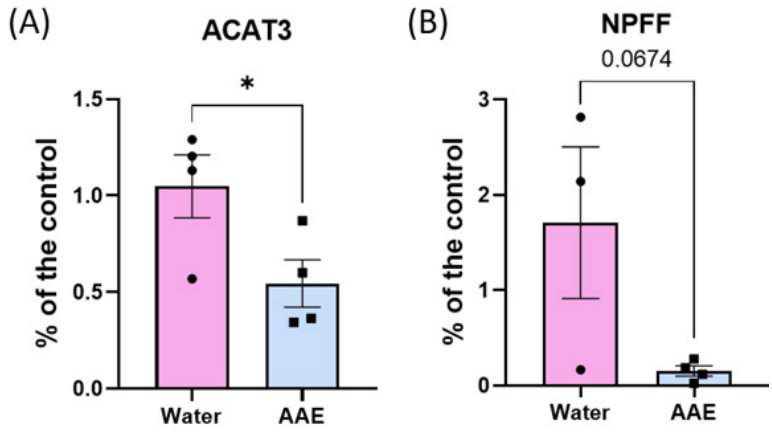

Figure 13: qRT-PCR analysis of ACAT3 and NPFF mRNAs in the IP and fraction after Ribotag IP in PFC samples at P43. (A) Unpaired t test showed ACAT3 mRNAs expression is decreased in alcohol-exposed mice as compared to water-exposed animals in IP fraction ($p=0.0488$). (B) NPFF mRNAs expression shows a tendency but is not significantly decreased in alcohol-exposed mice as compared to water-exposed mice in the IP fraction ($p=0.0674$). Data are presented as the average ratio of ACAT3 and NPFF to the mean of B2M and HPRT1 ± SEM and expressed as the percentage of water control; *$p<0.05$.

Additional potential targets have been identified, such as Nr4a1 and KDM6B, and are currently under qRT-PCR validation.

At P80, RNA-seq analysis has revealed 160 transcripts whose translation was increased or decreased in the PFC in the IP fraction (projection neurons only) by at least 1.2 or 0.8-fold in the AAE group compared to the water group. We first chose to follow upon the actin-binding protein Filamin A (FLNA), the Glutamate kainite receptor subunit GRIK1 and the microtubule scaffolding protein IQ motif containing GTPAse activating protein 1 (IQGAP1). qRT-PCR analysis showed significantly increased levels of the ribosome-bound FLNA and GRIK1 mRNAs content in IP fraction from PFC extracts of AAE animals as compared to water controls (**Figure 14**). In motor cortex (the control region), we did not report any significant difference in the level of FLNA and GRIK1 transcripts being translated in IP fraction (data not shown). In addition, we did not find any significant variation of ribosome-bound IQGAP1 transcripts expression between alcohol- and water-exposed mice in IP fraction in the prefrontal cortex (**Figure 14C**). Hence, we did not confirm RNA-seq data for this transcript.

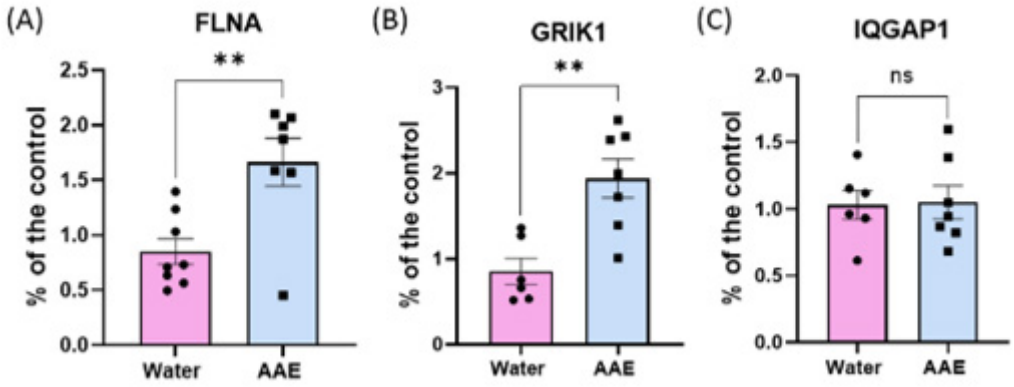

Figure 14. qRT-PCR analysis of FLNA, GRIK1 and IQGAP1 candidates at P80. Unpaired t test showed that (**A**) FLNA mRNAs expression is increased in the PFC IP fraction of alcohol-exposed mice as compared to water-exposed mice (p=0.0046). (**B**) GRIK1 mRNAs expression is also increased in the PFC IP fraction of alcohol-exposed mice as compared to water-exposed mice (p=0.0026). (**C**) No difference in the level of IQGAP1 mRNAs in the PFC IP fraction between the AAE and water groups was reported (p=0.9133). **p<0.01.

As for P43, additional potential targets are currently being validated. Next step will be further analysis of AAE-induced dysregulation of mRNA expression in projection neurons, by immunofluorescence and western blot following FACS sorting of PFC projection neurons. Finally, the involvement of candidates mRNAs in AAE-induced PFC defects will be studied by using the multidisciplinary method described in Task 4 of the proposal.

Geneeskundige Stichting Koningin Elisabeth
Fondation Médicale Reine Elisabeth
Königin-Elisabeth-Stiftung für Medizin
Queen Elisabeth Medical Foundation

Geneeskundige Stichting Koningin Elisabeth – G.S.K.E.
Fondation Médicale Reine Elisabeth – F.M.R.E.
Queen Elisabeth Medical Foundation – Q.E.M.F.

Mailing address:

The scientifique director:
Prof. dr. Jean-Marie Maloteaux
3, avenue J.J. Crocq laan
1020 Bruxelles – Brussel
Belgium
Tel.: +32 2 478 35 56
E-mail: jean-marie.maloteaux@uclouvain.be

Secretary:
Mr. Erik Dhondt
3, avenue J.J. Crocq laan
1020 Bruxelles – Brussel
Belgium
Tel.: +32 2 478 35 56
E-mail: fmre.gske@skynet.be
erik.dhondt@skynet.be
e.l.dhondt@skynet.be

www.fmre-gske.be
www.fmre-gske.eu
www.fmre-gske.com